ABSTRACT

Irene J. Abbene. RECONSTRUCTION OF THE RECENT PALEOENVIRONMENT OF PAMLICO SOUND, NORTH CAROLINA, USING FORAMINIFERA, STABLE ISOTOPES ($\delta^{13}C$ & $\delta^{15}N$), AND RADIONUCLIDE DATA. (under the co-direction of Dr. Stephen Culver and Dr. D. Reide Corbett) Department of Geology

Environmental conditions existing within Pamlico Sound over the last century were analyzed using foraminiferal data, stable isotope (C and N) data, C:N ratios, percent OC, and radionuclide data. Environmental conditions were evaluated at three time slices; (1) the modern environment as determined by surficial (0-2cm) sediments, (2) the intervals representing approximately 40 years BP, as determined by ^{137}Cs activity, and (3) the intervals representing approximately 120 years BP, as determined by ^{210}Pb activity.

Cluster analysis distinguished four foraminiferal assemblages at the surface (0-1cm); (1) Estuarine Biofacies A, (2) Estuarine Biofacies B, (3) Marsh Biofacies, and (4) Marine Biofacies. Estuarine Biofacies A is distinguished from Estuarine Biofacies B by the greater relative abundance of the agglutinated species *Ammotium salsum* and *Ammobaculites crassus* in the former and the greater relative abundance of *Elphidium excavatum* in the latter. The Marsh Biofacies is characterized by typical marsh foraminifera such as *Tiphotrocha comprimata, Trochammina inflata, Miliammina fusca,* and *Haplophragmoides wilberti.* The Marine Biofacies is comprised completely of calcareous foraminifera (e.g., *Elphidium excavatum, Hanzawaia strattoni, Cibicides lobatulus, Elphidium subarcticum, Quinqueloculina seminula,* and *Elphidium galvestonense*) and is restricted to tidal inlets.

The down-core foraminiferal data indicate that there has been a steadily increasing marine influence within Pamlico Sound over the last century; supportive

evidence is provided by down-core C:N ratios. Approximately 120 years BP, Pamlico Sound was dominated by Estuarine Biofacies A, which is indicative of brackish conditions. The particular abundance of hurricanes at this time may explain the brackish nature of the foraminiferal assemblage. Up-core, Estuarine Biofacies B becomes the more prominent assemblage within Pamlico Sound; this is indicative of increased salinity over time. C:N ratios steadily decrease up-core throughout the sound indicating an increase in marine influence over the last century.

$\delta^{15}N$ signatures began to steadily enrich at approximately 40 years BP. The resultant $\delta^{15}N$ signature is a combination of nitrogen cycling within the water column and the interaction with surficial sediment, as well as the organic matter source material. An increase in the amount of shrimp trawling during the early 1960s is a possible explanation for the enriched signatures. The average range for $\delta^{13}C$ signatures (-25 to –22) is typical of terrestrial sediment input and has not significantly changed over time. This suggests that the source area for the sediments being deposited within Pamlico Sound has not changed.

RECONSTRUCTION OF THE RECENT PALEOENVIRONMENT OF PAMLICO SOUND, NORTH CAROLINA, USING FORAMINIFERA, STABLE ISOTOPES ($\delta^{13}C$ & $\delta^{15}N$), AND RADIONUCLIDE DATA

A Thesis

Presented to

The Faculty of the Department of Geology

East Carolina University

In Partial Fulfillment

Of the Requirements for the Degree

Master of Science in Geology

By

Irene Johanna Abbene

July 2004

RECONSTRUCTION OF THE RECENT PALEOENVIRONMENT OF PAMLICO SOUND, NORTH CAROLINA, USING FORAMINIFERA, STABLE ISOTOPES ($\delta^{13}C$ & $\delta^{15}N$), AND RADIONUCLIDE DATA

By

Irene Johanna Abbene

APPROVED BY:

CO-DIRECTOR OF THESIS _____
Dr. Stephen J. Culver

CO-DIRECTOR OF THESIS _____
Dr. D. Reide Corbett

COMMITTEE MEMBER _____
Dr. David Mallinson

COMMITTEE MEMBER _____
Dr. Martin A. Buzas

CHAIR OF THE DEPARTMENT OF GEOLOGY

_____
Dr. Stephen J. Culver

DEAN OF THE GRADUATE SCHOOL

_____
Dr. Paul Tschetter

ACKNOWLEDGEMENTS

I wish to express my gratitude to Dr. Stephen Culver and Dr. D. Reide Corbett. The entire experience has been completely rewarding to me because of their encouragement, enthusiasm, patience, and friendship. I would like to thank my committee members, Dr. Dave Mallinson and Dr. Martin Buzas. I especially thank Dr. Buzas for helpful guidance with statistics. I would also like to thank the entire ECU crew for two full years of memories. Their support and companionship have made times of stress more bearable and will not be forgotten. And I would like to especially thank my family for always instilling confidence in me to be the person I am today.

TABLE OF CONTENTS

LIST OF TABLES vi

LIST OF FIGURES vii

INTRODUCTION 1

Objectives 8

PREVIOUS WORK 10

Foraminifera of marginal marine environments on the North American Atlantic Coast 10

Significance of $\delta^{13}C$ signatures 18

Significance of $\delta^{15}N$ signatures 21

Significance of C:N ratios 24

Estuarine studies using geochemical tracers 25

Radionuclides 27

METHODS 29

Foraminiferal analysis 30

Laboratory Methods 30

Cluster Analysis 33

Biofacies Fidelity and Constancy 34

Discriminant Analysis 34

Species Diversity 35

Geochemical Analysis 36

Carbon and Nitrogen 36

Radionuclides 37

One-way Analysis of Variance (ANOVA) 39

RESULTS 40

Foraminifera 40

Cluster Analysis: Live Foraminifera 40

Cluster Analysis: Dead Foraminifera 43

Biofacies Fidelity and Constancy 46

Discrimininant Analysis 49

Surficial Discriminant Analysis 49

Down-core Discriminant Analysis 54

Species Diversity 58

Geochemistry 61

Geochronology 61

Stable Isotopes 61

C:N Ratios 82

Percent Organic Carbon 84

One-way Analysis of Variance (ANOVA) for Geochemical Results 86

DISCUSSION 91

Description of the Modern Environment 91

Description of the Paleoenvironment 120 years Before Present 95

Description of the Paleoenvironment 40 years Before Present to Present Day..... 98

Explanations 101

CONCLUSIONS 109

REFERENCES 111

PLATES 121

APPENDIX A: REFERENCES USEFUL IN IDENTFYING TAXA 127

APPENDIX B: RAW CENSUS DATA (SURFACE) 131

APPENDIX C: RELATIVE ABUNDANCE DATA (SURFACE) 138

APPENDIX D: TRANSFORMED ABUNDANCE DATA (SUFACE) 142

APPENDIX E: RAW CENSUS DATA (DOWN-CORE) 147

APPENDIX F: RELATIVE ABUNDANCE DATA (DOWN-CORE) 149

APPENDIX G: TRANSFORMED ABUNDANCE DATA (DOWN-CORE) 151

APPENDIX H: GEOCHEMICAL DATA 153

LIST OF TABLES

1. Summary of the habitat zones and characteristic species described by Woo et al. (1997) in a barrier island lagoon system in Virginia (modified from Woo et al., 1997)..... 15

2. Biofacies Fidelity and Constancy for the four biofacies, using dead species comprising 2% or more of the assemblage in any one sample..... 48

3. Canonical discriminant functions including the percent of variability for each eigenvalue..... 50

4. Canonical discrimint function scores for group means (group centroids) along the three canonical variate axes (functions)..... 50

5. Canonical discriminant functions including the percent of variability for each eigenvalue..... 51

6. Canonical discriminant function scores for group means (group centroids along two canonical variate axes (functions)..... 52

7. Standardized canonical discriminant function coefficients from the analysis..... 59

8. Species diversity of foraminifera within the Pamlico Sound estuarine system.... 59

9. ANOVA test results for $\delta^{13}C$ signatures..... 87

10. ANOVA test results for $\delta^{15}N$ signatures..... 87

11. ANOVA test results for C:N ratios..... 88

12. Contrasts for geochemistry compared to the three time slices..... 90

13. Summary of modern biofacies described for Pamlico Sound, the key species, sites, and salinity readings..... 92

14. Dates of hurricanes to reach coastal North Carolina between the years 1876 and 1899 (Barnes, 2001)..... 103

LIST OF FIGURES

1. Location of study area, Pamlico Sound, North Carolina..... 2

2. Bathymetry of Pamlico Sound..... 4

3. Sediment distribution in Pamlico Sound..... 4

4. Distribution of organic matter in Pamlico Sound..... 4

5. Location of tidal exchange, freshwater sources, wind direction, and typical isohalines for Pamlico Sound (Wells and Kim, 1989)..... 7

6. Locality of sites for foraminiferal and geochemical analysis within Pamlico Sound..... 9

7. Generalized map of nearshore environments displaying typical foraminifera and thecamoebians (freshwater only) (after Scott et al., 2001).....10

8. Typical range for $\delta^{13}C$ signatures (after Letrick, 2003).....20

9. Typical range for $\delta^{15}N$ signatures (after Letrick, 2003)..... 24

10. Floating apparatus set-up..... 31

11. Cluster analysis of surface sites using live foraminifera..... 41

12. Spatial distribution plot of the results of the cluster analysis using only live species..... 42

13. Cluster analysis of surface sites using dead foraminifera..... 44

14. Spatial distribution plot of the results of the cluster analysis of dead foraminifera..... 46

15. Plot of Canonical Discriminant Function 1 versus Canonical Discriminant Function 2..... 53

16. Plot of Canonical Discriminant Function 1 versus Canonical Discriminant Function 2 including three *a priori* groups and 21 "unknown" down-core samples; Estuarine Biofacies A, Marsh Biofacies, and Estuarine Biofacies B..... 55

17. Spatial plot of samples indicated by 'a' in Figure 16..... 56

18. Spatial plot of samples indicated by 'b' in Figure 16..... 59

19. Species diversity distribution plot within biofacies determined using cluster analysis..... 60

20. Geochemistry data for PAM02S9..... 62

21. Geochemistry data for PAM02S10..... 63

22. Geochemistry data for PAM02S11..... 64

23. Geochemistry data for PAM02S12..... 65

24. Geochemistry data for PAM02S22..... 66

25. Geochemistry data for PAM02S23..... 67

26. Geochemistry data for PAM02S24..... 68

27. Geochemistry data for PAM02S27..... 69

28. Geochemistry data for PAM02S30..... 70

29. Geochemistry data for PAM02S31..... 71

30. Geochemistry data for PAM02S32..... 72

31. Geochemistry data for PAM02S41..... 73

32. Geochemistry data for PAM02S42..... 74

33. Geochemistry data for PAM03S50..... 75

34. Geochemistry data for PAM03S59..... 76

35. Geochemistry data for PAM03S60..... 77

36. Geochemistry data for PAM03S61..... 78

37. Surface (0-2cm) $\delta^{13}C$ signatures for Pamlico Sound..... 80

38. Surface (0-2cm) $\delta^{15}N$ signatures for Pamlico Sound..... 82

39. Surface (0-2cm) C:N ratios for Pamlico Sound..... 83

40. Surface (0-2cm) percent organic carbon values for Pamlico Sound..... 85

41. One-way ANOVA plot of means for time slices (as determined by radionuclides) vs $\delta^{13}C$ signatures..... 88

42. One-way ANOVA plot of means for time slices (as determined by radionuclides) vs. $\delta^{15}N$ signatures..... 89

43. One-way ANOVA plot of means for time slices (as determined by radionuclides) vs. C:N ratios..... 89

44. $\delta^{13}C$ signatures approximately 120 years BP (as determined by radionuclide data)..... 96

45. $\delta^{15}N$ signatures approximately 120 years BP (as determined by radionuclide data)..... 97

46. C:N ratios approximately 120 years BP (as determined by radionuclide data)..... 97

47. $\delta^{13}C$ signatures approximately 40 years BP (as determined by radionuclide data)..... 99

48. $\delta^{15}N$ signatures approximately 40 years BP (as determined by radionuclide data)..... 99

49. C:N ratios approximately 40 years BP (as determined by radionuclide data)..... 100

50. Comparison of foraminiferal assemblage changes over time..... 101

51. Comparison of C:N ratio changes over time..... 103

52. $\delta^{13}C$ signatures versus $\delta^{15}N$ signatures over the last approximate 120 years BP..... 107

INTRODUCTION

Pamlico Sound, North Carolina, is one of the largest embayments along the US east coast, encompassing approximately 5340km^2 (2060mi^2) (Giese et al., 1985; Pietrafesa et al., 1986). The Sound is separated from the ocean by a series of barrier islands, referred to as the Outer Banks. Three main inlets, Oregon, Hatteras, and Ocracoke promote access to the sound from the ocean. Two rivers, the Pamlico and the Neuse, discharge fresh water into the sound. The low brackish Albemarle Sound, located to the north, also drains into the Sound and affects environmental conditions in its northern section (Figure 1).

Pamlico Sound is an estuary, a partially enclosed body of water, characterized by the interaction of fresh and salt water. A number of processes (biological, chemical, physical, etc.) occurring within esturaries make them one of the most productive ecosystems. Estuaries are important filter systems for nutrients and pollutants carried in from rivers. They also provide humans with a source of food and recreational activites (Dyer, 1997).

Pamlico Sound is a drowned-river estuary (Riggs et al., 1995; Riggs and Ames, 2003). Paleo-rivers and tributaries drained through the system during the Pleistocence. As sea level rose, the system flooded with ocean waters forming the current estuarine system. The bathymetry of the sound is controlled by the paleogeomorphology of the river and tributary system (Riggs et al., 1995; Riggs and Ames, 2003).

Two large basins form the deep sections of the Sound. These basins are separated by Bluff Shoal, a bar of medium grained sand which extends across the Sound in a

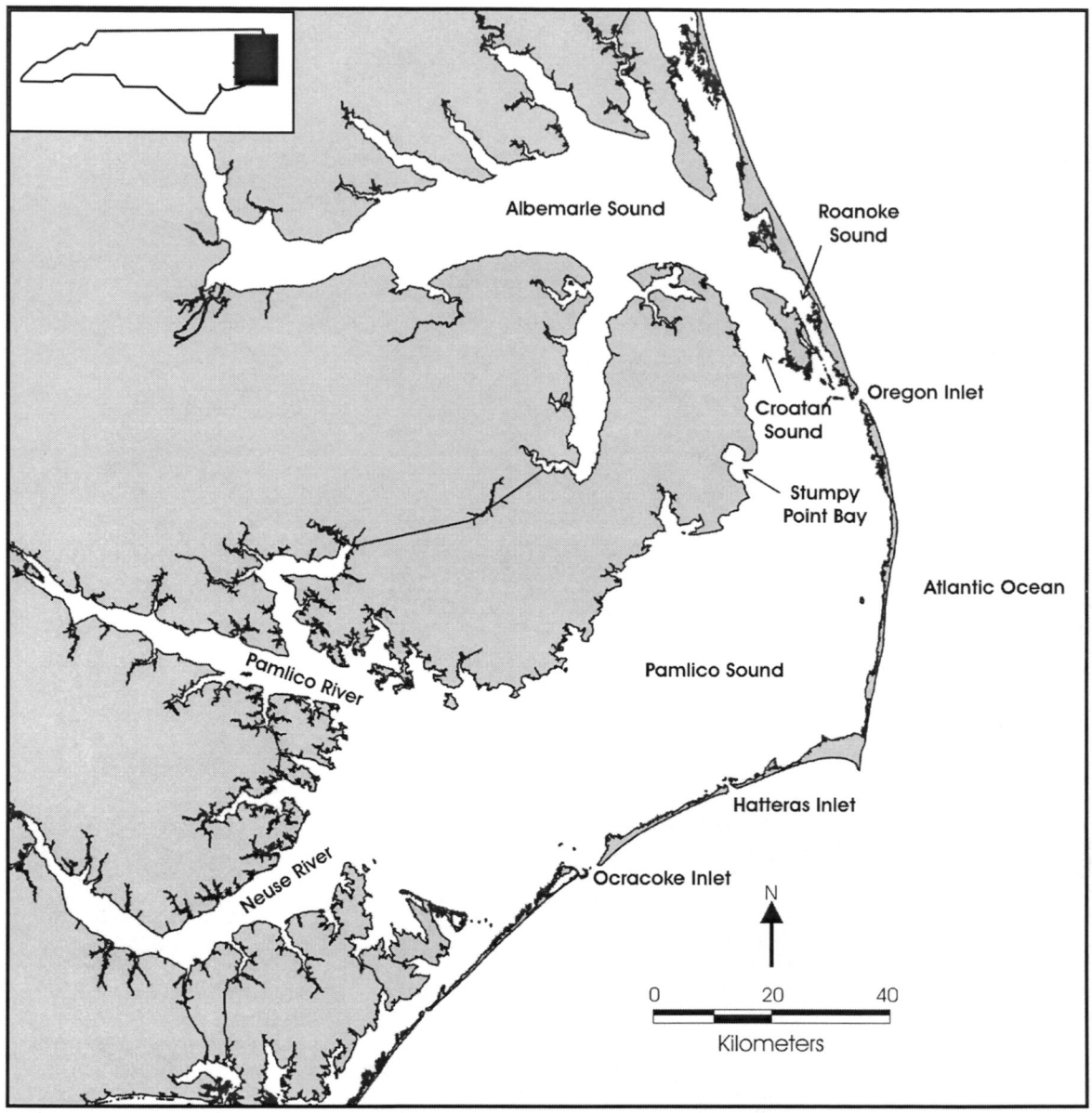

Figure 1: Location of study area, Pamlico Sound, North Carolina. Inset shows location within North Carolina.

northwest-southeast transect from the mainland to Ocracoke Inlet (Figure 2). Pamlico Sound is relatively shallow, with a maximum depth no more than 8m (26.4ft) (Giese et al., 1985). The four major sources for sediment deposition in the Sound are from river input, shoreline erosion, the continental shelf, and autochthonous biogenic production, whereas windblown silt from the dunes of the Outer Banks is a minor contribution (Wells and Kim, 1989). The floor of the Sound is generally covered in fine to very find grained sand, with silt and clay-sized particles concentrated in the basins and in the channels of the rivers (Neuse and Pamlico) that extend into the Sound (Figure 3). Medium grained sand is found at the inlets. Scattered pockets of medium grained sand form sand shoals within the Sound. The greatest amount of recorded organic matter and carbon correspond to regions of fine-grained material and the amount decreases with increasing grain size (Figure 4) (Giese et al., 1985; Pietrafesa et al., 1986; Wells and Kim, 1989).

Pamlico Sound, a microtidal estuary, has an astronomical tidal range between 10 to 100cm. Wind-tide currents dominate the movement of water and physiochemical conditions within the Sound. Strong winds associated with storms have a dramatic affect on the tidal range by increasing the water build up in the direction of the wind (Wells and Kim, 1989; Riggs and Ames, 2003). The large build up of water, or storm tide, floods and erodes shorelines sometimes causing an incredible amount of damage; up to 15m of mainland marsh recession during Hurricane Isabel in September 2003 (Riggs and Ames, 2003).

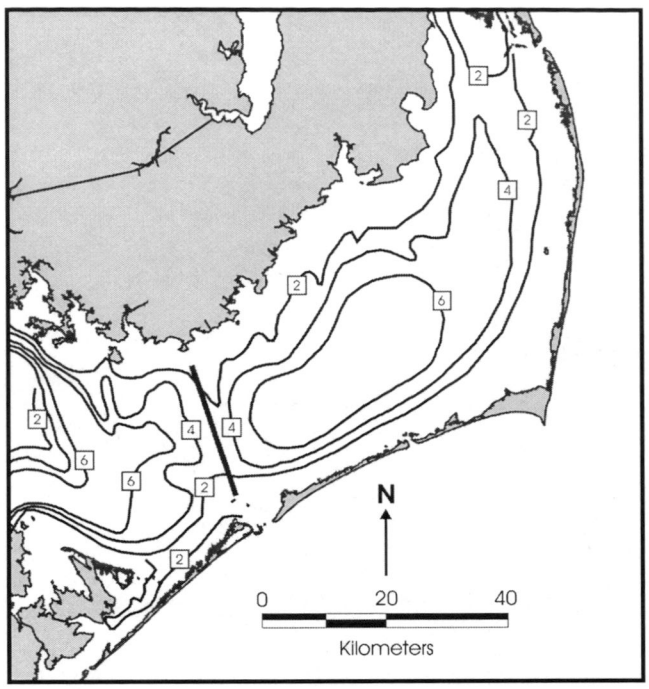

Figure 2: Bathymetry of Pamlico Sound. Black line indicates the location of Bluff Shoal. Contours are in meters (modified from Wells and Kim, 1989).

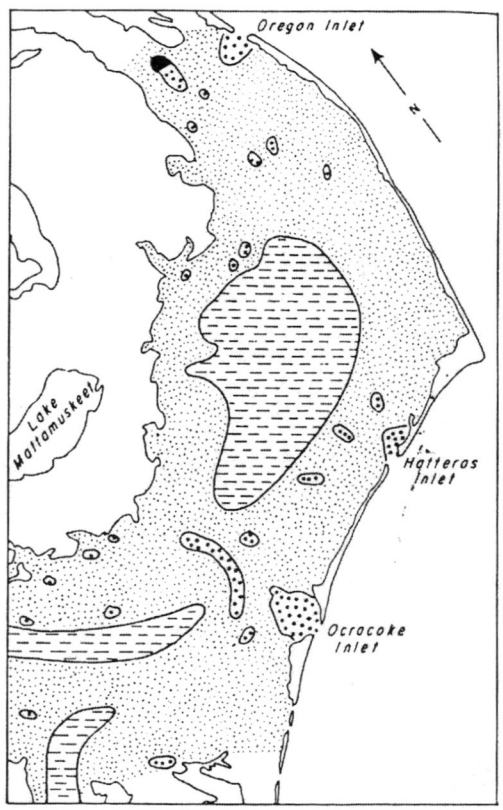

Figure 3: Sediment distribution in Pamlico Sound (from Giese et al., 1987).

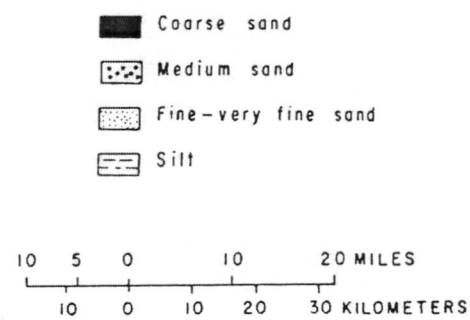

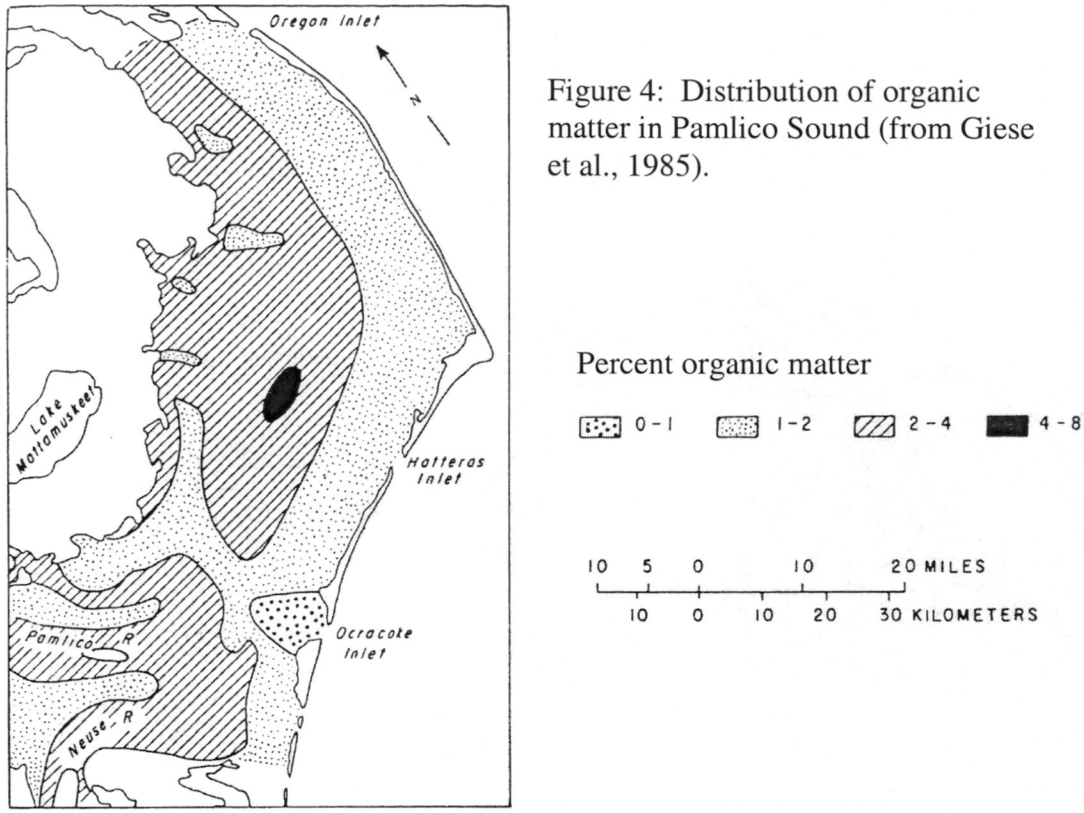

Figure 4: Distribution of organic matter in Pamlico Sound (from Giese et al., 1985).

The conditions that exist within the Sound are greatly affected by the freshwater/saltwater interface, mixing currents created by wind tides, and storm events. These conditions vary on a seasonal scale and a day-to-day basis. Salinity generally decreases with increasing distance from the inlets westward (Roelofs and Bumpus, 1953; Wells and Kim, 1989). The Pamlico and Neuse Rivers are the main source of freshwater for the Sound. Peak discharge from the rivers is during the spring. The direction of the wind and the volume of water within the rivers control the extent of freshwater into the sound. Winds are generally from the south/southwest during the spring and summer time. The increased amount of water draining from the rivers and the general wind direction form a freshwater wedge that extends far into the northern section of the Sound

during the spring and early summer seasons (Figure 5) (Wells and Kim, 1989). A difference of 6 between surface and bottom salinities was recorded in the southern basin of the Sound during the spring, summer, and fall, which was attributed to increased freshwater inflows from the rivers due to a "wetter" than average spring (Pietrafesa et al., 1986). Tidal exchange between the Sound and the Atlantic Ocean occurs at the inlets. The extent that the saline waters will disperse into the sound is also controlled by wind direction. Northerly winds dominate during the fall and winter seasons. Wind direction and the low flow out of the rivers allow saline water to disperse throughout the Sound and to extend further up into the rivers (Figure 5) (Wells and Kim, 1989). The salinity range for the entire Sound is between 0.5 (at the rivers) and 36 (at the inlets) with an average of 20 (Marshall, 1951; Roelofs and Bumpus, 1953; Pietrafesa et al., 1986; Wells and Kim, 1989).

The majority of the research conducted in Pamlico Sound has documented patterns of salinity, temperature, sediment distribution, and water movement throughout the Sound (Marshall, 1951, Roelofs and Bumpus, 1953, Williams et al., 1973; Singer and Knowles, 1975; Pietrafesa et al., 1986; Giese et al., 1985; Wells and Kim, 1989). Recent research has defined the underlying geology of portions of the Pamlico-Albemarle estuarine system (Riggs et al., 1992; Riggs et al., 1995; Riggs, 1996; Pilkey et al., 1998; Riggs et al., 2000; Riggs and Ames, 2003). Research involving geochemical and paleontological analysis has been conducted only for the southernmost section of the Sound (Grossman, 1967; Grossman and Benson, 1967; Paerl et al., 2001). Other research

documented biogeochemical processes occurring within the Neuse and Pamlico Rivers (Matson and Brinson, 1990; Benninger and Wells, 1993; MODMON, 2001).

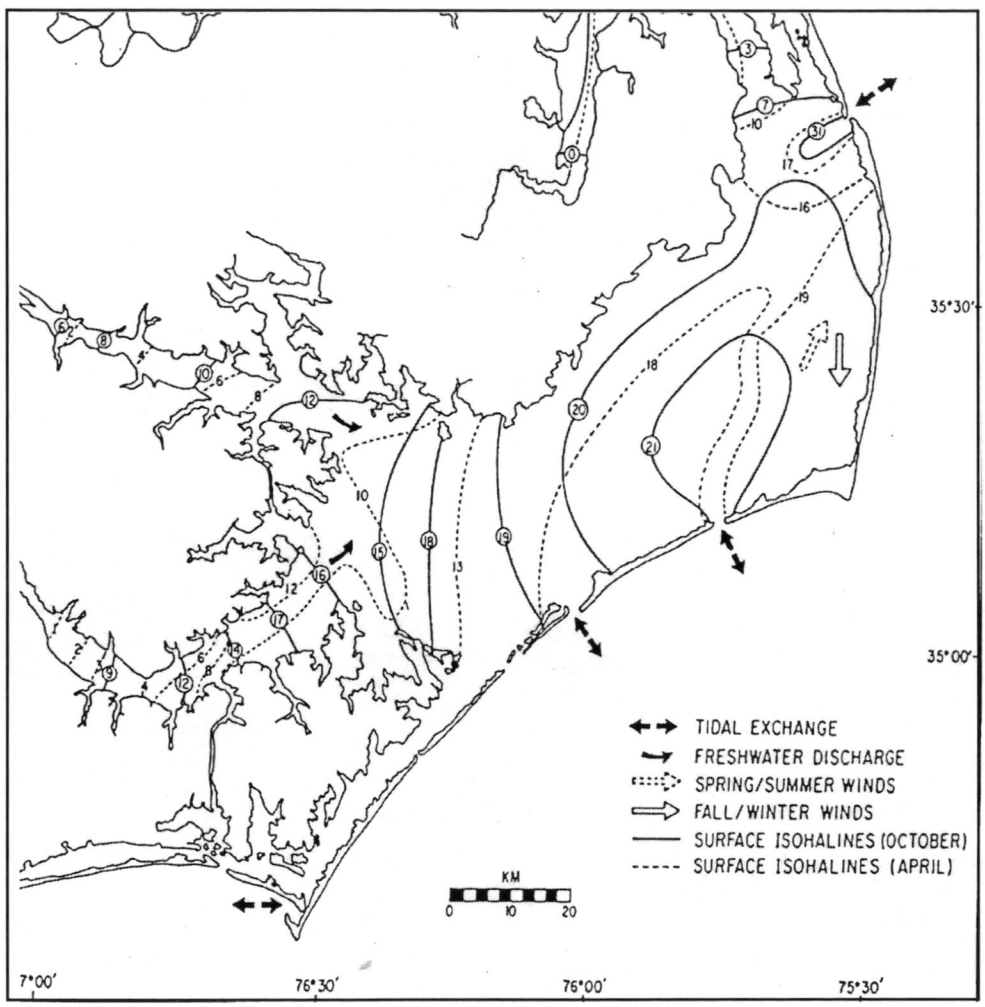

Figure 5: Location of tidal exchange, freshwater sources, wind direction, and typical isohalines for Pamlico Sound (Wells and Kim, 1989).

Objectives

This research is part of the North Carolina Coastal Geology Cooperative (NCCGC) program. The larger goal of the program is to describe the geologic framework and the modern anthropogenic/geologic processes of the coastal system. The purpose of the present study is to characterize the foraminiferal and geochemical (carbon and nitrogen) distribution patterns for the entire Pamlico Sound estuary and their change within the past 150 years. The objectives for this project are:

1) To map, for the first time, the distribution of modern foraminifera within the entire Pamlico Sound.

2) To create a model to interpret paleoenvironments represented by downcore foraminiferal assemblages.

3) To use stable isotopes of C and N, and C/N ratios to determine the dominant source of organic matter present in sediment (marine or terrestrial influence).

4) To describe environmental conditions that have existed within Pamlico Sound during the past 150 years BP (age determined by radionuclide data, provided by Tully, 2004).

A total of 40 sites throughout Pamlico Sound have been chosen for this study (Figure 6). The surface (0-1cm) sediment of each site has been analyzed to determine the modern distribution of foraminifera. Down-core geochemical data (stable isotopes C and N, C:N, percent organic carbon) have been analyzed for 17 of the 40 sites (Figure 6). Twelve of the 17 sites were chosen for analysis of down-core foraminiferal assemblages (Figure 6).

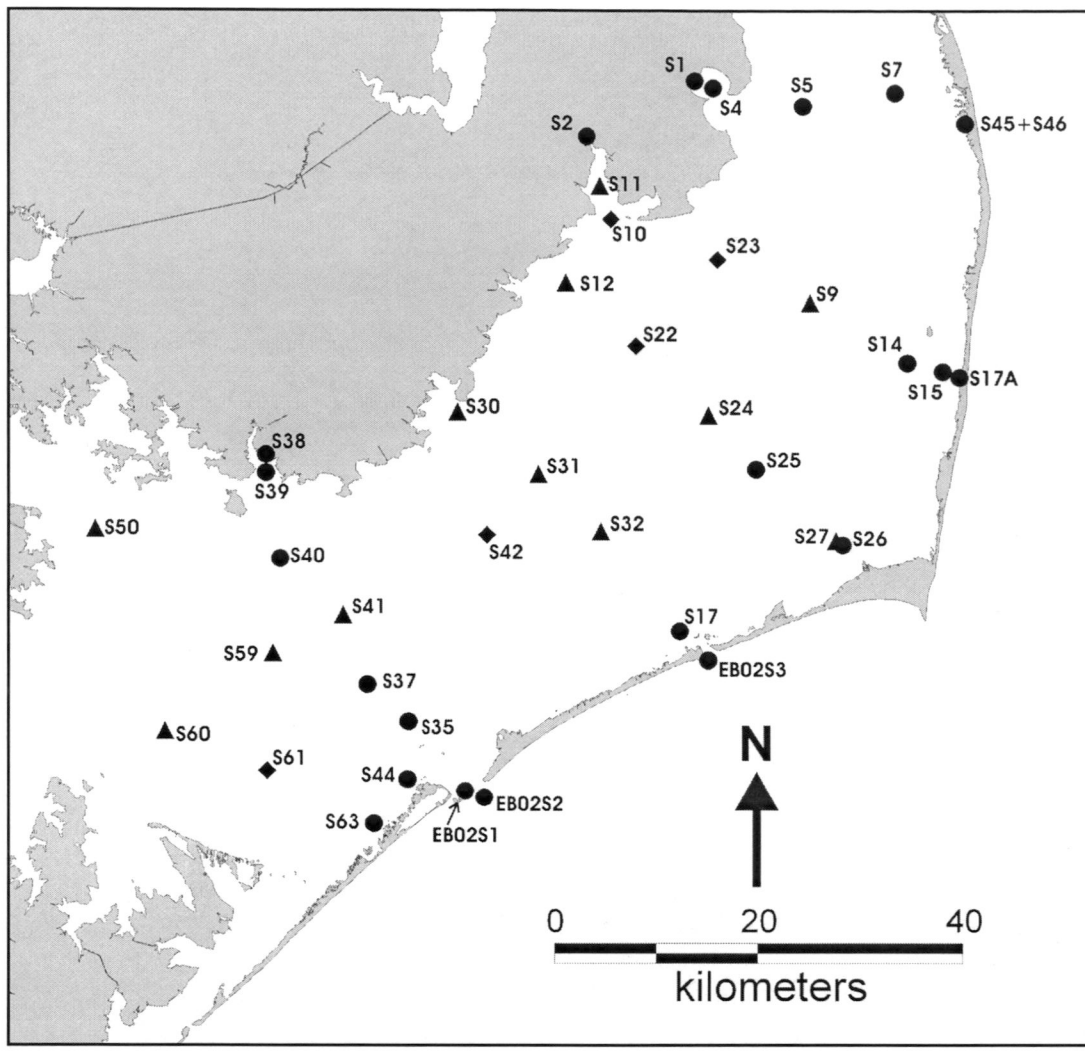

Figure 6: Locality of sites for foraminiferal and geochemical analysis within Pamlico Sound. The surface (0-1cm) of each site was used to determine surficial foraminiferal analysis. Closed triangles represent core locations for geochemcial and down-core foraminiferal analysis, and closed diamonds represent core locations for geochemical analysis. Closed circles represent those locations analyzed for surficial (0-1cm) foraminiferal assemblages only.

PREVIOUS WORK

Foraminifera of marginal marine environments on the North American Atlantic Coast

Each foraminiferal species is adapted to a particular set of abiotic and biotic environmental variables (e.g., food availability, competition, salinity, temperature, substrate, dissolved oxygen, etc); thus they are excellent indicators of modern and paleo-environments (Boltovoskoy and Wright, 1976; Scott et al., 2001). Many studies have used foraminiferal assemblages to define differences between shallow marine environments (Buzas, 1965; Nichols and Norton, 1969; Ellison and Nichols, 1970; Woo, 1992; Goldstein et al., 1995; Collins, 1996; Culver et al., 1996; Woo et al., 1997; Saffert

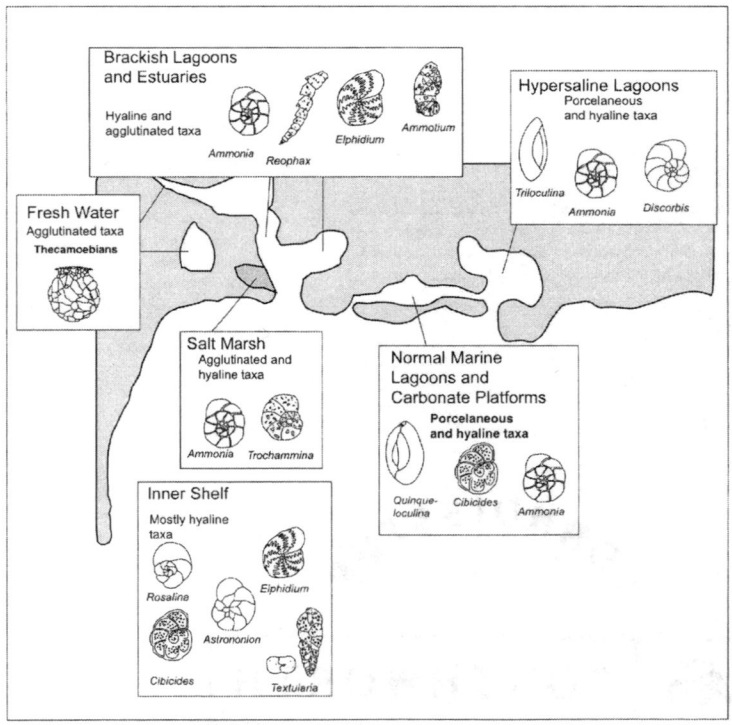

Figure 7: Generalized map of nearshore environments displaying typical foraminifera and thecamoebians (freshwater only) (after Scott et al., 2001).

and Thomas, 1998; Scott et al., 2001; Robinson and McBride, 2003; Vance, 2004) (Figure 7). Foraminifera have also proven to be valuable indicators of environmental stress, both natural (i.e., storm induced) and anthropogenic (e.g., Collins, 1996; Karlsen et al., 2000; Thomas et al., 2000; Scott et al., 2001; Bratton et al., 2003; Buzas-Stephens et al., 2003).

A considerable amount of research has described the distribution patterns of foraminifera on the Atlantic continental margin of North America (Culver and Buzas, 1980). This project involves foraminifera found within marginal environments along the east coast. Therefore, the following summary of previous work concentrates on foraminiferal distribution patterns recognized within marginal marine environments between Texas and Long Island Sound.

While much research has been conducted along the eastern seaboard, the only research in Pamlico Sound is in the southernmost part of the sound (Grossman, 1967; Grossman and Benson, 1967). Five foraminiferal assemblages were distinguished: an estuarine, an open-sound, a saltwater lagoon, a tidal-delta, and a marsh biofacies. *Ammobaculites* and *Elphidium* were the most abundant taxa found throughout the study area. *Ammobaculites* was dominant in the estuarine biofacies, and, when present with *Elphidium,* characterized the open-sound biofacies. The presence of *Quinqueloculina* distinguished the tidal-delta biofacies from the saltwater lagoon biofacies. The saltwater lagoon was distinguished by several species of *Elphidium,* such as *E. gunteri* and *E. tumidum* (= *E. excavatum* of this study). Typical marsh foraminifera, such as *Arenoparrella mexicana, Trochmmina,* and *Haplophragmoides wilberti,* distinguished the

marsh biofacies. The distribution of these assemblages was considered to be strongly influenced by salinity, vegetation, and tidal currents (Grossman, 1967).

Research conducted by LeFurgey (1976) defined a foraminiferal transition zone between the Albermarle and Pamlico Sounds. The upper Roanoke Sound, Croatan Sound, and Stumpy Point Bay (Figure 1) contained foraminifera characteristic of a lagoonal environment (*Miliammina fusca* and *Ammobaculites crassus*) where salinities, temperatures, and availability of calcium carbonate are low. With the influence of the adjacent Oregon Inlet, environmental conditions present within the lower Roanoke Sound were reported as having moderate temperatures, salinity, and calcium carbonate availability. *M. fusca* and *Elphidium selseyense* (=*E. excavatum* of this study) were considered to be the characteristic foraminifera for this nearshore marine environment (LeFurgey, 1976).

Research in the Albemarle Sound estuarine system using dead foraminifera distinguished five assemblages (Vance, 2004); nearshore marine and inlets, estuarine shoal, estuarine, inner estuarine, and marsh biofacies. Sediment type and salinity were determined to be the controlling factors for the distribution of the assemblages. Agglutinated species dominated the study area; *Ammobaculites crassus* was the most widespread species (present in four out of five biofacies). *Elphidium excavatum, Ammonia parkinsoniana, Hanzawaia strattoni* were the dominant and characteristic species of the normal salinity nearshore marine and inlet biofacies. Two species, *A. crassus* and *Ammotium salsum,* characterized the estuarine sandy shoal biofacies. The estuarine biofacies was dominated by three agglutinated species, *A. salsum, A. crassus,*

and *Miliammina fusca.* The inner estuarine biofacies was located near areas of freshwater inflow. Characteristic species for the inner estuarine biofacies were *Ammobaculities subcatenulatus, A. salsum, M. fusca,* and *A. crassus.* The foraminifera that distinguished the marsh biofacies were *A. crassus, M. fusca, Haplophragmoides wilberti,* and *Jadammina macrescens*. Foraminiferal assemblages present in two short cores were used to reconstruct the recent (ca. 150 years) paleoenvironment for the Albemarle estuarine system. Two biofacies were recognized down-core (inner estuarine and estuarine). The presence of these biofacies, as well as sedimentation rates (as determined using radionuclides), determined a change in depositional patterns for Albemarle Sound (Vance, 2004).

At St. Catherines Island, Georgia, marsh foraminifera were used to differentiate between marsh zones (high, transitional, and low). *Miliammina fusca, Ammonia beccarii, Ammotium salsum, Ammobaculites dilatatus, Trochammina inflata,* and *Arenoparrella mexicana* were dispersed throughout the marsh. *Siphotrochammina lobata* and *Haplophragmoides wilberti* were determined to be the key species to distinguish between the three marsh zones. *S. lobata* was only found at low marsh zones and *H. wilberti* was found at low and transitional marsh zones (Goldstein et al., 1995; Goldstein and Watkins, 1999).

In South Carolina, Collins (1996) also used foraminifera to delineate marsh zones and compared his findings between three marsh field sites. He found that the distribution of foraminifera was sensitive to salinity, sea level, river discharge, and anthropogenic influences. Only one marsh location was recognized to have "typical" marsh

foraminiferal assemblages present. Foraminifera found at the low marsh region were *Ammotium salsum* and *Miliammina fusca*, while the high marsh region was defined by the presence of four species; *Haplophragmoides wilberti, Ammoastuta inepta, Trochammina inflata,* and *Arenoparrella mexicana.* An unusual localized abundance of *Ammonia beccarii* and *Elphidium* spp. was recognized at a higher elevations (>40cm). Since these particular species are not generally found in these marsh settings, it was concluded that they represented an overwash deposit associated with a storm surge from Hurricane Hugo in 1989. Foraminiferal assemblages were not easily recognized at the other two marsh locations due to anthropogenic influence at one and a high river discharge at the other (Collins, 1996).

Foraminifera have been used to classify subenvironments in a barrier-island lagoon system in Virginia (Woo, 1992; Culver et al., 1996; Woo et al., 1997). This region is virtually untouched by human activity and the initial survey of foraminiferal assemblages provides a baseline of expected foraminiferal biofacies under natural conditions. Particular species were found to be distinct indicators of back barrier lagoonal environments and sensitive to a variety of environmental conditions (wave energy, sediment, and salinity). Seven environments (habitat zones) were distinguished based on the distribution of characteristic species. A summary of the seven habitat zones and characteristic species is given in Table 1.

Recent research in Long Island Sound compared changes in foraminiferal species abundance and distribution in the late 1940s (Parker, 1952a) and the early 1960s (Buzas, 1965) to species abundance and distribution documented in the 1990s (Thomas et al.,

Table 1: Summary of the habitat zones and characteristic species described by Woo et al. (1997) in a barrier island lagoon sytem in Virginia (modified from Woo et al., 1997).

Habit Zone	**Characteristic Species**
Brackish environments	*Ammonia beccarii* *Trochmmina inflata* *Trochammina squamata*
Fringe Marsh	*Ammobaculites exiguus* *Ammonia beccarii* *Elphidium excavatum* *Jadammina macrescens* *Miliammina fusca* *Textularia earlandi* *Trochammina inflata*
Valley marsh and tidal channel margins	*Ammonia beccarii* *Elphidium excavatum* *Haynesina germanica* *Miliammina fusca*
Inner and mid-lagoon environments	*Ammonia beccarii* *Elphidium excavatum* *Haynesina germanica*
Washover fan	*Ammonia beccarii* *Elphidium excavatum* *Quinqueloculina seminula*
Outer lagoon (sandy)	*Elphidium excavatum*
Shoreface and delta shoals	*Elphidium excavatum* *Elphidum mexicanum*

2000). *Elphidium, Buccella frigida,* and *Eggerella advena* were the dominant taxa and assemblages were of low diversity in Long Island Sound during the 1940s and 1960s. However, research from the late 1990s indicated that the relative abundance of *Eggerella advena* decreased while the relative abundance of *Buccella frigida* increased. Also, the relative abundance of *Ammonia beccarii,* a species that can withstand extreme variability

in oxygenation, has steadily increased since the 1960s. The change was attributed to the increased delivery of organic matter into Long Island Sound since the 1960s. An increase in algal blooms (which create episodes of anoxia/hypoxia) has occurred since the 1970s as a result of increased local nutrient loading in the sound from wastewater treatment plants. The research concluded that the observed change in the relative abundance of species over the years is a result of the increased anthropogenic influence in Long Island Sound (Thomas et al., 2000).

Foraminiferal distributions and abundances are used to delineate zones within estuaries. Estuaries generally have few species of foraminifera with only one or two dominant genera, usually *Elphidium* and an agglutinated taxon, *Ammobaculites* or *Ammotium*. The distribution and abundance of species in these two genera is related to salinity and depth (Nichols and Norton, 1969; Ellison and Nichols, 1970). Ellison and Nichols (1970) distinguished foraminiferal assemblages based on salinity and depth in their study in the Rappahannock Estuary of Chesapeake Bay. In particular, *Elphidium clavatum* (= *E. excavatum* of this study) inhabited deep areas of the estuary with higher salinities (Basin Biofacies). The presence of *Ammbaculites crassus* delineated a transition zone (Shoal Biofacies) between the Basin Biofacies and the Marsh (outer and inner) Biofacies. The Shoal Biofacies was comprised of mainly agglutinated foraminifera, such as *A. crassus* and *Miliammina fusca,* and extended over a wide range of fairly brackish water, with a salinity range of 0.5 to 16. Similar seasonal variations were observed in the Rappahannock Estuary (Ellison and Nichols, 1970) and the James River Estuary (Nichols and Norton, 1969), both part of the Chesapeake Bay estuarine

system. *Elphidium* increased in abundance with an increase in salinity during the summer months of low river flow (>14), while *Ammobaculites* was dominant in regions containing brackish water (0.5-14) (Nichols and Norton, 1969; Ellison and Nichols, 1970).

Recent research has combined foraminferal assemblages and geochemical analyses for recognition and explanation of changes in estuarine environmental conditions over time (e.g., Karlsen et al., 2000; Bratton et al., 2003; Buzas-Stephens et al., 2003). The abundance of *Ammonia parkinsoniana* was found to increase up-core in deep cores (4.5m) collected in Chesapeake Bay (Karlsen et al., 2000). *A. parkinsoniana* is tolerant of a variety of environmental conditions and can be associated with low dissolved oxygen. Using a number of dating techniques (radiocarbon analysis, pollen stratigraphy, ^{210}Pb and ^{137}Cs, and paleomagnetic correlation), the first presence of *A. parkinsoniana* was found to be in intervals dating back to the turn of the 19th century. The change in foraminiferal abundances at this time coincides with a boom in agriculture. The research concluded that the increased abundance of *A. parkinsoniana* was a direct result of anthropogenic influences (Karlsen et al., 2000; Bratton et al., 2003).

Recent research analyzed four areas in the Texas Gulf coast for the possible effects of pollutants on foraminifera (Buzas-Stephens et al., 2003). While no direct geochemical evidence of pollution was present, change in down-core foraminiferal assemblages within one area, the Arroyo Colorado, was determined to be an effect of anthropogenic influence. The present day surface foraminiferal assemblage of the Arroyo Colorado is classified as an estuarine river assemblage dominated by *Elphidum*

with a small percentage of *Ammonia*. However, as the amount of sand and grain size increases down-core, the number *Elphidium* species decreases as the number of *Ammonia* species increases. The foraminiferal assemblage at the bottom of the 70cm core is dominated by *Ammonia* with a small percentage of *Elphidium*. Radiounuclides (^{210}Pb and ^{137}Cs) determined that the age of the down-core change in sediment coincided with the construction of a shipping channel. The study noted coincidence of the change in the foraminiferal assemblage down-core with the dredging of the channel. However, the cause of the assemblage change was not evident to the authors (Buzas-Stephens et al., 2003).

Significance of δ^{13}C signatures

Carbon is one of the most abundant elements on Earth; it is found in all living things and the atmosphere. The two stable isotopes of carbon are ^{12}C and ^{13}C. The ^{13}C/^{12}C ratio varies among plants as a result of isotope fractionation. The δ^{13}C notation defines the isotope signature of carbon. The value for δ^{13}C is found by the following equation:

$$\delta^{13}C = \frac{\left(^{13}C/_{12}C\right)_{spl} - \left(^{13}C/_{12}C\right)_{std}}{\left(^{13}C/_{12}C\right)_{std}} * 1000 \qquad \text{(Eq. 1)}$$

Where 'spl' is for the sample and 'std' is for the standard. Calcite from a belemnite within the PeeDee Formation is the standard for δ^{13}C and is assigned a value of 0 parts

per thousand (‰). Values with a negative $\delta^{13}C$ are depleted in ^{13}C and values with a positive $\delta^{13}C$ are enriched (Cifuentes et al., 1996; Schlesinger, 1997; Faure, 1998).

Photosynthesis is the primary cause of carbon fractionation. Fractionation of carbon occurs at different rates based on photosynthetic metabolic pathways (Faure, 1998). The varying rates cause different $\delta^{13}C$ signatures in plants (marine and terrestrial), the atmosphere, and ocean. Photosynthesis begins the fractionation process by extracting CO_2 gas from the atmosphere and diffuses into the cells of the plants. Kinetics dictates a more rapid uptake of ^{12}C into plant cells because it is the lighter of the two isotopes. As a result of the diffusion, the CO_2 in the plant cells is depleted in ^{13}C (Schlesinger, 1997). Most plants are divided into two categories based on their photosynthetic pathways (C_3 or C_4), which is based on the number of carbon atoms used to convert CO_2 into simple sugars. Most terrestrial plants use the Calvin-Benson Cycle (C_3) to carry out photosynthesis. In contrast, many grasses, including salt marsh grasses (such as *Spartina alterniflora*), which are classified as C_4 plants, carryout photosynthesis using the Hatch-Slack cycle (Waller and Lewis, 1979; Smith and Smith, 1998).

The atmosphere has a $\delta^{13}C$ signature of -7 ‰. When plants uptake CO_2 from the atmosphere, the CO_2 becomes depleted in ^{13}C (a more negative $\delta^{13}C$ value). In general, organic matter derived from terrestrial sources (plants) is recognized by strongly depleted (more negative) $\delta^{13}C$ signatures. The biogenic release of CO_2 from HCO_3^- in marine waters has a $\delta^{13}C$ signature of 0‰. Therefore, the uptake of CO_2 by marine plants is generally more enriched (less negative) in ^{13}C than that of their terrestrial counter parts. As a result, greater enriched $\delta^{13}C$ signatures, in comparison to terrestrially derived

organic matter, allow the recognition of marine derived organic matter (Waller and Lewis, 1979; Faure, 1998; Thornton and McManus, 1994). Letrick (2003) summarized typical range values of $\delta^{13}C$ derived from various sources (Figure 8).

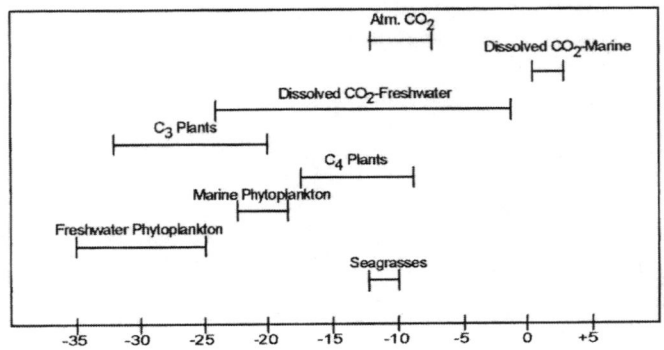

Figure 8: Typical range for $\delta^{13}C$ signatures (after Letrick, 2003).

The specific isotopic signatures of the ^{13}C allow researchers to determine whether marine or terrestrial biological processes dominate the production of organic matter present in their study area. Organic matter present in any coastal system has a specific $\delta^{13}C$ signature. However it is important to remember that there are several sources of carbon and that a $\delta^{13}C$ signature is a resultant of all the organic matter present in the sample. Carbon values obtained from organic matter in sediment have proved to be important indicators to determine whether estuaries and marshes are marine, riverine, or terrestrially dominated (Matson and Brinson, 1990; Thornton and McManus, 1994; Middleburg and Nieuwenhuize, 1998; Maksymowska et al., 2000; Neubauer et al., 2002).

Significance of $\delta^{15}N$ signatures

The stable isotopes for nitrogen are ^{14}N and ^{15}N. Variations in $^{15}N/^{14}N$ ratios are the result of fractionation occurring during biogeochemical processes. The $\delta^{15}N$ notation defines the isotope signature of nitrogen. $\delta^{15}N$ signatures are expressed in terms of parts per thousand (‰). The isotopic signature is calculated as follows:

$$\delta^{15}N = \frac{\left(^{15}N/_{14}N\right)_{spl} - \left(^{15}N/_{14}N\right)_{std}}{\left(^{15}N/_{14}N\right)_{std}} * 1000 \qquad \text{(Eq. 2)}$$

Where 'spl' is for the sample and 'std' is for the standard. The standard for nitrogen isotopes is atmospheric nitrogen (N_2), which has an isotopic signature equal to zero (Cifuentes et al., 1988; Cifuentes et al., 1996).

Stable nitrogen isotopes ($\delta^{15}N$) have proved to be a useful tool in determining possible sources (allochthonous or autochthonous) of organic matter within an estuarine system (Peters et al., 1978; Cifuentes et al., 1988; Thornton and McManus, 1994; Middleburg and Nieuwenhuize, 1998; Maksymowska et al., 2000; Graham et al., 2001; Neubauer et al., 2002; Bratton et al., 2003). The resultant signature is a combination between nitrogen cycling within the water column and the interaction with surficial sediment, as well as the organic matter source material (Bratton et al., 2003). Therefore, it is important to understand the biogeochemical processes occurring within the water column and sediment before deposition to obtain the conditions that exist within a system.

Nitrogen signatures are altered in the sediment and water-column by a number of different biogeochemical processes such as ammonification, nitrification, denitrification, bioturbation, assimilation, and physical mixing of sediment (Thornton and McManus, 1994). Ammonification is the formation of ammonium (NH_4^+) by the decomposition of organic matter (Kemp et al., 1990). Ammonium (NH_4^+) is delivered to the estuarine system via rivers (Maksymowska et al., 2000; Middleburg and Nieuwenhuize, 2001). In the estuary, NH_4^+ is either oxidized to nitrate (NO_3^-) (nitrification) within the water-column (Middleburg and Nieuwenhuize, 2001) or taken up by organisms, such as phytoplankton (assimilation) (Kemp, et al., 1990). Isotopic fractionation during assimilation of NH_4^+ by phytoplankton has been reported to enrich $\delta^{15}N$ signatures up to 6.4 ‰ (Montoya et al., 1991). The process of denitrification removes NO_3^- from the water-column and sediment in gas form as either N_2 or N_2O (Kemp et al., 1990; Middleburg and Nieuwenhuize, 2001; Usui et al., 2001), which is composed of the lighter isotope ^{14}N, leaving behind the heavier isotope ^{15}N (Anderson and Fourqurean, 2003). Denitrification produces the greatest fractionation (up to as much as 40 ‰) in comparison to all other biogeochemical processes (Bratton et al., 2003). The longer organic matter is suspended, the longer period of time it is exposed to biogeochemical processes within the water-column. In general, marine plankton and plants have a more enriched $\delta^{15}N$ signature in comparison to terrestrial vegetation (Peterson et al., 1985; Anderson and Fourqurean, 2003) as a result of these biogeochemical processes. Therefore, sediment deposited in marginal marine estuaries is typically enriched in $\delta^{15}N$.

$\delta^{15}N$ values can also determine the extant of anthropogenic influence in estuaries (Voss et al., 2000). Agriculture of the land (adding fertilizers) and direct addition of sewage increase $\delta^{15}N$ signatures (Peters et al., 1978; Thornton and McManus, 1994; Zimmerman and Canuel, 2000; Bratton et al., 2003). Many times, the increased nutrient loading into the water stimulates eutrophication, which will also enrich nitrogen signatures (Zimmerman and Canuel, 2000; Bratton et al, 2003). Algal blooms associated with increased nutrient loading into estuaries have disturbed natural nitrogen levels (Dortch et al., 1998; MODMON, 2001). Letrick (2003) summarized typical $\delta^{15}N$ signatures from various sources (Figure 9).

Once deposited, both aerobic and anaerobic microbial processes continue to modify the $\delta^{15}N$ of sediment. Continued denitrification of deposited sediment is expected to readily continue to remove ^{14}N, displaying increased enrichment of sediment down-core. However, a study conducted in Chesapeake Bay reported $\delta^{15}N$ signatures to deplete down-core (Bratton et al., 2003). The depletion found down-core was attributed to bacterial growth during anoxic decay of organic matter. Bacterial growth adds biomass depleted in ^{15}N to the sediment (Lehmann et al., 2002).

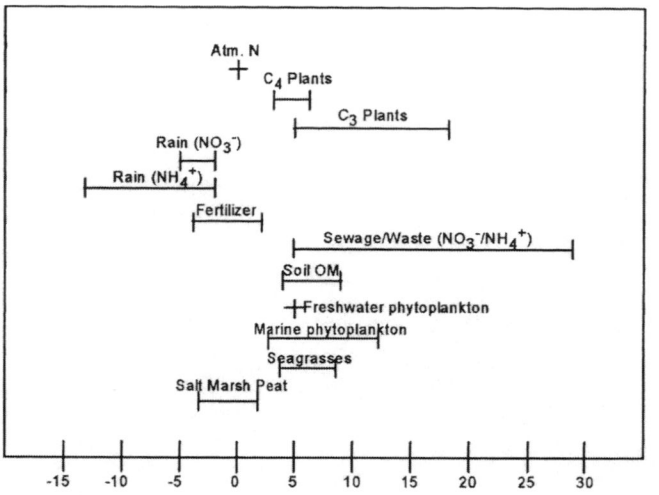

Figure 9: Typical range for $\delta^{15}N$ signatures (after Letrick, 2003).

Significance of C:N Ratios

C:N ratios (carbon to nitrogen weight ratio) have proven to be valuable indicators of possible sources for organic matter present within estuaries. In general, regions that are influenced by delivery of terrestrially derived organic matter have high ratios (>12). In contrast, regions that are influenced by marine processes have lower ratios (~9). Many studies have used C:N ratios to trace patterns in estuaries between terrestrially influenced regions and marine influenced regions. In most cases, C:N ratios decrease with increasing distance from source areas (down-river) (Matson and Brinson, 1990; Thornton and McManus, 1994; Middleburg and Nieuwenhuize, 1998; Gordon et al., 2001; Graham et al., 2001). C:N ratios are heavily influenced by processes (such as mixing) occurring within the sampling region and vary among field areas. Therefore, it is important to use other geochemcial tracers ($\delta^{13}C$, $\delta^{15}N$) to help understand the mechanics of the estuary and not to rely on C:N ratios alone.

Estuarine studies using geochemical tracers

Several studies have used C and N stable isotopes and C/N ratios to determine dominant source for organic matter present in estuaries (Thornton and McManus, 1994; Middleburg and Nieuwenhuize, 1998; Müller and Voss, 1999; Struck et al., 2000; Graham et al., 2001; Neubauer et al., 2002). According to Cifuentes (1988), isotopic signatures are conserved and the determined signature found in sediments is a result of the physical mixing between sources (terrestrial versus marine). For this reason, many studies have defined signatures and ratio values for terrestrial and marine environments to explain the values found in estuaries. Research in the Schelde Estuary determined four pools of organic matter: terrestrial, marine, riverine, and estuarine. The estuary was divided into an upper and lower section. Both sections of the estuary displayed C:N, $\delta^{13}C$, and $\delta^{15}N$ (upper: 17, -26, 7 and lower: 10, -23, 9, respectively) indicating mixing between several sources. However, the observed change between the two sections determined the upper estuary was more terrestrially influenced where as the lower estuary was more estuarine influenced (Middleburg and Nieuwenhuize, 1998).

Recent research in the Chesapeake Bay estuary has also used $\delta^{13}C$ and $\delta^{15}N$ signatures and C:N ratios from sediment in deep cores (4.5m) to described the paleoenvironment. The observed profile changes down-core were attributed to an increase in anthropogenic influence since the turn of the 19th century (as determined by various dating techniques) (Zimmerman and Canuel, 2000; Bratton et al., 2003). $\delta^{13}C$ and C:N profiles, as displayed down-core, signified changes in the estuarine productivity and delivery of terrestrially derived carbon to the estuary. $\delta^{15}N$ profiles displayed periods

of oxygen depletion down-core that indicated an increase in denitrification and nutrient recycling on seasonal scales (Bratton et al., 2003). An overall $\delta^{15}N$ enrichment in the cores began at the intervals representing approximately the years 1750-1800 (as determined by pollen and diatoms). The enrichment was attributed to increased eutrophication. The time period associated with the change coincides with an intense boom of agriculture of the land (land clearing and tillage), which also caused an increased in erosion of the land and sedimentation into the bay (Bratton et al., 2003).

Letrick (2003) used stable isotopes ($\delta^{13}C$ and $\delta^{15}N$), C:N ratios, and sedimentology to describe changes within Albemarle Sound estuarine system, North Carolina, over the last century. The data presented indicate that the system has changed in the last approximately 150 years from a primarily marine dominated estuary to the present day terrestrially dominated estuary. Cores collected in the Pasqutank River, a tributary to Albemarle Sound, indicate $\delta^{15}N$ enriches continually up-core over the last century (as determined by radionuclide data; Vance, 2004). This region of the estuary is densely populated. The increased enriched values were attributed to the increase in anthropogenic influence over time (Letrick, 2003).

Stable carbon isotopes and C:N ratios have been used to determine sources of organic carbon in the Pamlico and Neuse River estuaries of North Carolina. Matson and Brinson (1990) determined sediment present in the upper part of the estuaries to have $\delta^{13}C$ values characteristic of terrestrial plant material. $\delta^{13}C$ values continually enriched downstream, which signified less terrestrial plant input and more marine influence. Organic carbon produced from marine phytoplankton is more enriched in ^{13}C. The

increased levels of ^{13}C resulted in a decrease in C:N ratios present downstream. The change in isotope values and the C:N ratios delineate between the upper and lower waters within the Neuse River estuary (Matson and Brinson, 1990).

Radionuclides

Lead-210 (^{210}Pb) is part of the Uranium-238 (^{238}U) decay series. ^{238}U decays through a sequence of four radionuclides before it decays to Radium-226 (^{226}Ra). In soil, ^{226}Ra decays to the short-lived radionuclide to Radon-222 (^{222}Rn) and escapes to the atmosphere. Once in the atmosphere, ^{222}Rn (with a half-life of 3.82 days) continues the decay series through a series of short-lived radionuclides to ^{210}Pb. Lead-210 may be removed from the atmosphere in two ways: (1) dry deposition or (2) precipitation. In normal climate conditions, it can be assumed that ^{210}Pb fall-out is constant over the years (Appleby and Oldfield, 1992). With a half-life of approximately 22 years, ^{210}Pb can be used as a dating technique to construct sedimentation rates in sediment cores up to approximately 150 years before present (BP). In general, ^{210}Pb activities will decrease with increasing depth, which is a result of the radioactive decay of ^{210}Pb overtime (Jetter, 2000).

Cesium-137 (^{137}Cs) can also be used to determine calendar dates for core samples. The source for ^{137}Cs in the system is from the atmospheric testing of nuclear bombs beginning in 1954. Continued testing of nuclear bombs through the 1950's and the early 1960's places a prominent peak concentration in the record in 1963. Since 1963, a smaller quantity of ^{137}Cs is recorded in the sedimentary record (Jeter, 2000).

Radionuclides have been used in several studies to obtain sedimentation rates and ages within estuaries (Ravichandran et al., 1995; Dellapenna, et al., 1998; Buzas-Stephens et al., 2003; Corbett et al., 2004; Vance, 2004). Cesium-137 has also proven to be a useful tool to track sediment deposition from hurricanes and other major storms along the east coast of the United States (Chmura and Kosters, 1994; Donnelly et al., 2001a; Donnelly et al., 2001b; Corbett et al., 2004).

METHODS

Samples were collected during the summers of 2002 and 2003 using a 1-meter length manual push coring device and a Ponar grab sampler. Separate samples were collected for geochemical and foraminiferal analysis. For geochemical analysis, cores were sectioned into two-centimeter intervals between zero and 30 cm, then three-centimeter intervals for the remainder of each core. Sediment to be analyzed for radionuclides was placed into plastic bags while sediment for stable isotope analysis was placed in plastic vials and kept on ice in the field until they could be frozen in the lab. For foraminiferal analysis, each core was divided into surface intervals (0-1 and 1-2 cm), then into 2 cm intervals for the first 30 cm, and 3 cm intervals for the remainder of the core. Approximately 20 ml of sediment was placed into bottles and preserved in buffered alcohol for foraminiferal analysis. Two grab samples were collected at each site wherever a short core was collected. Twenty ml samples from the top 1 cm (0-1 cm) of sediment were acquired from each Ponar grab sample. Three grab samples were collected at sites where short cores were not collected. Each site was visited once and the temperature, salinity, water depth, as well as position were recorded.

Foraminiferal Analysis

Laboratory Methods

Forty surface samples (0-1 cm interval) were used for analysis of the modern distribution of foraminifera (Figure 6). Preparation of the samples followed the same procedure used by Culver et al. (1996) and Woo et al. (1997).

The samples were washed over a nest of 710-μm and 63-μm sieves to remove the mud (silt and clay) and the alcohol used to preserve foraminifera within the sample. The coarse material (> 710 μm) was placed into a plastic weigh boat then placed in an oven set a 60°C to be dried. The remaining material (63 to 710 μm) was washed into a 400 ml glass beaker with tap water. A small amount (< 1 g) of sodium metaphosphate ($(NaPO_3)_x \bullet Na_2O$ calgon) was added to every sample to help break apart any remaining mud aggregates. One to two small tablets of sodium hydroxide (NaOH) were added to extremely muddy samples in order to help break apart the larger mud aggregates. Rose Bengal (Walton, 1952) was added to all the surface samples. Rose Bengal stains cytoplasm of the preserved foraminifera to allow the distinction of live from dead foraminifera at the time of collection. After eight to twelve hours, the sample was washed over the sieves once more to remove any excess clay and silt the chemicals may have disaggregated, as well as the stain. The samples were then washed into plastic weigh boats and placed in an oven to be dried at 60°C.

Foraminifera were separated from samples containing a high amount of sand using sodium polytungstate (Munsterman and Kerstholt, 1996). The density of the heavy liquid can be controlled by the addition or subtraction (by evaporation) of de-ionized

water. The density of the heavy liquid is set to allow a piece of gypsum to float and a piece of feldspar to sink. This allowed foraminifera to float on the surface because they are composed of chambers filled with air, while sand and other heavy minerals sank in the solution.

The apparatus for the 'floating technique' is set-up as shown in Figure 10. Sodium polytungstate was poured into the funnel and tubing. The sandy sample was then sprinkled into the liquid. Once the sample had separated (approximately 15-20 minutes),

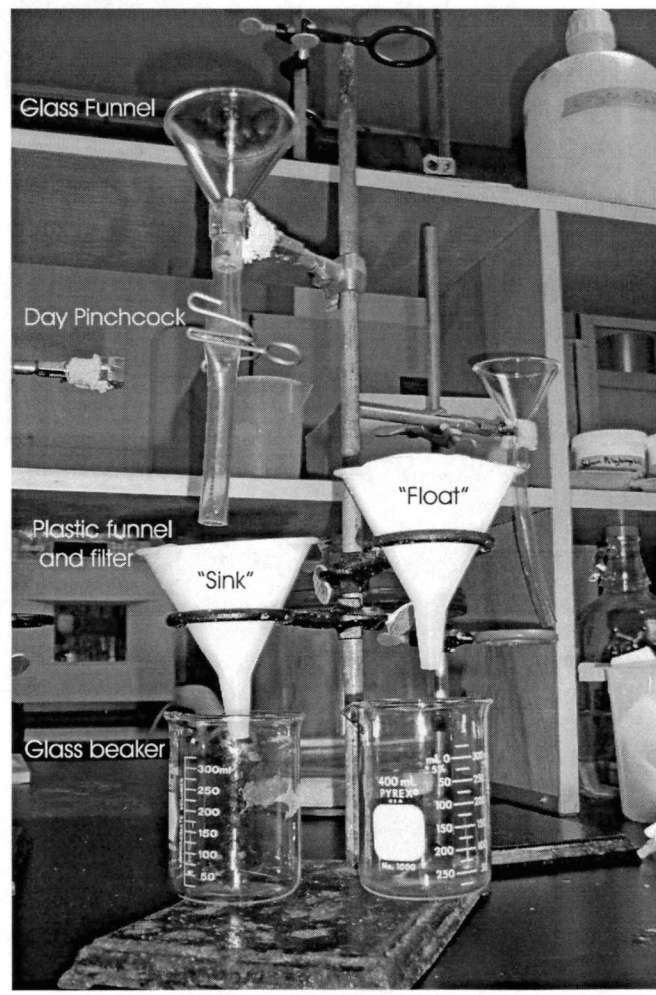

Figure 10: Floating apparatus set-up.

the liquid and the sand were drained into a plastic funnel lined by an 18.5 cm (diameter) paper filter with a coarse porosity to allow liquid to readily flow through (pore size should be no larger than 63μm). The sand ('sink') was captured in the filter while the liquid drained into a 400 ml glass beaker. Once the sand had drained out, the remaining liquid containing the foraminifera and lighter material ('float') was drained into a separate funnel lined with another paper filter. The float remained in the filter while liquid drained into the 400 ml glass beaker. Both the float and the sink were continuously washed with de-ionized water until all sodium polytungstate had been removed from the sample. The sediment was then washed from the filters into a plastic weigh boat, which was placed into an oven to be dried.

Each sample was split into aliquots using a microsplitter. A small portion of the sample was sprinkled evenly onto a 45-square picking tray to be viewed under a microscope. Foraminifera were picked out of the sediment using a fine (000 scale) paintbrush. The foraminifera were placed onto a 60-squared cardboard slide that had been brushed with gum tragacanth (a water soluble glue). Specimens were sorted based on their morphologies and whether or not they were alive or dead (surface samples only) at the time of collection. Live foraminifera were distinguished from the dead by the presence of cytoplasm stained pink by rose Bengal. Foraminifera identification was confirmed by comparison with type figured and unfigured specimens kept in the Smithsonian Institution's Cushman Collection. Once identification was confirmed, specimens were counted (both live and dead) and the numbers were tabulated into an Excel spreadsheet for further manipulation.

Down-core foraminiferal assemblages from two intervals representing approximately 40 and 120 years ago (based on Cs-137 and Pb-210 data, respectively) were studied in 12 cores. The lack of geochemical indicators in a few cores reduced the number of down-core samples from 24 to 21. Down-core samples were prepared as for surface samples except they were not stained with rose Bengal.

Cluster Analysis

A Q-mode cluster analysis was utilized to help recognize foraminiferal assemblages located within the Pamlico Sound region. The resulting dendrogram, based on transformed abundance data, reveals patterns of foraminiferal distribution and allows determination of biofacies (Mello and Buzas, 1968; Culver and Buzas, 1981). Approximately 300 foraminifera were picked from each surface sample (Buzas, 1990). Analyses were run using the program SYSTAT for surficial, live and dead assemblages. Rare species were excluded from the analysis. Only those taxa comprising two percent or more of the assemblage at any one station were used in the cluster analysis. The abundance data for each species at each station were transformed using the equation, $2\arcsin\sqrt{p}$ (p = abundance). The Q-mode method was used to compare the species present at each station to species present at other stations (Mello and Buzas, 1968; Davis, 1973). Q-mode analysis uses the transformed abundance data to allow stations to be compared geographically to recognize a spatial distribution. The amount of similarity between samples was measured using Euclidean distances, on a scale from zero to infinity, with zero distance being most similar. Ward's linkage method was used to

group 'objects' together based on similarities between the 'objects,' thus creating a cluster. Clusters were continuously formed until there were no remaining relationships between unclustered stations, thus forming a dendrogram (Mello and Buzas, 1968; Buzas, 1979).

Biofacies Fidelity and Constancy

Biofacies Fidelity and Constancy (Hazel, 1977) were calculated to determine which species dominate within each assemblage (biofacies). Constancy (C) refers to how often the species occurs in an assemblage. Biofacies fidelity (BF) is calculated by dividing the constancy of the species by the total sum for all constancies.

$$\text{Constancy (C)} = \frac{\text{Occurrence}}{\text{Total number of stations in cluster}} \times 10 \qquad \text{(Eq. 3)}$$

$$\text{Biofacies Fidelity (BF)} = \frac{C}{\Sigma \text{ for all C}} \times 10 \qquad \text{(Eq. 4)}$$

BF and C are expressed on a scale between zero and ten. If a species scores high for both C and BF, then that species can be considered a characteristic for a particular biofacies (Hazel, 1977).

Discriminant Analysis

Multivariate discriminant (canonical variate) analysis was used to test the hypothesis that the (*a priori*) groups defined by the cluster analysis are distinguishable statistically. The analysis, based on the amount of variability and similarity between groups (Davis, 1973; Buzas, 1979; Hayek and Buzas, 1997), determines which species

contribute most to the discrimination between the *a priori* groups, thus providing a way to check the biofacies fidelity results. The analysis uses transformed abundance data for the calculation. A discriminant analysis was run for the surficial groups defined by the cluster analysis. A second discriminant analysis was run on the same data with subsurface (down-core) samples included as 'unknowns'. The program classifies each 'unknown' into the most similar *a priori* group. SPSS (Statistical Package for the Social Sciences) version 12 was used to run the analyses.

Species Diversity

Benthic foraminiferal species diversity varies spatially. In general, the number of species increases with decreasing latitudes (Hayek and Buzas, 1997) and with increasing depth across a continental margin (Buzas and Gibson, 1969). Species diversity is defined as the relationship between the number of species and number of specimens within an assemblage (Murray, 1973).

There are a number of ways to determine species diversity. One simple way is the calculation of the Fisher alpha (α) index:

$$\frac{N}{S} = \frac{e^{\frac{S}{\alpha}} - 1}{\frac{S}{\alpha}} \qquad \text{(Eq. 5)}$$

Where 'N' is the number of observations and 'S' is the number of species. Graphs and charts have been constructed for easier determination of α, which is based on N and S (Murray, 1973; Hayek and Buzas, 1997).

Geochemical Analysis

Carbon and Nitrogen

Once collected from the push cores, samples for stable carbon and nitrogen isotopes and C:N were placed in vials, and stored in an ice cooler, which was later transferred to a freezer. In the lab, the sediment was dried in an oven at 60°C. Any shell material and organics (i.e., root fragments) were removed to avoid interference with the true isotopic signature of the sediment. The sediment was then ground into a fine powder using a mortar and pestle.

Initial percent organic matter present within each sample was determined by the loss on ignition (LOI) method. Ground sediment (approximately 1-2 grams) was placed into pre-weighed porcelain crucibles and placed into a desiccator overnight to remove any moisture. The samples were weighed and placed into a muffle furnace set at 450°C for four hours. Samples were then placed back into the desiccator to cool. Once cooled, the samples were reweighed. The difference between the sample weights before and after the furnace was determined to be the percent of organic matter.

Stable isotopic analysis requires approximately 800-1200 mg of organic carbon. Assuming that total organic matter (measured by loss on ignition) contains 40% organic carbon, the range of sediment for analysis can be calculated by:

$$\text{Minimum sediment (g)} = \frac{8.0 \times 10^{-6} \text{ g of organic carbon}}{\text{LOI}(0.40)} \qquad \text{(Eq. 6)}$$

$$\text{Maximum sediment (g)} = \frac{1.2 \times 10^{-6} \text{ g of organic carbon}}{\text{LOI}(0.40)} \qquad \text{(Eq. 7)}$$

The calculated amount of sediment was then weighed out into silver capsules and placed into a micro titre plate. Any inorganic carbon present within the sample can interfere with the isotopic signature of organic carbon. To ensure that all inorganic carbon was removed, the samples were fumigated with acid. Each sample was wetted with 50 µl of de-ionized water and placed in a desiccator for four to six hours with 100 ml of 12 M hydrochloric acid (HCL). Harris et al. (2001) demonstrated how this fumigation process removes the inorganic carbon without affecting the stable organic carbon and nitrogen values. Once the fumigation process was complete, the samples were dried in an oven at 60°C, and shipped to the University of California Stable Isotope Laboratory.

Samples were analyzed on a Europa 20-20 continuous flow isotope ratio mass spectrometer followed by combustion at 1000°C in a Europa ANCA-GSL CN analyzer to determine total nitrogen and carbon, as well as nitrogen and carbon signatures. The isotopic signatures are relative to atmospheric N_2 and to Vienna-Pee Dee Belemnite (Harris et al., 2001).

Radionuclides

The approximate age of the sediment was calculated by evaluating ^{210}Pb and ^{137}Cs activity levels down-core. The total amount of ^{210}Pb contained within the sediments down-core was determined using an alpha spectrometer following an acid leach technique. ^{210}Pb can be quantified indirectly using its daughter isotope ^{210}Po, and assuming secular equilibrium decay of ^{210}Pb and ^{210}Po, ^{210}Pb activities can be determined by counting the alpha decay of ^{210}Po (Ravichandran et al., 1995). To analyze the

sediments for ^{210}Po, 15 ml of 8 M nitric acid (HNO_3) and 1 ml of ^{209}Po (used as a yield determinant) was added to approximately one gram of dry sediment and digested using a high-pressure microwave digestion technique. Samples are digested at a constant pressure of 75psi for approximately 50 minutes. Samples typically reach a temperature of approximately 150ºC for 40 minutes during digestion. Once digestion was complete, the sample was then centrifuged three times and washed with 8 M HNO_3 twice. The solution was poured into a Teflon beaker and placed onto a hot plate. Hydrogen peroxide (H_2O_2) was added to the solution to help remove any residual organics. The samples were evaporated until approximately 10 ml of solution remained. Ammonium hydroxide was added until the solution reached a pH of 8, precipitating FeO(OH). The samples were then centrifuged three more times and rinsed with de-ionized water into Teflon beakers. Nickel disks, resting on magnetic Teflon stir bars, were placed in the Teflon beakers with the solution. The beakers were left on a magnetic spinning plate for 24-48 hours to allow the Po to spontaneously plate onto the disks. Ascorbic acid was added to each beaker to avoid any reaction between the Fe^{3+} in solution with the nickel disks (Ravichandran et al., 1995; Lewis et al., 2002).

Activity levels (dpm/g) of the ^{209}Po were graphed against depth (cm) to determine the depth at which excess ^{210}Pb activity (supported minus unsupported) was absent (dead), which represents approximately 120 years before present. The supported activity levels for each core were determined by averaging the tight-ranged, low-level ^{210}Pb activities found towards the bottom of the core (Lewis et al., 2002). The supported activity is the result of the natural decay process of ^{222}Rn within the sediments, and does

not represent the constant amount of ^{210}Pb deposition from the atmosphere (Appleby and Oldfield, 1992). This process determined which down-core interval (representing approximately 120 years ago) was analyzed for foraminifera.

Cesium-137 activities were determined by gamma emission using a low-background, high resolution Germanium detector. Samples were dried in an oven (set at 60°C) and crushed into a fine powder using a mortar and pestle. The sediment samples were packed into plastic vials or aluminum tins and counted for at least 24 hours. The ^{137}Cs activity was measured using the 661 keV peak. The measured activities (dpm/g) were plotted against depth (cm). The observed peak in ^{137}Cs was assumed to represent the early 1960s, when atmospheric nuclear testing reached a maximum (Jeter, 2000). This age determinant marked which down-core interval (representing approximately 40 years ago) was analyzed for foraminifera.

One-way Analysis of Variance (ANOVA)

The ANOVA statistical analyses were conducted using SPSS version 12.0. The one-way ANOVA with contrasts was used to show if there are significant differences in the means between the three time frame/intervals (~120 yrs BP, ~40 yrs BP, and modern) for the stable isotopes and ratios. An explanation of the program and mathematical computation for the analysis can be found in the tutorial section of the program.

RESULTS

Foraminifera

Cluster Analysis: Live Foraminifera

Twenty-one species were found living (rose Bengal stained) at the surface (0-1cm) at the time of collection. The number of live foraminifera found per site is shown in Figure 11 and Appendix B. The cluster analyses using only live foraminifera recognized five groups (Figure 11). However, two of these groups (A and C) were distinguished based on the presence of only one species (*Elphidium excavatum* and *Ammonina parkinsoniana*, respectively) (Figure 12). The cluster analysis using only live foraminifera did not result in any meaningful faunal patterns, probably because of the generally low number of specimens per sample (Figure 11). In addition, the clustering technique may force samples into groups when they contains very different kinds of species. For example, the analysis grouped sites located at marshes, comprised of *Siphotrochammina lobata, Tiphotrocha comprimata,* and *Trochammina inflata*, with sites located at inlets, comprised of *Quinqueloculina jugosa, Quinqueloculina seminula,* and *Elphidium mexicanum,* and did not create a clear distinction between any sub-environments within the Sound. The analysis also excluded six sites (S2, S9, S12, S23, S35, and EB02S1) because live foraminifera were not present. An analysis only using live foraminifera only reflects environmental conditions (i.e., temperature and salinity) at the time of collection. These conditions change on a seasonal basis and often on a day-to-day basis in Pamlico Sound.

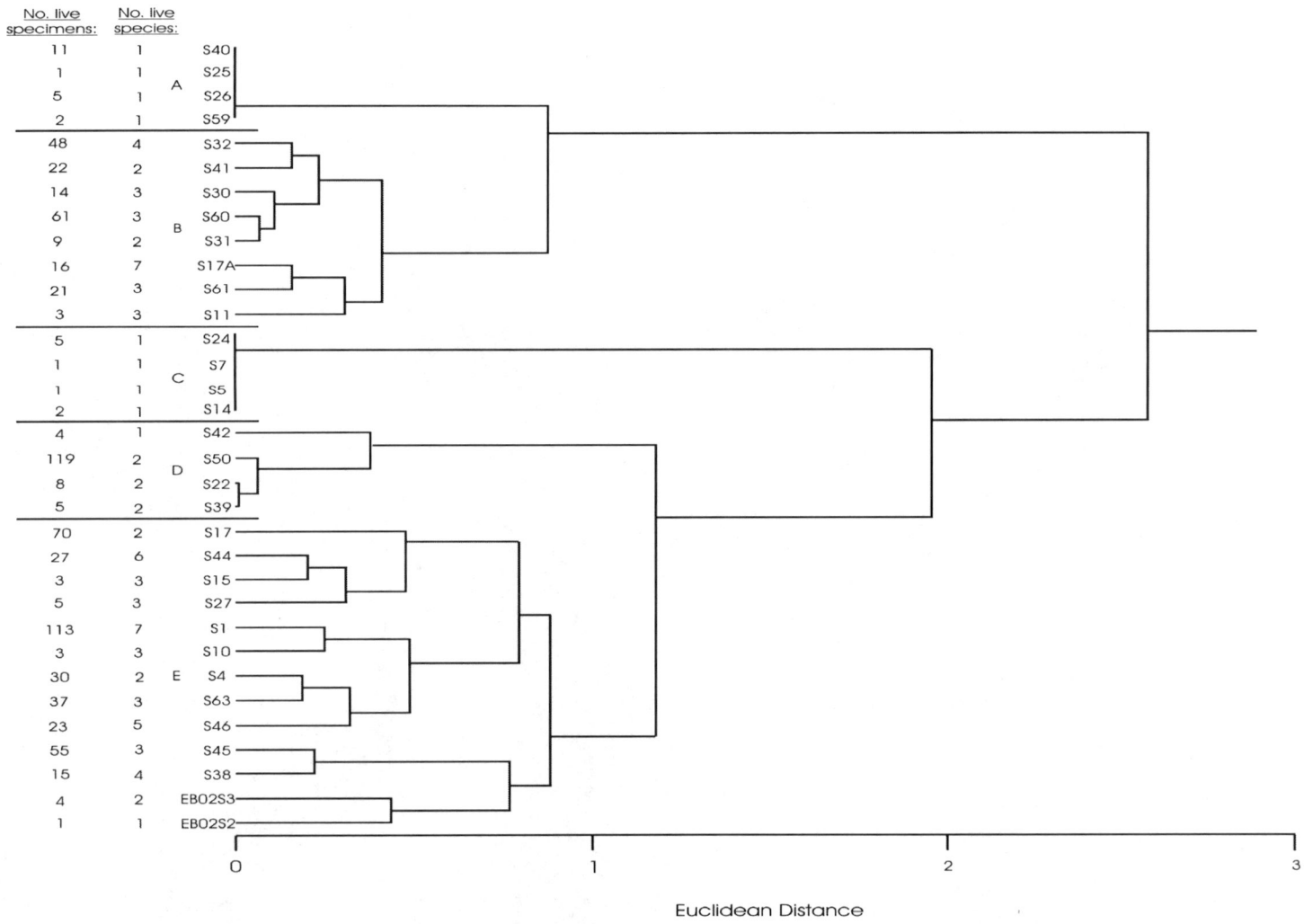

Figure 11: Cluster analysis of surface sites using live foraminifera. Dendrogram resulting from using transformed abundance data of all live species. Biofacies are labeled A-E.

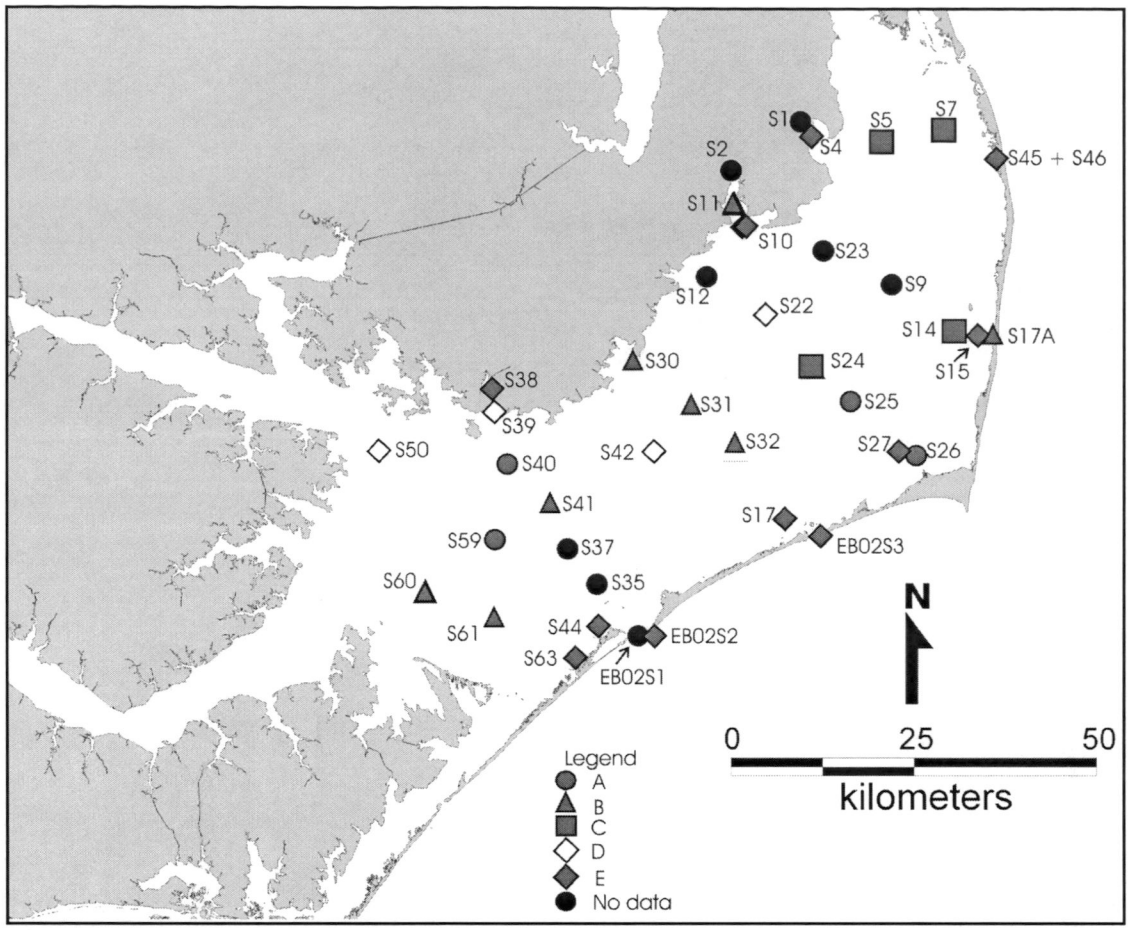

Figure 12: Spatial distribution plot of the results of the cluster analysis using only live species. The plot is based on the clusters indicated in Figure 11.

Some researchers (Scott and Medioli, 1980) argue that studying just the live foraminiferal populations is of limited use. Benthic foraminifera living in shallow water do not have a long life span. The typical reproductive cycle of foraminifera within Pamlico Sound may last several days to a year. The duration is dependant upon the species and the environmental conditions, including season (Boltovoskoy and Wright, 1976). At any one time, a collection will have a greater number of dead specimens versus live specimens. Analysis of the total population (live + dead foraminifera) integrates the small seasonal and spatial variation that is often not seen when analyzing just the live population. The

total assemblage gives a better representation of the environmental conditions that exist in any one region (Scott and Medioli, 1980).

Cluster Analysis: Dead Foraminifera

Forty-four species were found in the surface (0-1 cm) sediment of Pamlico Sound (Appendices A and B). Several cluster analyses were run using the dead foraminiferal surface data; one including all species and others using only the dominant species (abundance greater than 2% or 5%) thus eliminating the rare species. In general, all of the analyses displayed similar patterns. However, rare species are not reliable indicators of foraminiferal patterns (Koch, 1987). Therefore, the results of only one analysis is presented, that utilizing only those dead species comprising two percent or more of the assemblage (based on abundance data (Appendix C)) at any one station. The data were entered into the cluster analysis program as transformed relative abundance data (Appendix D). The resulting dendrogram divided the stations into three main clusters. A nested set of four samples within group three are geographically distinct from other samples in that group (Figure 13). Hence, they are treated as a distinct group. The group names were determined based on species present within each group and location of the site within the Pamlico Sound. These groups are: (1) Estuarine Biofacies A, (2) Marsh Biofacies, (3) Estuarine Biofacies B, and (4) Marine Biofacies (Figure 13).

Estuarine Biofacies A contains 16 samples and is dominated by the agglutinated species *Ammotium salsum* (approximately 83%). Approximately ten percent of the assemblage was comprised of calcareous foraminifera; *Ammonia parkinsoniana* (6%),

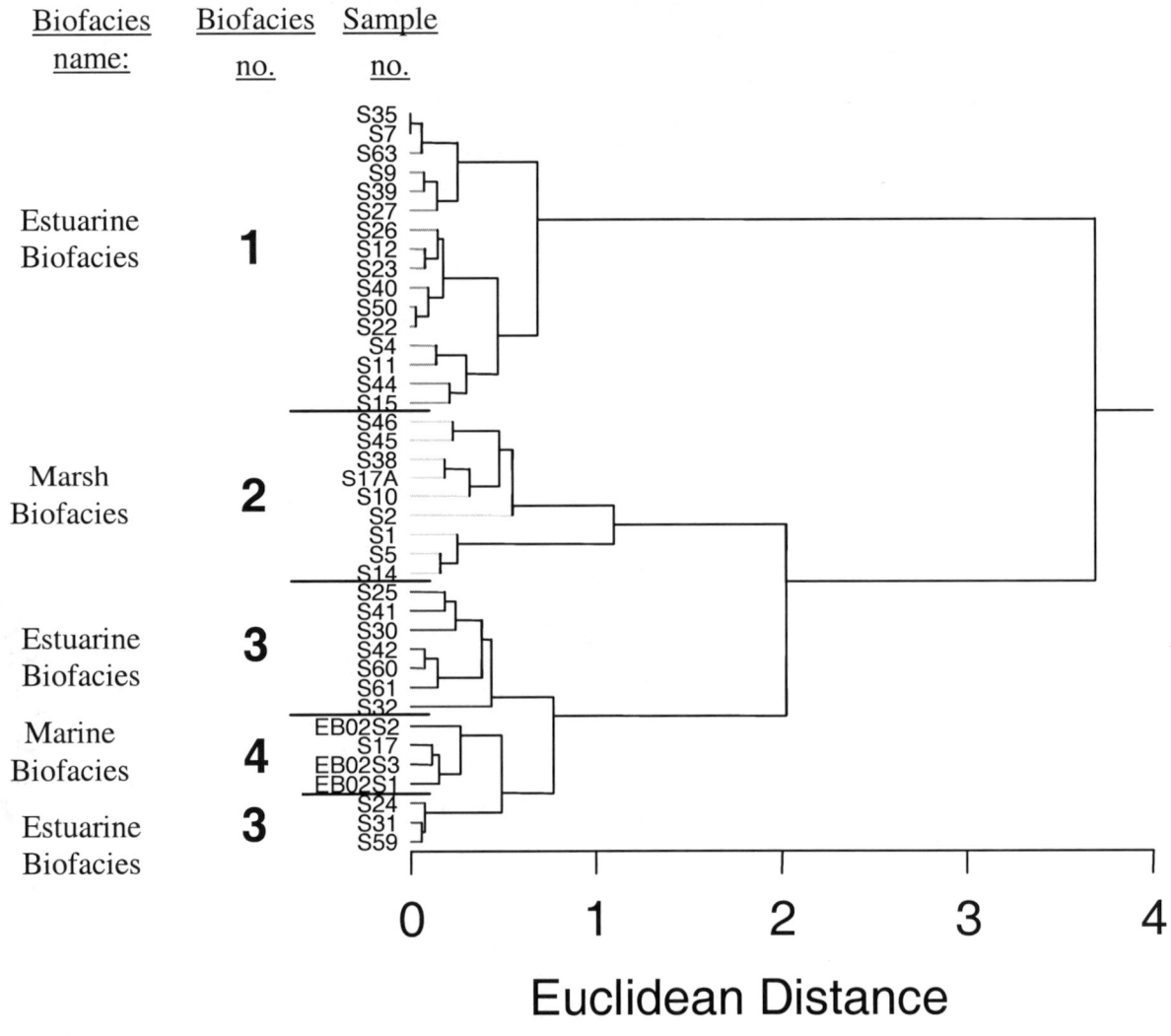

Figure 13: Cluster analysis of surface sites. Dendrogram resulting from cluster analysis of transformed abundance data of those species comprising of 2% or more of the assemblage in any one sample.

and *Elphidium excavatum* (4%). When plotted spatially, Estuarine Biofacies A is located along the margins and in the north-central basin of Pamlico Sound (Figure 14).

The Marsh Biofacies (9 samples) is dominated by *Ammonia parkinsoniana* (33%), followed by *Ammotium salsum* (13%). This biofacies is distinguished from the others by the presence of typical finely agglutinated marsh foraminifera (e.g., *Trochammina inflata* and *Haplophragmoides wilberti*). Many of the species present in this group are not found in any of the other biofacies. The nine stations assigned to this group are generally found close to shores of the sound (Figure 14), with two exceptions (S5 and S14).

Estuarine Biofacies B is comprised of ten samples. Approximately 77% of the assemblage is comprised of calcareous foraminifera. *Elphidium excavatum* (65%), *Ammotium salsum* (15%), and *Ammonia parkinisoniana* (12%), are the dominant species. Estuarine Biofacies B, with the exception of station S30, is located in the south and the central sections of Pamlico Sound (Figure 14).

The four stations comprising the Marine Biofacies are located at Ocracoke and Hatteras Inlets (Figure 14), and are composed completely of calcareous foraminifera; *Elphidium excavatum* (70%) is the dominant species. Many of the species (*Cibicides lobatulus, Cibicides refulgens, Elphidium subarticum, Quiniqueloculina lamarckiana,* and *Quiniqueloculina seminula*) found within this assemblage are not found in any of the other assemblages and are typical open shelf species (Schnitker, 1971; Workman, 1981).

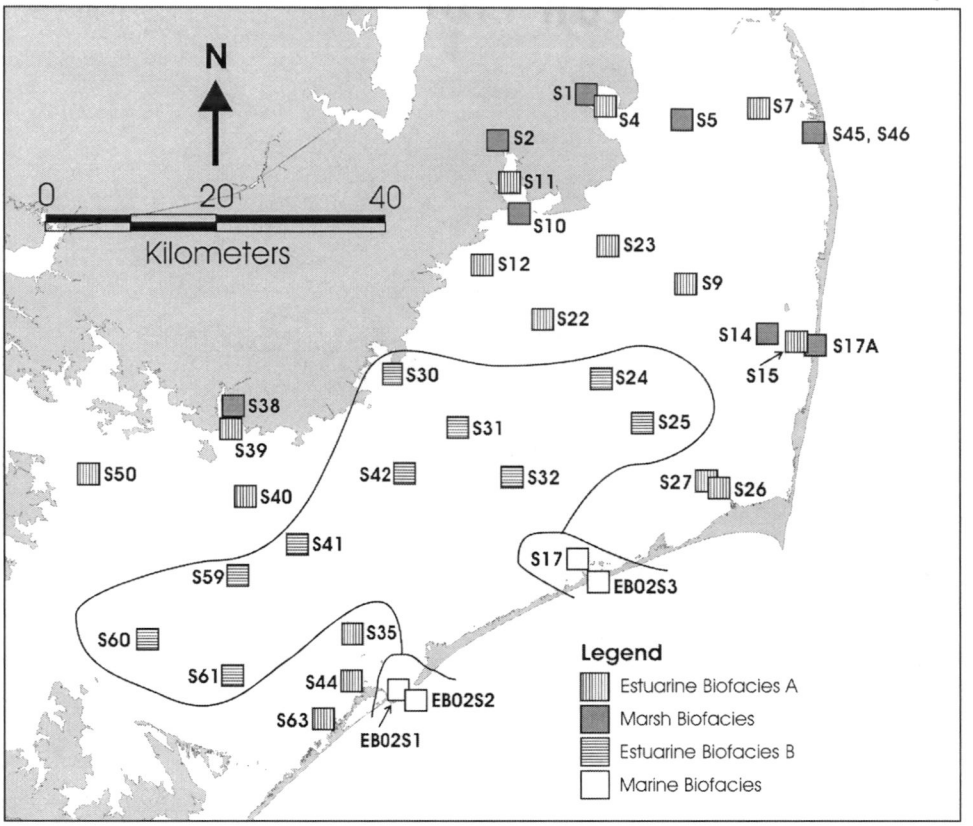

Figure 14: Spatial distribution plot of the results of the cluster analysis of dead foraminifera. The plot is based on the clusters indicated in Figure 13.

Biofacies Fidelity and Constancy

In order to determine which taxa were most important in distinguishing biofacies, Biofacies Fidelity and Constancy (Hazel, 1977) were calculated for those dead taxa comprising two percent or more of the assemblage at any one station (Appendix C). A species was considered to be characteristic for the assemblage if it received a score of six or greater for both Constancy (C) and Biofacies Fidelity (BF). No species are characteristic for Estuarine Biofacies A (Table 2). However, *Ammobaculites dilatatus, Ammobaculites exiguus,* and *Textularia earlandi*, although occurring rarely (Table 1), are

present only in this assemblage. *Ammotium salsum* occurs at every station within this assemblage, but it has a BF of only four. Coarsely agglutinated foraminifera dominate Estuarine Biofacies A in comparison to other assemblages.

Haplophragmoides wilberti, Miliammina fusca, Tiphotrocha comprimata, and Trochammina inflata are characteristic of the Marsh Biofacies (Table 2). *Ammoasuta inepta* and *Haplophragmoides bonplandi* are restricted to this assemblage, but they occur at few stations (Table 2). In general, the foraminifera of this assemblage are finely agglutinated.

Estuarine Biofacies B, like Estuarine Biofacies A, does not contain characteristic species (C and BF values > 6) (Table 2). However, *Ammotium salsum* and *Elphidium excavatum* occur at all ten stations within the assemblage but they have a low BF value. *Elphidium* cf. *E. mexicanum* is restricted to this assemblage but it occurs only at one station. Estuarine Biofacies B is distinguished from Estuarine Biofacies A by a greater proportion of calcareous foraminifera (averages of 77% and 10% respectively).

Six species are considered to be characteristic of the Marine Biofacies; *Cibicides lobatulus, Elphidium galvestonense, Elphidium mexicanum, Elphidium subarcticum, Hanzawaia strattoni,* and *Quinqueloculina seminula* (Table 2). Three additional species, *Cibicides refulgens, Quinqueloculina lamarckiana,* and *Quinqueloculina* sp. C, are only found in this assemblage but do not occur in as many samples as the six characteristic species.

Table 2: Biofacies Fidelity and Constancy for the four biofacies, using dead species comprising 2% or more of the assemblage in any one sample. O = Occurrence, C = Constancy, and BF = Biofacies Fidelity (see equations (1) and (2) in Methods section). Boxed values indicate characteristic species, defined arbitrarily or those species with values of >6 for C and BF.

	Estuarine Biofacies A			Marsh Biofacies			Estuarine Biofacies B			Marine Biofacies		
Species:	**O**	**C**	**BF**	**O**	**C**	**BF**	**O**	**C**	**BF**	**O**	**C**	**BF**
Ammoastuta inepta	0	0	0	2	2	10	0	0	0	0	0	0
Ammonia parkinsoniana	6	4	1	6	7	2	9	9	3	4	10	3
Ammonia tepida	1	1	1	1	1	2	1	1	2	1	3	5
Ammotium salsum	16	10	4	7	8	3	10	10	4	0	0	0
Arenoparrella mexicana	3	2	3	4	4	6	1	1	1	0	0	0
Asterigerina carinata	0	0	0	0	0	0	1	1	2	2	5	8
Ammobaculites crassus	5	3	4	3	3	4	1	1	1	0	0	0
Ammobaculites dilatatus	1	1	10	0	0	0	0	0	0	0	0	0
Ammobaculites exiguus	3	2	10	0	0	0	0	0	0	0	0	0
Cibicides lobatulus	0	0	0	0	0	0	0	0	0	3	8	10
Cibicides refulgens	0	0	0	0	0	0	0	0	0	1	3	10
Elphidium excavatum	11	7	2	5	6	2	10	10	3	4	10	3
Elphidium galvestonense	1	1	1	1	1	1	0	0	0	3	8	8
Elphidium mexicanum	0	0	0	0	0	0	0	0	0	4	10	10
Elphidium c.f. *E. mexicanum*	0	0	0	0	0	0	1	1	10	0	0	0
Elphidium subarcticum	0	0	0	0	0	0	0	0	0	3	8	10
Hanzawaia strattoni	0	0	0	0	0	0	1	1	1	4	10	9
Haplophragmoides bonplandi	0	0	0	2	2	10	0	0	0	0	0	0
Haplophragmoides wilberti	5	3	3	5	6	6	1	1	1	0	0	0
Jadammina macrescens	1	1	1	4	4	7	1	1	2	0	0	0
Miliammina fusca	3	2	2	6	7	6	2	2	2	0	0	0
Quinqueloculina lamarckiana	0	0	0	0	0	0	0	0	0	2	5	10
Quinqueloculina seminula	0	0	0	0	0	0	0	0	0	3	8	10
Quinqueloculina sp C	0	0	0	0	0	0	0	0	0	1	3	10
Siphotrochammina lobata	1	1	1	4	4	9	0	0	0	0	0	0
Textularia earlandi	4	3	10	0	0	0	0	0	0	0	0	0
Tiphotrocha comprimata	2	1	1	6	7	7	1	1	1	0	0	0
Trochammina inflata	4	3	2	6	7	6	2	2	2	0	0	0
Indeterminate agglutinated	0	0	0	1	1	10	0	0	0	0	0	0
Indeterminate calcareous	0	0	0	0	0	0	3	3	5	1	3	5
Organic lining	3	2	3	4	4	6	1	1	1	0	0	0

Discriminant Analysis

Surficial discriminant analysis. The cluster analysis of dead foraminifera in surface (0-1cm) samples distinguished four biofacies. Discriminant analysis was used to test the hypothesis that these four *a priori* biofacies were statistically distinguishable. All taxa representing two percent or more of the assemblage were included in the analysis; indeterminate agglutinated, and organic linings were excluded. Therefore, there were 28 species (number of variables, P = 28), and 39 sites (observations, N = 39). S37 was barren of foraminifera. Four groups (h) were analyzed, and since P is greater than h, a total of three canonical variates were possible (h -1 = 3).

The first two eigenvalues account for 99.6 percent of the variance between the four *a priori* groups (Table 3). The canonical discriminant scores for the group means (group centroids) can be found on Table 4. Since the fourth group (Marine Biofacies) proved to be so different from the other three groups (Table 4), the analysis was re-run excluding those samples belonging to the fourth group.

In this second analysis, where P = 28, N = 39, and h = 3, because P>h, there are h–1 =2 canonical variates. The first eigenvalue accounts for 84 percent of the variance between the three *a priori* groups (Estuarine Biofacies A, Marsh Biofacies, and Estuarine Biofacies B) (Table 5), and discriminates the Marsh Biofacies from Estuarine Biofacies A and B. The second axis (function) accounts for approximately 16 percent of the total variance between the groups (Table 5). The scores for the group centroids along the two canonical variates (functions) are given in Table 6. Table 7 indicates which species

Table 3: Canonical discriminant functions including the percent of variability for each eigenvalue. These values result from the analysis including all four *a priori* groups (Estuarine Biofacies A, Marsh Biofacies, Estuarine Biofacies B, and Marine Biofacies).

Function	Eigenvalue	% of Variance	Cumulative %
1	1437.128	97.2	97.2
2	35.012	2.4	99.6
3	6.588	0.4	100.0

Table 4: Canonical discriminant function scores for group means (group centroids) along the three canonical variate axes (functions). These values result from the analysis including all four *a priori* groups. Group number (1) Estuarine Biofacies A, (2) Marsh Biofacies, (3) Estuarine Biofacies B, and (4) Marine Biofacies.

a priori group number	Function		
	1	2	3
1	-11.415	4.663	1.952
2	-13.132	-9.756	1.004
3	-12.402	1.436	-4.007
4	106.213	-0.290	-0.051

Table 5: Canonical discriminant functions including the percent of variability for each eigenvalue. These values result from the analysis of Estuarine Biofacies A, B, and the Marsh Biofacies.

Function	Eigenvalue	% of Variance	Cumulative %
1	35.443	84.2	84.2
2	6.659	15.8	100.0

Table 6: Canonical discriminant function scores for group means (group centroids) along two canonical variate axes (functions). These values result from the analysis of Estuarine Biofacies A, B, and Marsh Biofacies. Group number (1) Estuarine Biofacies A, (2) Marsh Biofacies, and (3) Estuarine Biofacies B.

a priori group number	Function	
	1	2
1	4.481	1.859
2	-9.405	0.984
3	1.295	-3.861

(those with large positive or negative values) are most important in distinguishing between the groups. *Ammoasuta inepta, Haplophragmoides wilberti,* and *Haplophragmoides bonplandi* are responsible for the separation along function 1, which distinguishes the Marsh Biofacies from the other two biofacies (Table 6). *Trochammina inflata, Elphidium galvestonense,* and *Siphotrochammina lobata* are responsible for separation of the groups along function 2, which distinguishes Estuarine Biofacies A and B (Table 6).

The three groups are clearly distinguished from each other when plotted (Figure 15) with 95% confident circles. Therefore, the hypothesis that the three *a priori* groups, Estuarine Biofacies A, Marsh Biofacies, and Estuarine Biofacies B, are statistically different can be accepted.

Table 7: Standardized canonical discriminant function coefficients from the analysis. Foraminifera listed are the source of variability along each axis.

	Function	
	1	2
A. inepta	-9.645	-0.199
A. park	-0.082	0.214
A. tepida	4.336	0.357
A. salsum	3.480	0.538
A mex	3.911	0.079
A. car	-0.693	-0.518
A. crassus	-0.866	-0.363
A. dila	2.417	0.262
A. exiguus	2.166	0.098
E. excav	2.885	-0.812
E. galv	-1.123	-1.261
H. strattoni	-0.661	-0.290
H. bon	8.163	-0.515
H. wilberti	-6.196	1.100
J. mac	-1.920	0.233
M. fusca	4.857	0.403
S. lobata	-0.144	3.261
T. earlandi	0.660	1.123
T. comp	1.947	0.184
T. inflata	-0.781	-2.625

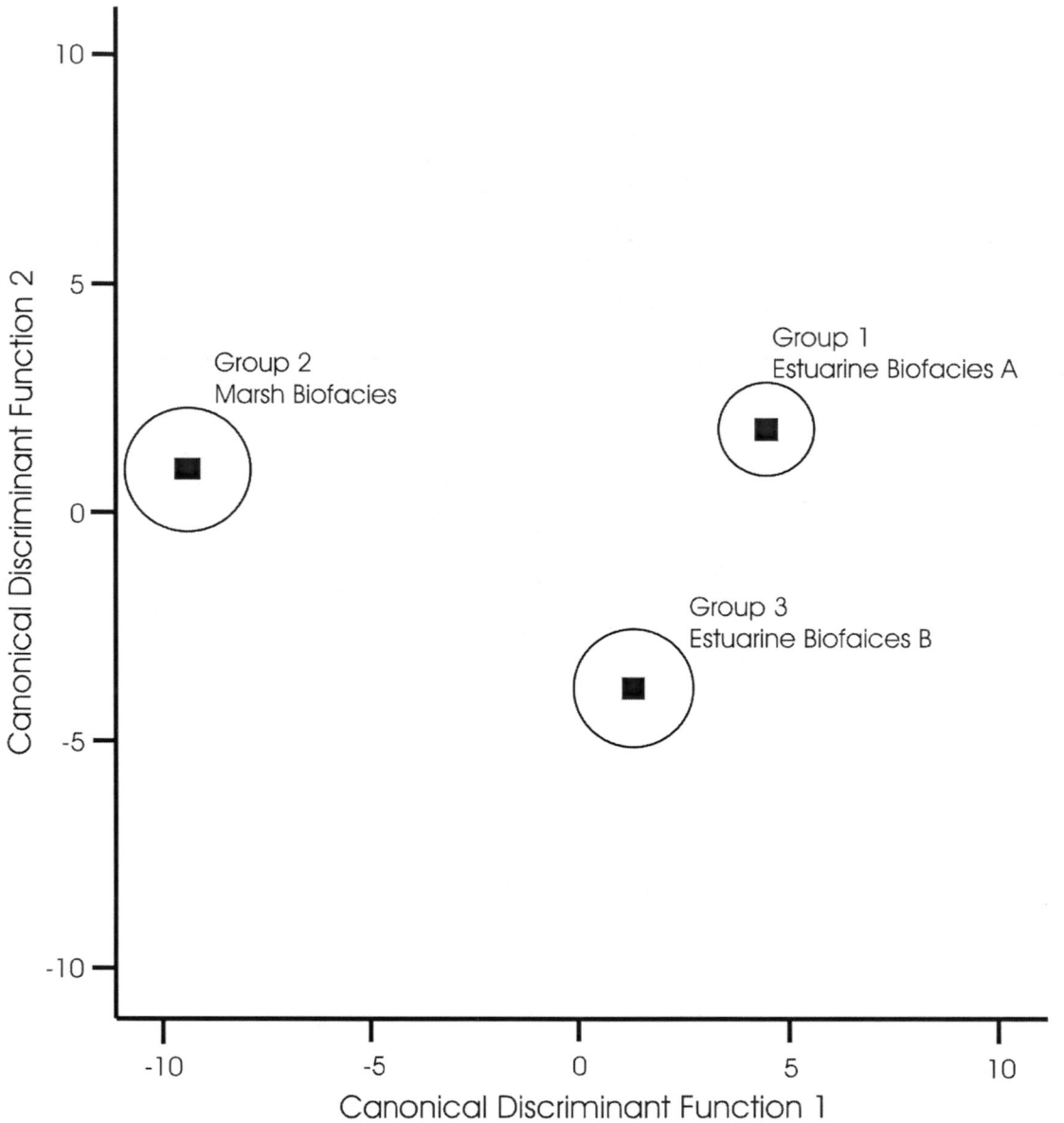

Figure 15: Plot of Canonical Discriminant Function 1 versus Canonical Discriminant Function 2. The three *a priori* groups, (1) Estuarine Biofacies A, (2) Marsh Biofacies, and (3) Estuarine Biofacies B, represented by a box (group centroids) and 95 % confidence circles, are clearly distinguished from each other.

Down-core discriminant analysis. The combined results of the cluster analysis and discriminant analysis of the surface data provide a model that was used to interpret foraminiferal assemblages down-core. Discriminant analysis was used to assign down-core samples into surface biofacies.

To determine the change in environmental conditions over the last approximate 150 years, two separated intervals, representing two separate time slices, were chosen from each core. Sediment dated using 137Cs represents approximately 40 years BP; while sediment dated using 210Pb represents approximately 120 years BP. The sediment accumulation rate for Pamlico Sound is approximately 0.5cm/yr, however, the rate varies from time to time and regionally (Tully, 2004). Therefore, the two-centimeter intervals chosen may represent period of several years (approximately 20 years).

Twenty-one taxa were found in 21 down-core samples (Appendices E, F, and G). These were included in the discriminant analysis including three biofacies (Estuarine Biofacies A, Marsh Biofacies, and Estuarine Biofacies B) described at the surface. The Marine Biofacies was excluded because none of the species restricted to this group were found down-core. Thus, it was assumed that none of the down-core samples represented an inlet assemblage. In this analysis, N (number of sites/stations) equals 60 and P (number of variables) was again 28. Therefore, since $P > h$, a total of two canonical variates is possible ($h - 1 = 2$). The down-core samples were not assigned an *a priori* group number but were treated as "unknowns" by the statistical model.

Site numbers labeled 'a' correspond to samples analyzed at the ^{137}Cs down-core interval of peak activity (early 1960's) down-core (Figure 16). The distribution pattern of

the foraminiferal assemblage (Figure 17) is similar to the surficial plot (Figure 14), with a few exceptions. The presence of marsh foraminifera at S9a changes the assemblage from the dominantly coarsely agglutinated Estuarine Biofacies A at the surface to a Marsh Biofacies down-core. At the surface, S30 is included in Estuarine Biofacies B, comprised mostly of calcareous foraminifera. Down-core, typical marsh foraminifera are present and thus sample S30a is classified as Marsh Biofacies. At S60, the environment changes

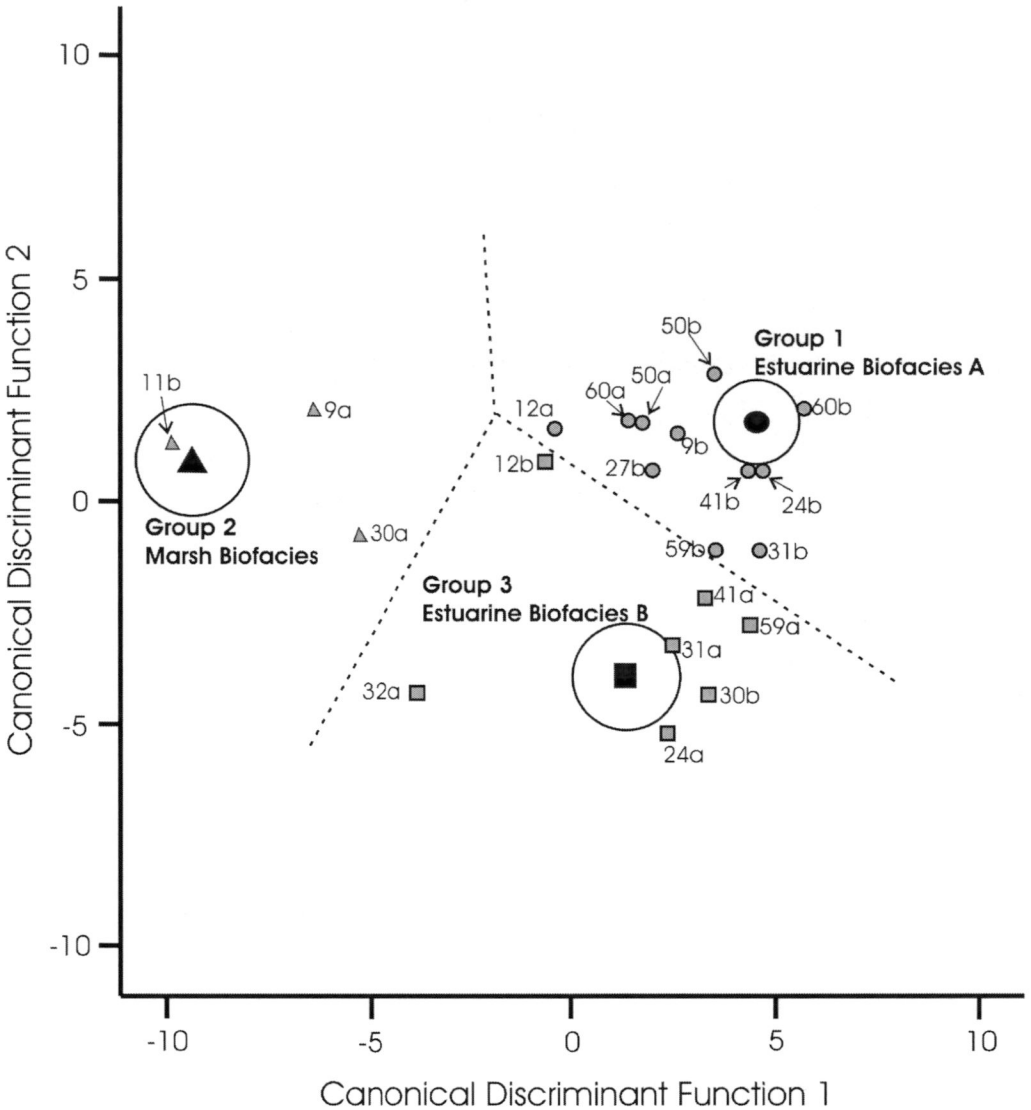

Figure 16: Plot of Canonical Discriminant Function 1 versus Canonical Discriminant Function 2 including three *a priori* groups and 21 "unknown" down-core samples; Estuarine Biofacies A, Marsh Biofacies, and Estuarine Biofacies B. 'a' denotes the ^{137}Cs peak interval samples and 'b' denotes samples from the interval where ^{210}Pb activity is absent. Shapes correspond to the biofacies that each sample was most similar to. Dashed line represents territory boundary determined by the computer program.

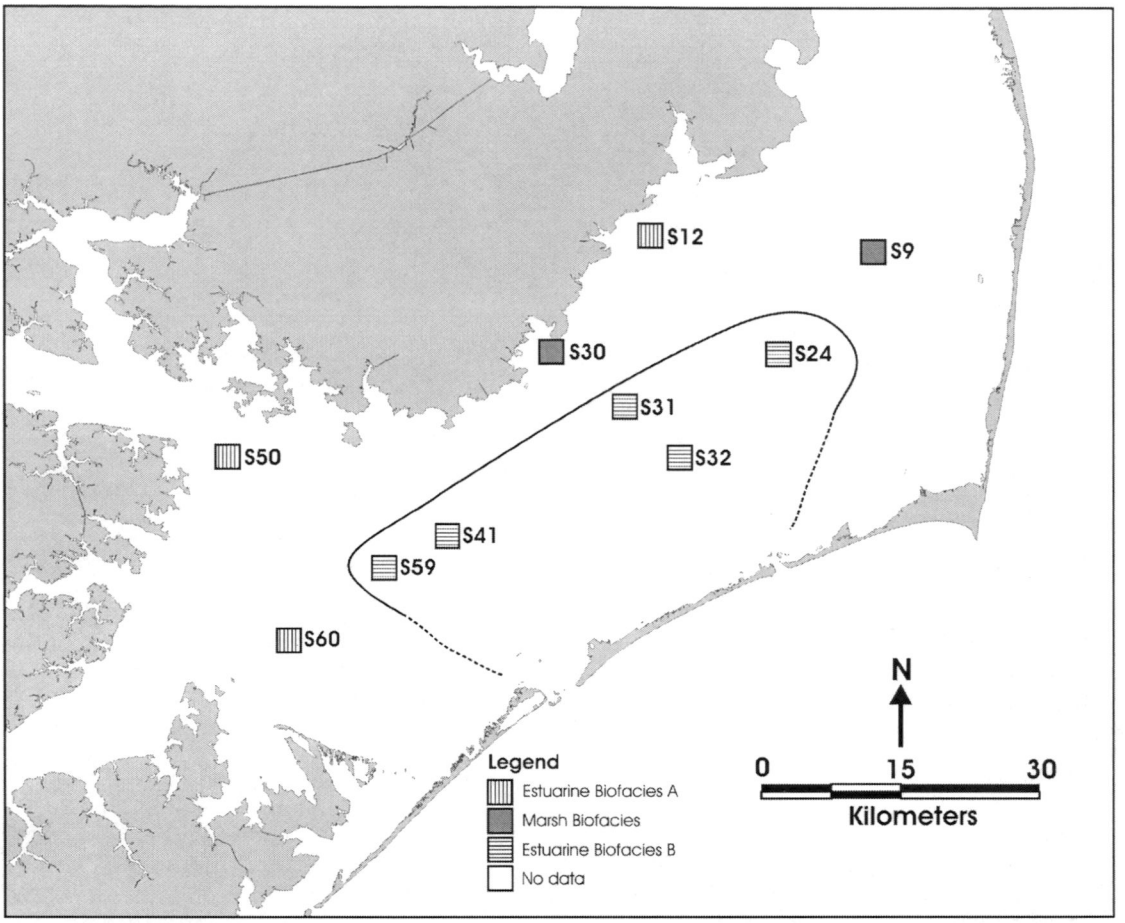

Figure 17: Spatial plot of samples indicated by 'a' in Figure 16. The sediment comprising those samples was deposited in the early 1960s, as determined by ^{137}Cs dating. The solid/dashed line represents the inferred boundary between Estuarine Biofacies A and Estuarine Biofacies B.

from Estuarine Biofacies B at the surface, to Estuarine Biofacies A down-core. This is due to the increased proportion of agglutinated foraminifera down-core. In general, during the early 1960s, the Estuarine Biofacies B (dominated by calcareous taxa) was not as widespread throughout the Pamlico Sound as it is today. Marsh foraminifera were also present further into the central sound, as seen at S9 and S30 (Figure 17). It is possible that these foraminifera were washed into these sites from another location.

Site numbers labeled 'b' correspond to down-core intervals lacking the presence of excess ^{210}Pb activity, which indicates deposition approximately 120 years before present (Figure 16). A significant change in assemblage characteristics down-core is indicated by the analysis (Figure 18). Estuarine Biofacies A dominates the Sound. Only two sites were classified with Estuarine Biofacies B (S12 and S30), and one station (S11) was classified with the Marsh Biofacies.

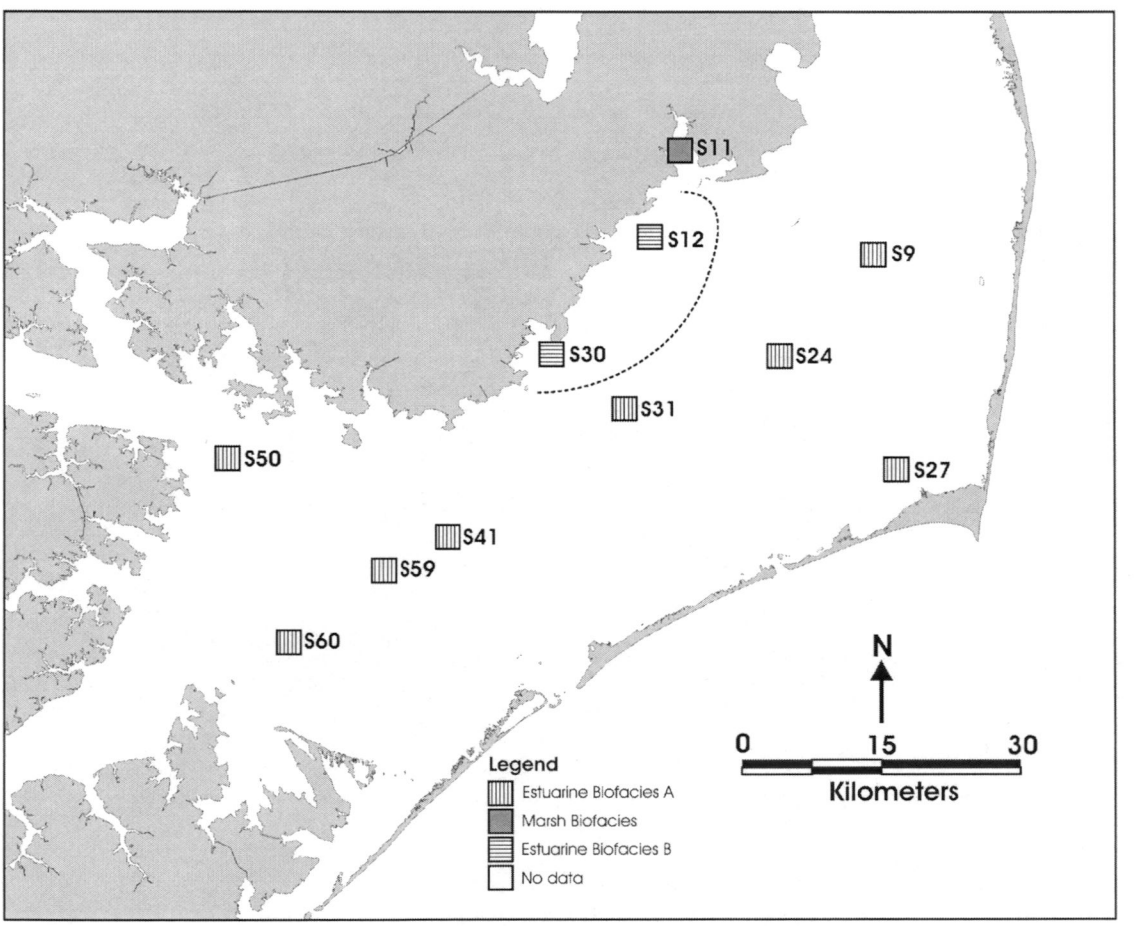

Figure 18: Spatial plot of samples indicated by 'b' in Figure 16. The sediment comprise those samples was deposited approximately 120 years before present, as determine by ^{210}Pb dating. The dashed line represents the inferred boundary between Estuarine Biofacies A and Estuarine Biofacies B.

Species Diversity

The diversity of total assemblages was analyzed using S (number of species per sample) and N (number of specimens observed) to calculate alpha (α). Alpha values can be obtained by using equation 3 (see Methods) or can be found in Appendix 4 of Hayek and Buzas (1997).

Table 8 lists the results of the diversity analysis and the plot of the α values can be found on Figure 19. Values for α within the Pamlico Sound estuarine system range from 0.455 in the sound (S59) to 4.149 at the inlets (EB02S3). The Marine Biofacies proves to be the most diverse with an average α value of 3.767, followed by the Marsh Biofacies with an average α value of 1.932 (Table 8). Estuarine Biofaces A and Estuarine Biofacies B have very similar low diversity α values of 0.999 and 0.909, respectively (Table 8).

Site	Biofacies	S	N	α
S1	Marsh Biofacies	287	10	2.008
S2		9	268	1.792
S5		5	349	0.826
S17A		16	299	3.61
S38		10	194	2.248
S45		7	220	1.378
S46		6	59	1.66
Mean		49	200	1.932
S4	Estuarine Biofacies A	5	307	0.847
S9		4	249	0.676
S11		11	286	2.263
S12		2	251	0.297
S22		5	297	0.852
S23		6	183	0.953
S27		6	232	1.127
S39		6	216	0.694
S40		4	329	0.688
S44		8	102	2.046
S50		3	317	0.458
S63		6	271	1.087
Mean		6	253	0.999
S24	Estuarine Biofacies B	3	263	0.476
S30		11	144	2.797
S31		3	282	0.469
S32		8	307	1.51
S41		4	338	0.483
S42		5	306	0.852
S59		3	332	0.455
S60		3	303	0.463
S61		4	250	0.676
Mean		5	281	0.909
S17	Marine Biofacies	16	272	3.723
EB02S1		12	111	3.43
EB02S3		15	147	4.149
Mean		14	177	3.767

Table 8: Species diversity of foraminifera within the Pamlico Sound estuarine system (S = No. of species, N = No. of specimens observed, and α = Fishers alpha index). Eight sites (S7, S10, S14, S15, S25, S26, S35, and EB02S2) contained less than 50 specimens were excluded from the analysis. The plotted α values can be found on Figure 19.

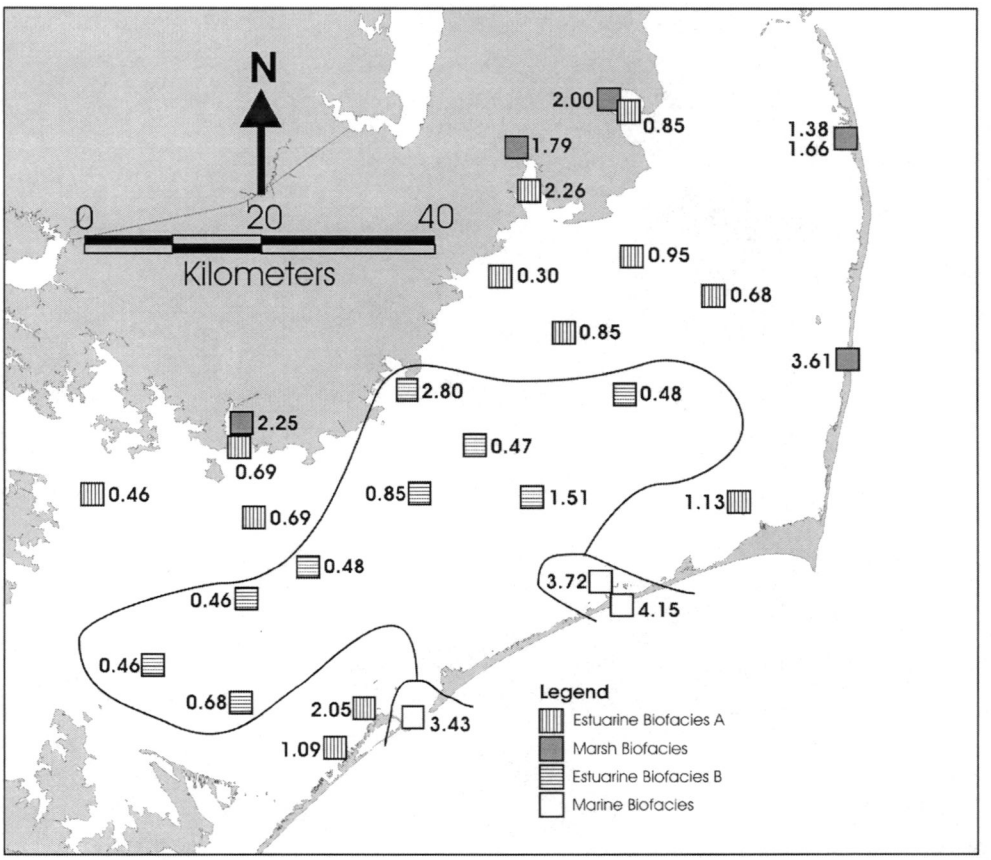

Figure 19: Species diversity distribution plot within biofacies determined using cluster analysis for the surface (0-1cm).

Geochemistry

Geochronology

Cesium-137 and ^{210}Pb data were obtained from a geochemical study (Tully, 2004), which used the same cores within Pamlico Sound. The intervals representing peak activity for ^{137}Cs (40yrs BP) and absence of ^{210}Pb activity (120yrs BP) are represented by lines found on Figures 20-36.

Stable Isotopes

Each interval in all 17 cores were analyzed at the Stable Isotope Lab Facility at UC Davis. All samples were analyzed at least once via the acid fumigation method described by Harris et al. (2001; see Methods). The results of the first set of samples that were sent to the lab had very high fluctuations in $\delta^{15}N$ values in comparison to the rest of the samples. Acid fumigation always increased the $\delta^{15}N$ signatures (approximately 0.04 to 0.11 $^{0}/_{00}$) of soils used by Harris et al. (2001), but did not have an affect on the $\delta^{13}C$ signature. However, Bratton et al. (2003), found no statistical difference between acidified and non-acidified subsurface samples collected from Chesapeake Bay. Reports from the lab also stated machine malfunction and as a result, some of the readings were a combined value of several samples. Regardless, several values from the first set of samples were questionable. Rather than disregard the questionable samples, several samples were chosen at random for re-analysis. There were two reasons for re-analysis: (1) to test whether or not acid fumigation had a significant affect on the isotopic signatures of ^{15}N, and (2) if the reported error was a direct result of machine malfunction.

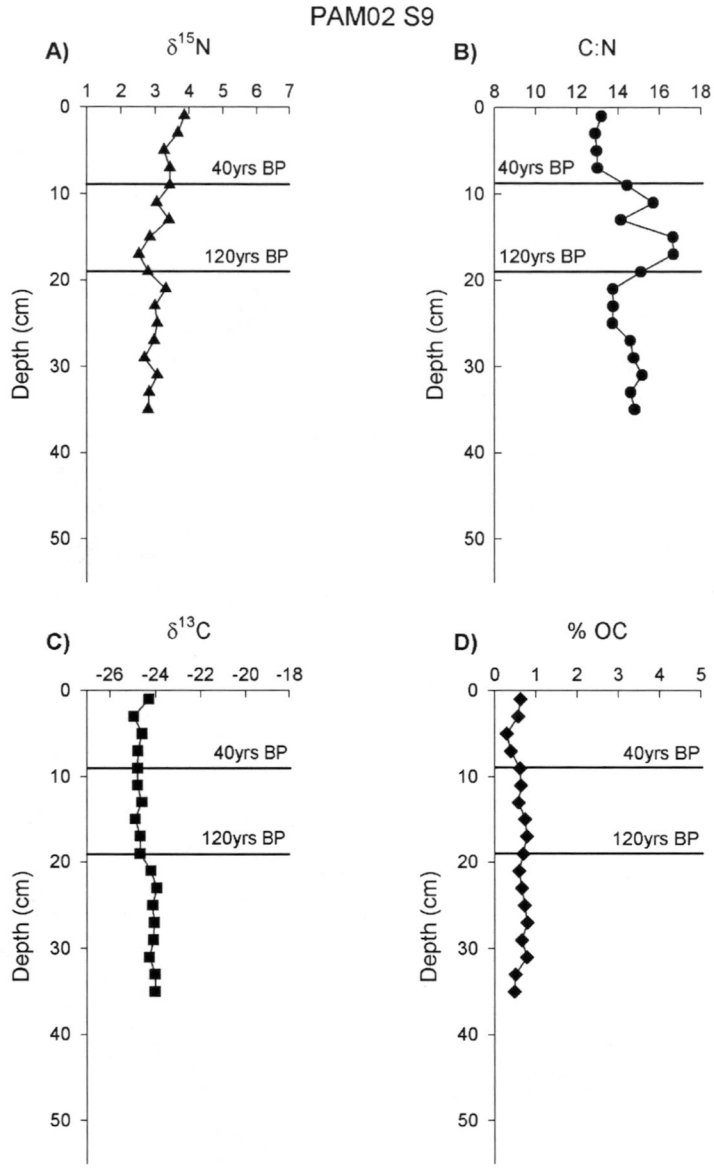

Figure 20: Geochemistry data for PAM02S9. A) $\delta^{15}N$ (‰) signatures vs depth (cm). B) C:N ratio vs depth (cm). C) $\delta^{13}C$ (‰) signatures vs depth (cm). D) Percent organic carbon vs depth (cm). The 40yrs BP line represents the ^{137}Cs peak and the 120yrs BP line represents the interval at which ^{210}Pb is considered to be inactive as determined by radionuclide data (Tully, 2004).

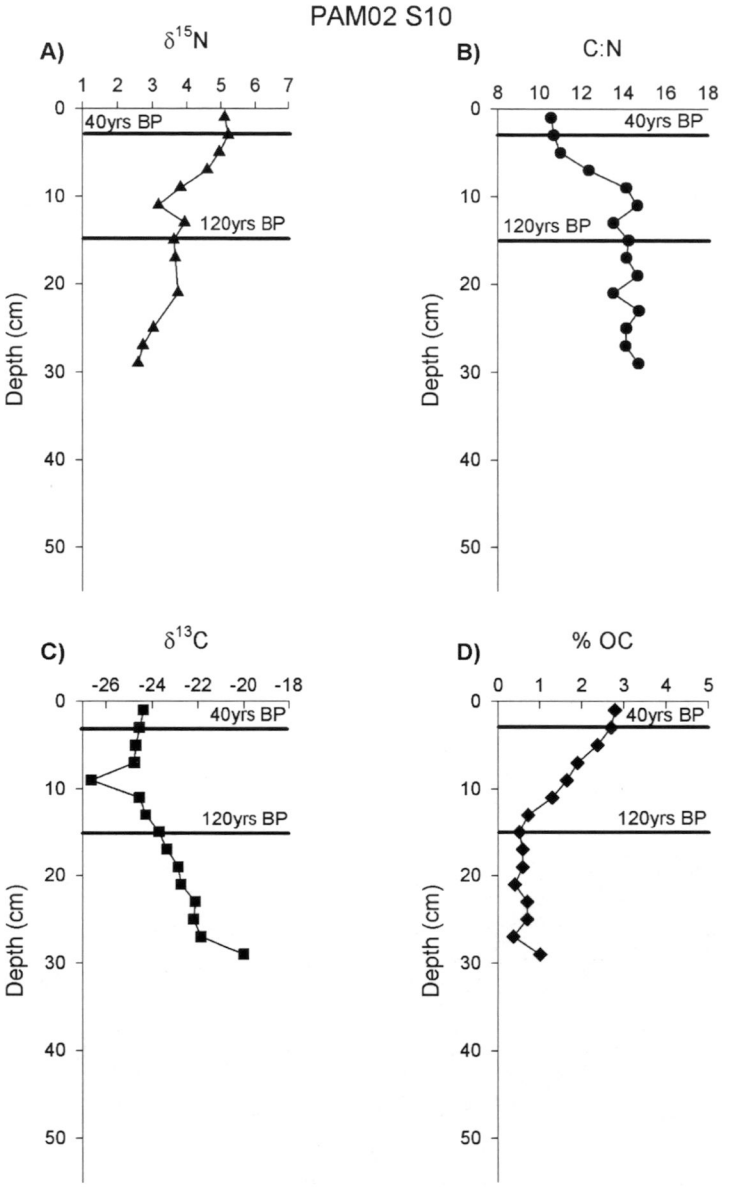

Figure 21: Geochemistry data for PAM02S10. A) $\delta^{15}N$ (‰) signatures vs depth (cm). B) C:N ratio vs depth (cm). C) $\delta^{13}C$ (‰) signatures vs depth (cm). D) Percent organic carbon vs depth (cm). The 40yrs BP line represents the ^{137}Cs peak and the 120yrs BP line represents the interval at which ^{210}Pb is considered to be inactive as determined by radionuclide data (Tully, 2004).

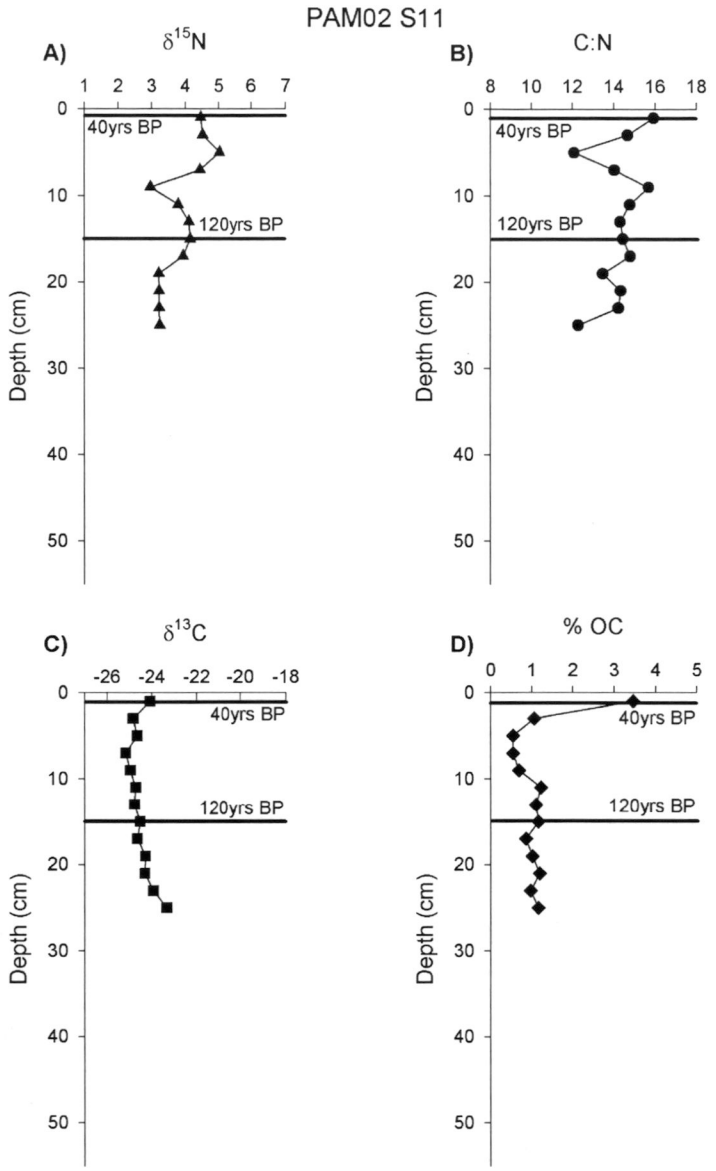

Figure 22: Geochemistry data for PAM02S11. A) δ^{15}N (‰) signatures vs depth (cm). B) C:N ratio vs depth (cm). C) δ^{13}C (‰) signatures vs depth (cm). D) Percent organic carbon vs depth (cm). The 40yrs BP line represents the ^{137}Cs peak and the 120yrs BP line represents the interval at which ^{210}Pb is considered to be inactive as determined by radionuclide data (Tully, 2004).

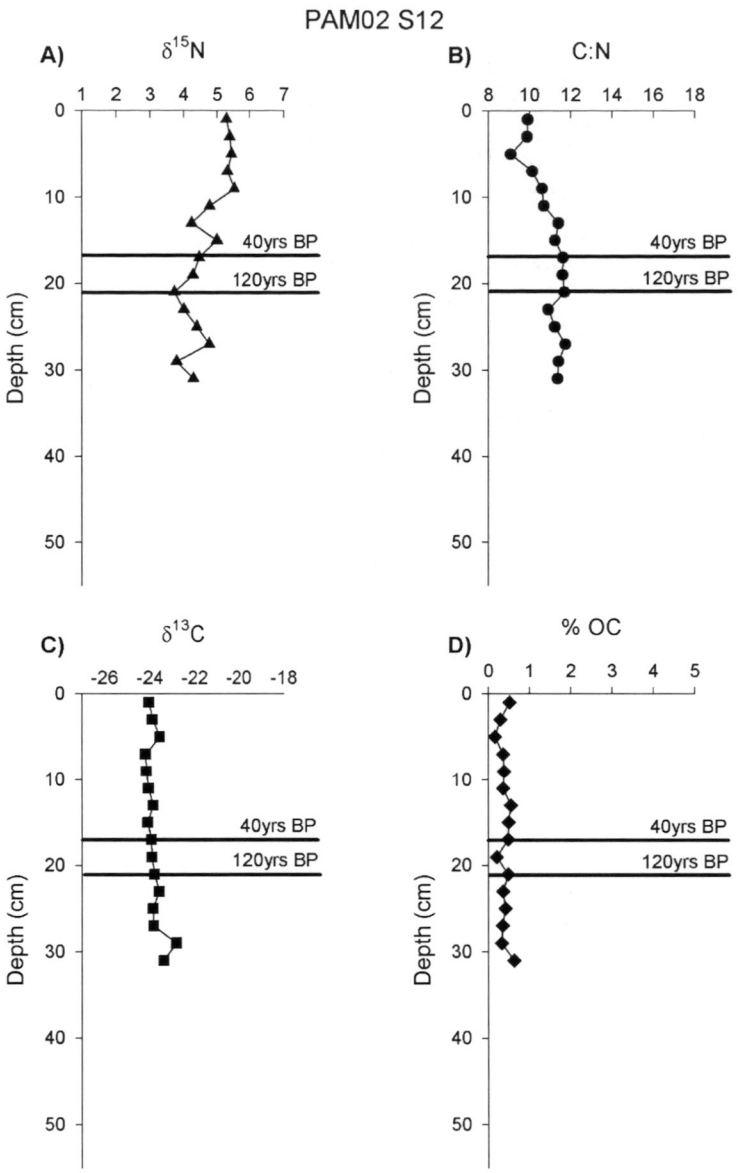

Figure 23: Geochemistry data for PAM02S12. A) $\delta^{15}N$ (‰) signatures vs depth (cm). B) C:N ratio vs depth (cm). C) $\delta^{13}C$ (‰) signatures vs depth (cm). D) Percent organic carbon vs depth (cm). The 40yrs BP line represents the ^{137}Cs peak and the 120yrs BP line represents the interval at which ^{210}Pb is considered to be inactive as determined by radionuclide data (Tully, 2004).

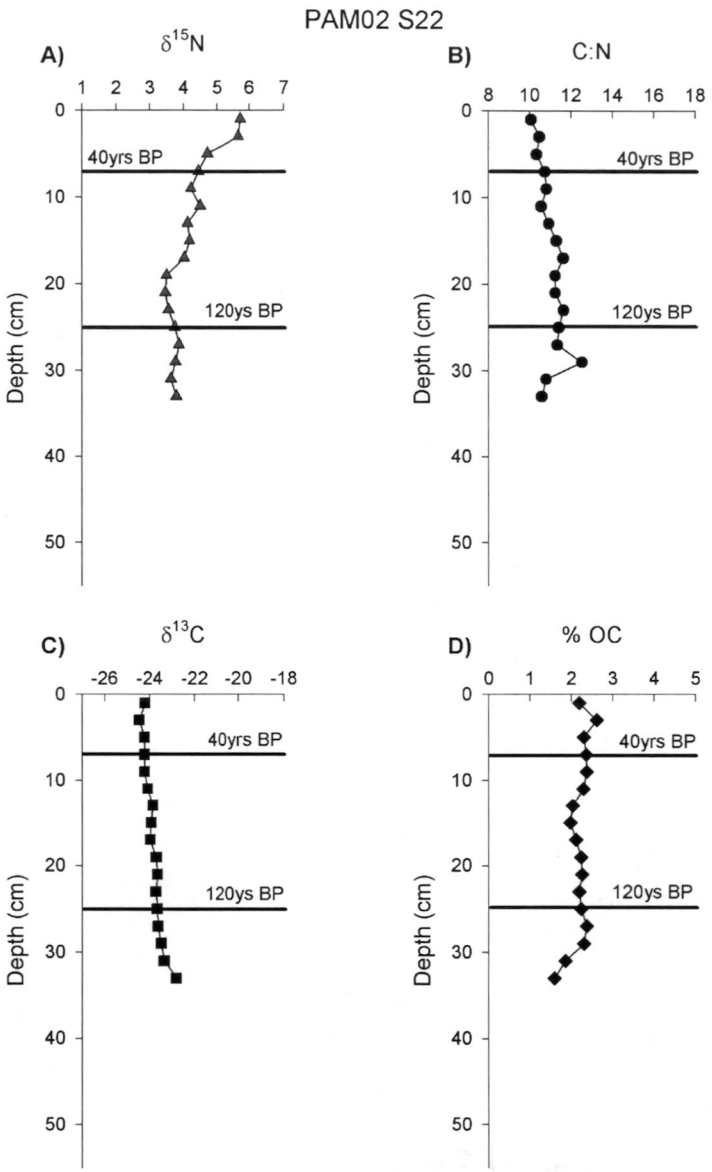

Figure 24: Geochemistry data for PAM02S22. A) δ^{15}N (‰) signatures vs depth (cm). B) C:N ratio vs depth (cm). C) δ^{13}C (‰) signatures vs depth (cm). D) Percent organic carbon vs depth (cm). The 40yrs BP line represents the ^{137}Cs peak and the 120yrs BP line represents the interval at which ^{210}Pb is considered to be inactive as determined by radionuclide data (Tully, 2004).

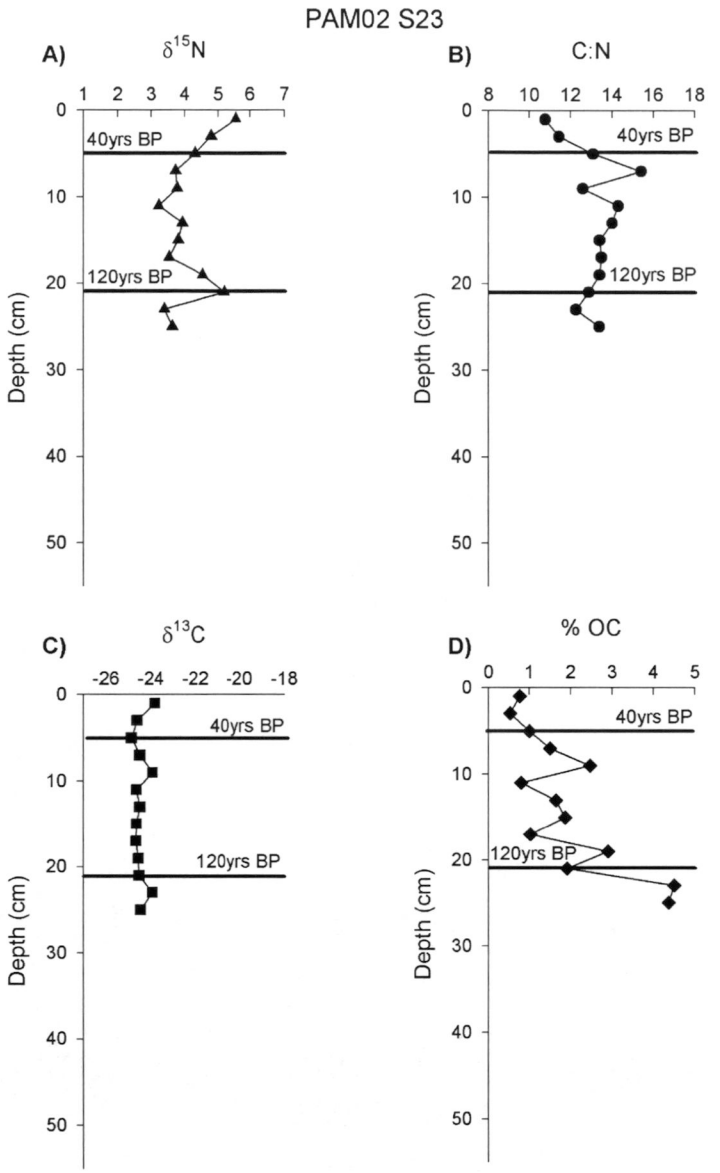

Figure 25: Geochemistry data for PAM02S23. A) $\delta^{15}N$ (‰) signatures vs depth (cm). B) C:N ratio vs depth (cm). C) $\delta^{13}C$ (‰) signatures vs depth (cm). D) Percent organic carbon vs depth (cm). The 40yrs BP line represents the ^{137}Cs peak and the 120yrs BP line represents the interval at which ^{210}Pb is considered to be inactive as determined by radionuclide data (Tully, 2004).

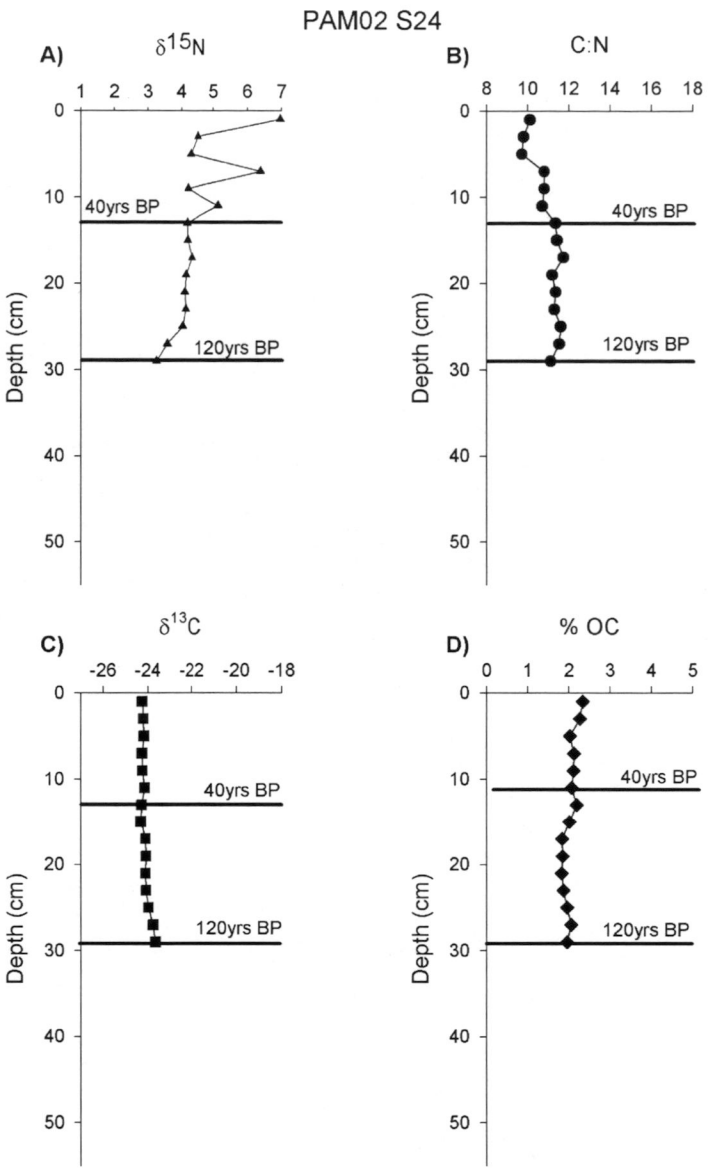

Figure 26: Geochemistry data for PAM02S24. A) $\delta^{15}N$ (‰) signatures vs depth (cm). B) C:N ratio vs depth (cm). C) $\delta^{13}C$ (‰) signatures vs depth (cm). D) Percent organic carbon vs depth (cm). The 40yrs BP line represents the ^{137}Cs peak and the 120yrs BP line represents the interval at which ^{210}Pb is considered to be inactive as determined by radionuclide data (Tully, 2004).

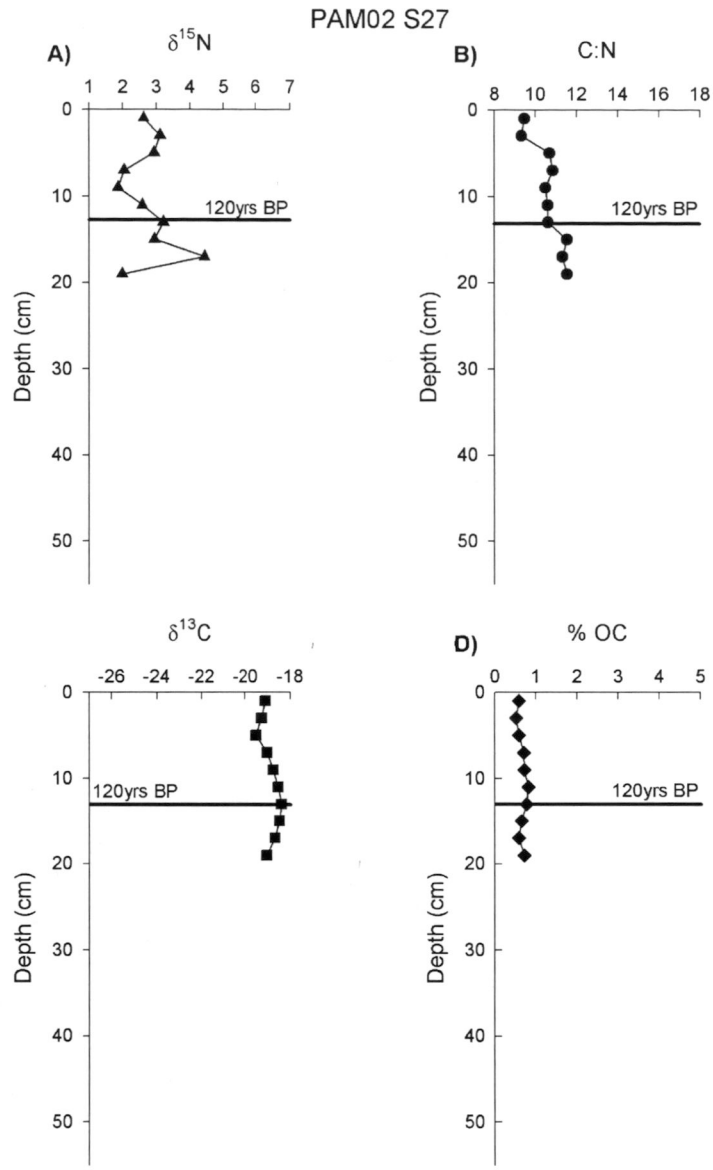

Figure 27: Geochemistry data for PAM02S27. A) $\delta^{15}N$ (‰) signatures vs depth (cm). B) C:N ratio vs depth (cm). C) $\delta^{13}C$ (‰) signatures vs depth (cm). D) Percent organic carbon vs depth (cm). The 120yrs BP line represents the interval at which ^{210}Pb is considered to be inactive as determined by radionuclide data. A ^{137}Cs peak was not present at this location (Tully, 2004).

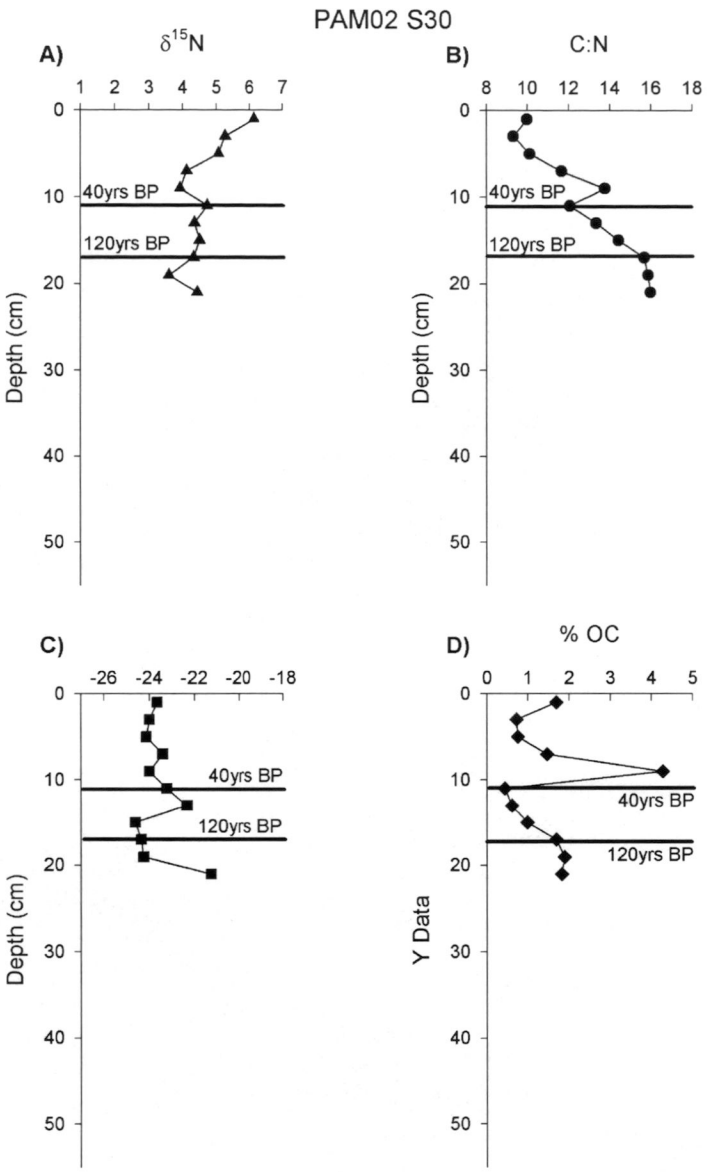

Figure 28: Geochemistry data for PAM02S30. A) $\delta^{15}N$ (‰) signatures vs depth (cm). B) C:N ratio vs depth (cm). C) $\delta^{13}C$ (‰) signatures vs depth (cm). D) Percent organic carbon vs depth (cm). The 40yrs BP line represents the ^{137}Cs peak and the 120yrs BP line represents the interval at which ^{210}Pb is considered to be inactive as determined by radionuclide data (Tully, 2004).

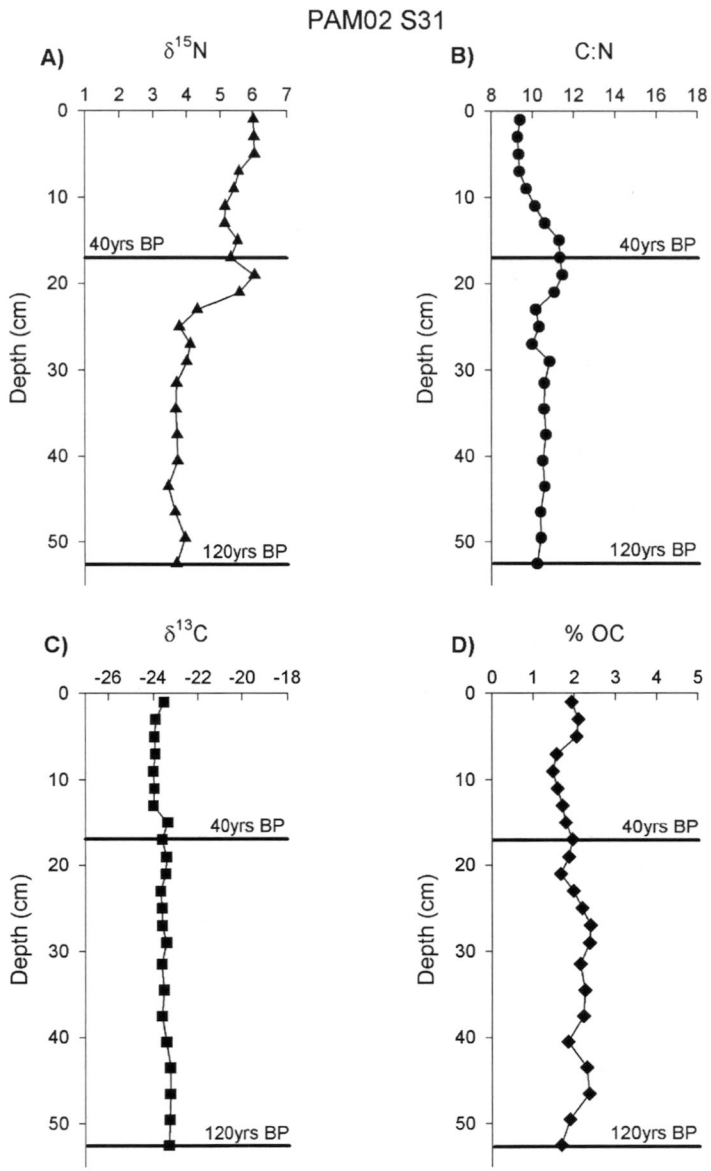

Figure 29: Geochemistry data for PAM02S31. A) $\delta^{15}N$ (‰) signatures vs depth (cm). B) C:N ratio vs depth (cm). C) $\delta^{13}C$ (‰) signatures vs depth (cm). D) Percent organic carbon vs depth (cm). The 40yrs BP line represents the ^{137}Cs peak and the 120yrs BP line represents the interval at which ^{210}Pb is considered to be inactive as determined by radionuclide data (Tully, 2004).

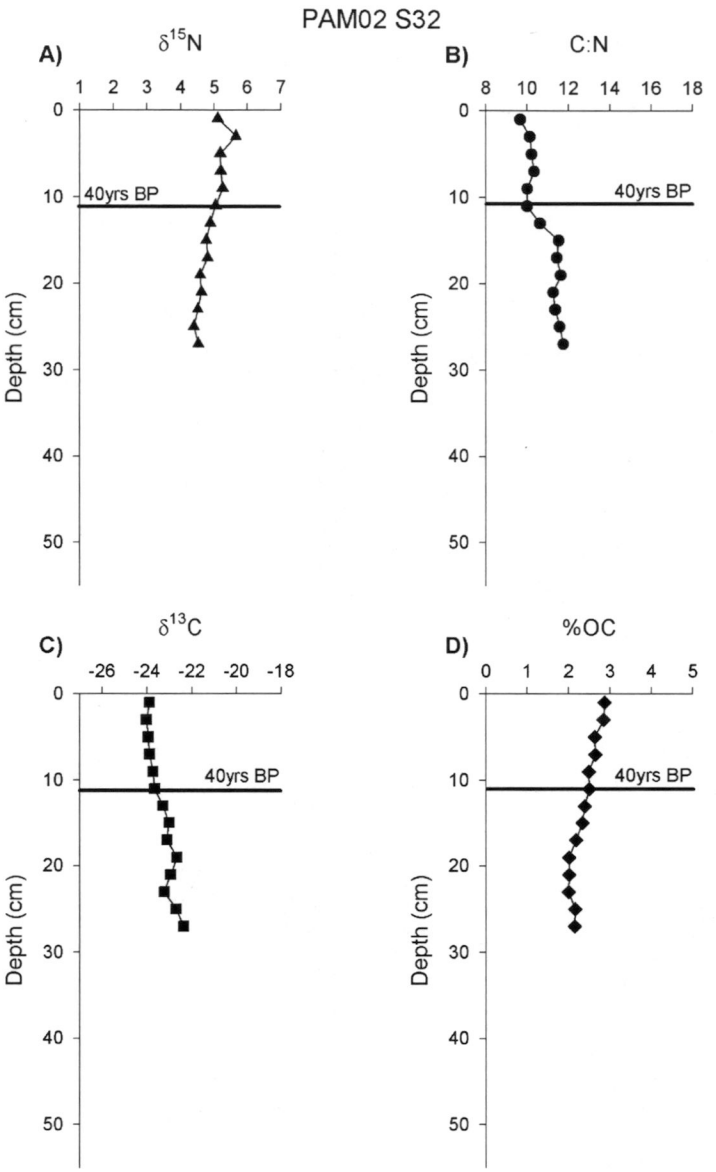

Figure 30: Geochemistry data for PAM02S32. A) $\delta^{15}N$ (‰) signatures vs depth (cm). B) C:N ratio vs depth (cm). C) $\delta^{13}C$ (‰) signatures vs depth (cm). D) Percent organic carbon vs depth (cm). The 40yrs BP line represents the ^{137}Cs peak as determined by radionuclide data. ^{210}Pb was still active at the base of the core (Tully, 2004).

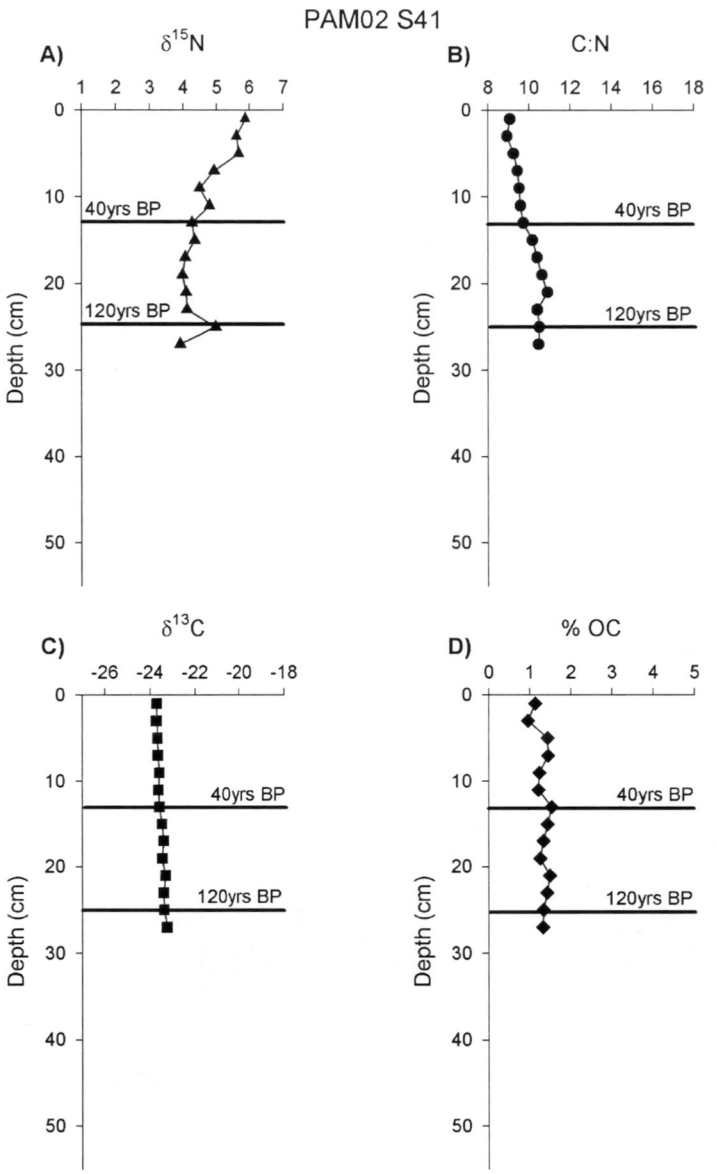

Figure 31: Geochemistry data for PAM02S41. A) $\delta^{15}N$ (‰) signatures vs depth (cm). B) C:N ratio vs depth (cm). C) $\delta^{13}C$ (‰) signatures vs depth (cm). D) Percent organic carbon vs depth (cm). The 40yrs BP line represents the ^{137}Cs peak and the 120yrs BP line represents the interval at which ^{210}Pb is considered to be inactive as determined by radionuclide data (Tully, 2004).

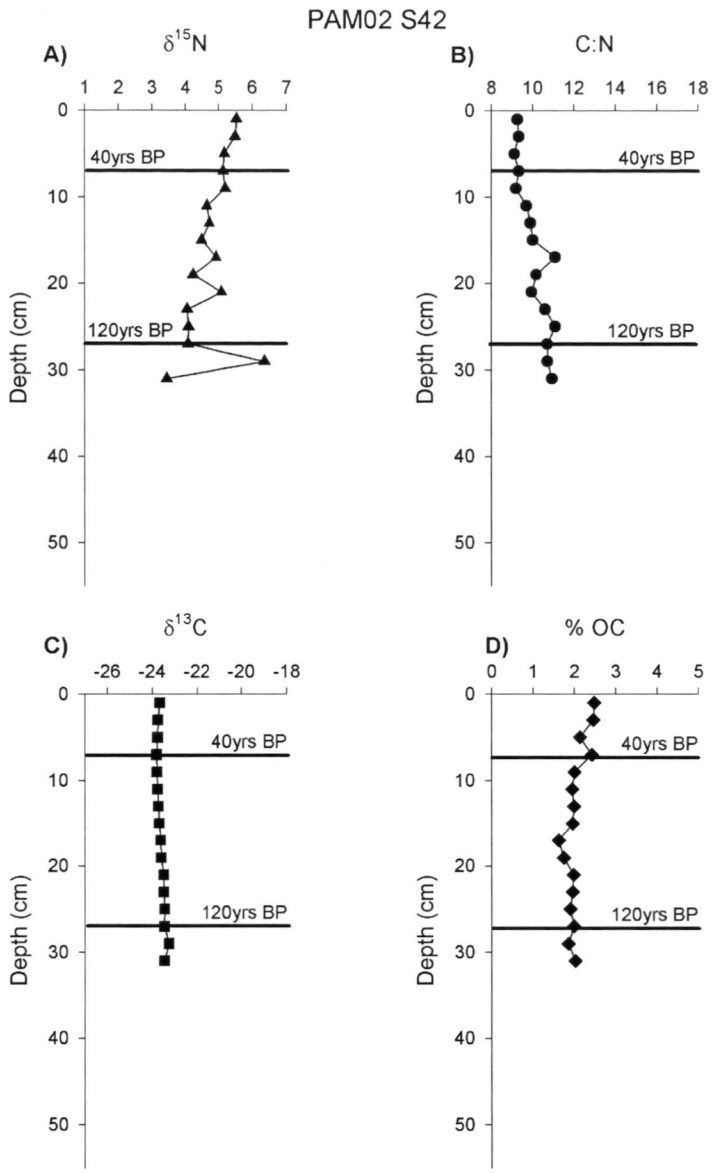

Figure 32: Geochemistry data for PAM02S42. A) $\delta^{15}N$ (‰) signatures vs depth (cm). B) C:N ratio vs depth (cm). C) $\delta^{13}C$ (‰) signatures vs depth (cm). D) Percent organic carbon vs depth (cm). The 40yrs BP line represents the ^{137}Cs peak and the 120yrs BP line represents the interval at which ^{210}Pb is considered to be inactive as determined by radionuclide data (Tully, 2004).

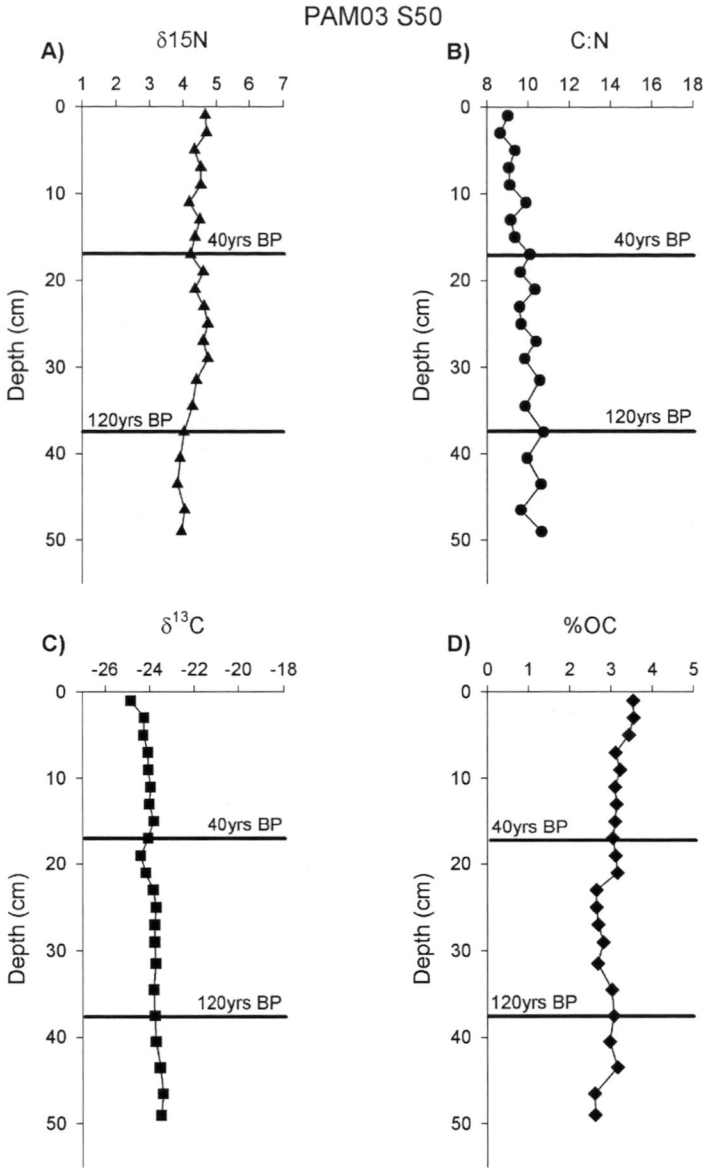

Figure 33: Geochemistry data for PAM03S50. A) $\delta^{15}N$ (‰) signatures vs depth (cm). B) C:N ratio vs depth (cm). C) $\delta^{13}C$ (‰) signatures vs depth (cm). D) Percent organic carbon vs depth (cm). The 40yrs BP line represents the ^{137}Cs peak and the 120yrs BP line represents the interval at which ^{210}Pb is considered to be inactive as determined by radionuclide data (Tully, 2004).

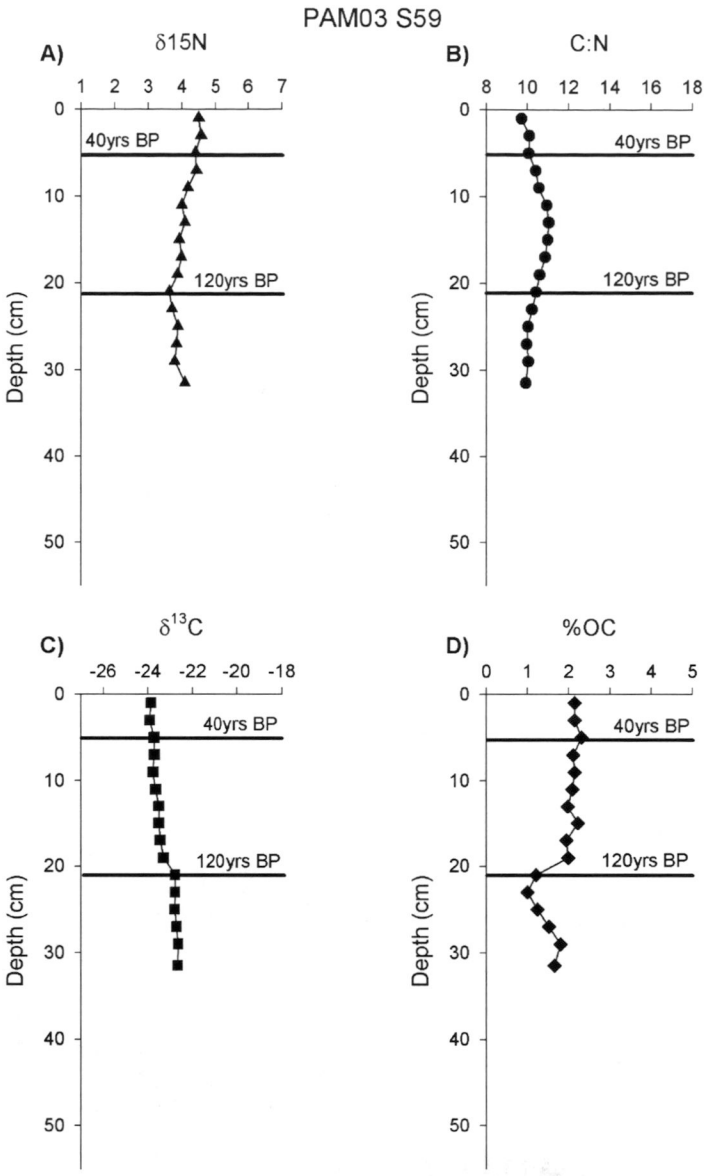

Figure 34: Geochemistry data for PAM03S59. A) $\delta^{15}N$ (‰) signatures vs depth (cm). B) C:N ratio vs depth (cm). C) $\delta^{13}C$ (‰) signatures vs depth (cm). D) Percent organic carbon vs depth (cm). The 40yrs BP line represents the ^{137}Cs peak and the 120yrs BP line represents the interval at which ^{210}Pb is considered to be inactive as determined by radionuclide data (Tully, 2004).

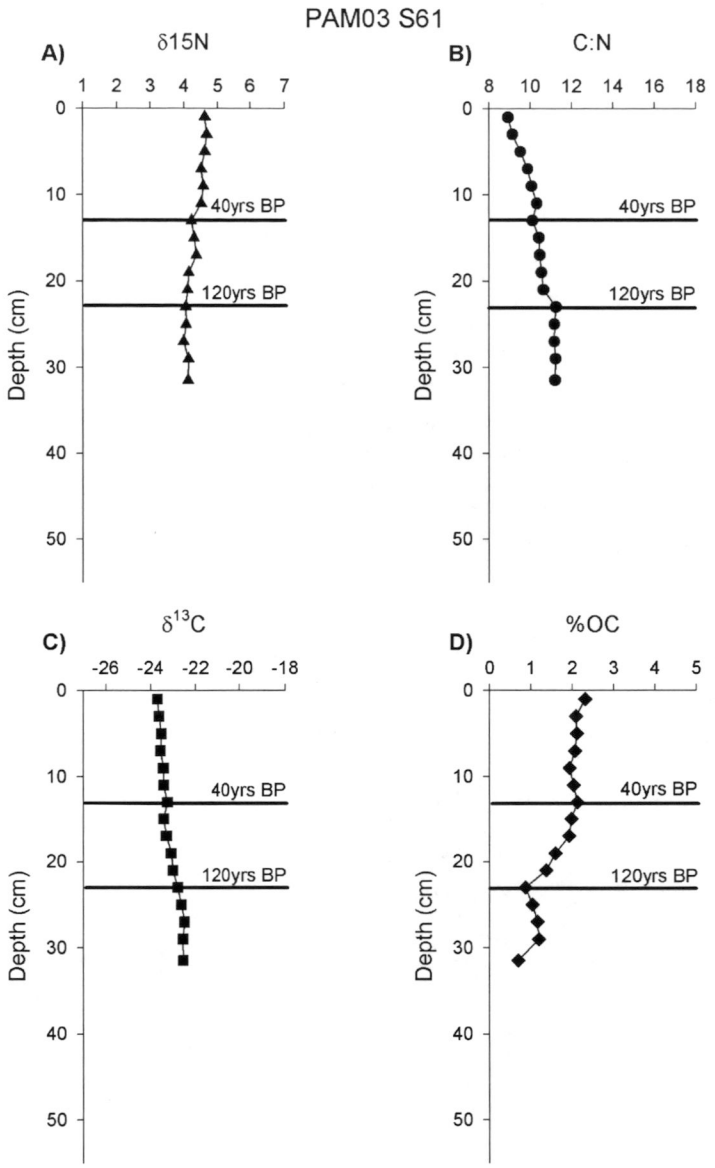

Figure 36: Geochemistry data for PAM03S61. A) $\delta^{15}N$ (‰) signatures vs depth (cm). B) C:N ratio vs depth (cm). C) $\delta^{13}C$ (‰) signatures vs depth (cm). D) Percent organic carbon vs depth (cm). The 40yrs BP line represents the ^{137}Cs peak and the 120yrs BP line represents the interval at which ^{210}Pb is considered to be inactive as determined by radionuclide data (Tully, 2004).

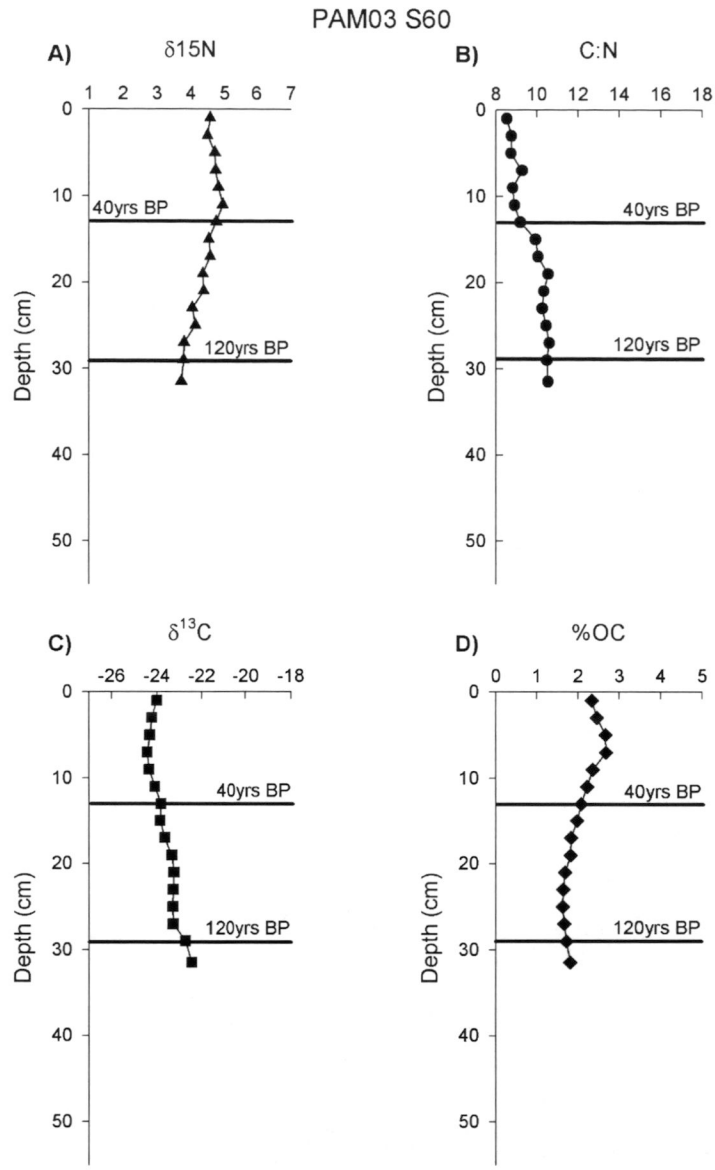

Figure 35: Geochemistry data for PAM03S60. A) $\delta^{15}N$ (‰) signatures vs depth (cm). B) C:N ratio vs depth (cm). C) $\delta^{13}C$ (‰) signatures vs depth (cm). D) Percent organic carbon vs depth (cm). The 40yrs BP line represents the ^{137}Cs peak and the 120yrs BP line represents the interval at which ^{210}Pb is considered to be inactive as determined by radionuclide data (Tully, 2004).

To do this, several samples were chosen at random from all sample sets and sent to the lab, untreated and treated (non-fumigated and acid fumigated). Some samples were re-analyzed three times. At least four samples were sent as a control (i.e., no reported problems from the lab and no discrepancies were observed in the values of the samples). The new values did not show any significant difference in $\delta^{15}N$ signatures between fumigated and non-fumigated samples (range of difference: 0.08-0.56) for the control samples. After review of the data, it was found that only those samples from the first set displayed some discrepancy. It was concluded that the observed high $\delta^{15}N$ signatures were a result of machine malfunction. The new results for those samples that displayed questionable values were either averaged with the original data (only if there were no reported problems with that particular sample) or they completely replaced the original values. Data used, including the corrected values, are given in Appendix H.

In general, all of the cores display a slight depletion in $\delta^{13}C$ values up-core. This suggests a slight change in the estuarine environment over time. Surface signatures vary between –23.51, in the center of the Sound (S31), and –24.86, at the mouth of the Pamlico River (S50), with the exception of S27, which has a value of –19.10 (Figure 37). A similar spatial pattern is recognized down-core (Figures 20-36).

S10 displays the greatest depletion observed up-core for the Sound (Figure 21). At the base of the core (28-30cm), the $\delta^{13}C$ signature is –20.01, while at the surface (0-2cm), the $\delta^{13}C$ signature is –24.40. A peak in depletion is observed at interval 8-10cm

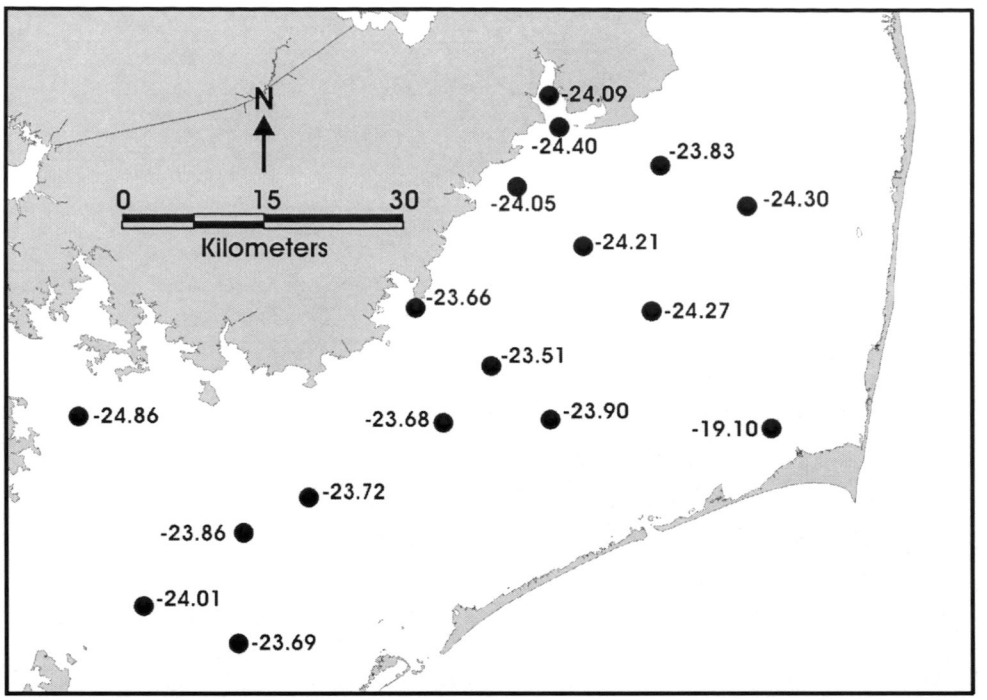

Figure 37: Surface (0-2cm) $\delta^{13}C$ signatures for Pamlico Sound.

with a signature of –26.64. The overall up-core shift in isotopic signature may be an indication of a change in source of organic matter.

The most enriched $\delta^{13}C$ values are found at S27 (Figure 27). The signature at the base of the core (18-20cm) is –19.04. The interval representing approximately 120 years BP (12-14cm), as determined by radionuclide data, has a peak enrichment value of –18.39. From this interval upwards, the signatures steadily depleted to –19.10 at the surface (0-2cm). S27 has an isotopic signature that is different from the rest of the Sound, which indicates the source of organic matter for this area is different than the rest of the Sound.

The general trend of $\delta^{15}N$ values increase (enrich) up-core throughout Pamlico Sound (Figures 20-36). Some cores show steeper gradients than others, as well as greater

variations in signatures. S22, S23, S30, and S41 (Figures 24, 25, 28, and 31) show a steeper gradient increase in the last 40 years BP opposed to the gradual trend seen at these sites down-core. The top 12cm of S24 fluctuates in signatures between 4.20 (8-10cm) and 6.96 (0-2cm) (Figure 26). Overall, the most enriched values for the surface (0-2cm) recorded across Pamlico Sound are found in the center of the Sound (S24, S30, and S31), while the less enriched values are located along the perimeter of the Sound (S9 and S27) (Figure 38). This pattern varies throughout the Sound down-core; however, S12, S22, S23, S24, S30, S31, S32, S42, S50, S59, S60, and S61 all appear to enrich at the same rate up-core (Figure 23, 24, 25, 26, 28, 29, 30, 32, 33, 34, 35, and 36).

The least amount of variation (small isotopic range) in nitrogen signatures down-core is observed at S32, located near the center of the Sound (Figure 30) and at sites located in the southern section where the rivers (Pamlico and Tar) drain into the Sound (S50, S59, S60, and S61) (Figures 33, 34, 35, and 36). At S31 (Figure 29), there is a shift towards more enriched nitrogen values mid-core for approximately 12cm beginning with interval 22-24cm up to interval 12-14cm. Above this interval (12-14cm), nitrogen signatures follow the general increasing upward trend with the rest of core. This shift coincides with the activity peak of ^{137}Cs as determined by radionuclide data. This suggests that there has been an increase in nitrogen-rich sediment deposited in this region beginning approximately 40 years BP.

S27 reports the lowest average $\delta^{15}N$ value (2.77 for entire core) (Figure 27). The signature for this particular site varies between 1.98, at the base (18-20cm), and 4.42 just above the base (16-18). The recorded signature at the surface (0-2cm) is 2.62.

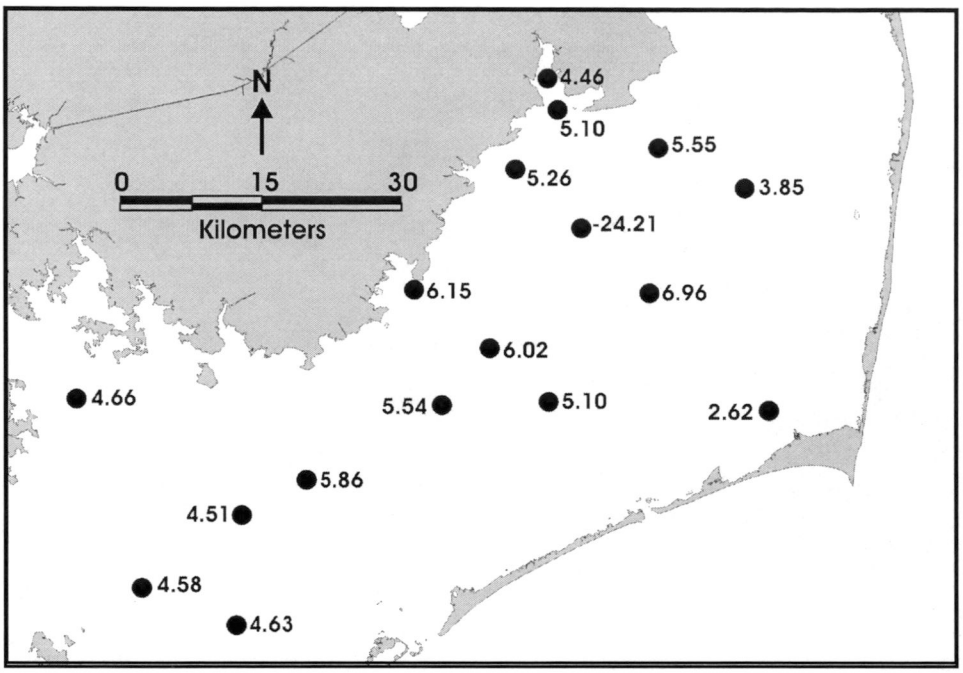

Figure 38: Surface (0-2cm) $\delta^{15}N$ signatures for Pamlico Sound.

C:N Ratios

The greatest surface (0-2cm) C:N values are found in the northern section of Pamlico Sound (Figure 39). This general pattern of greater C:N values to the north can be found down-core as well (Figures 20-36). An overall gradual decrease in C:N ratios up-core is observed at all sites throughout Pamlico Sound, except one (S11). S11 is the only core where C:N values increase up-core (Figure 22). At the base of the core (24-26cm), the C:N value is 12.27, while at the surface (0-2cm), the C:N value is 15.93. Between the intervals representing 120 and 40 years BP, the C:N values vary between 12.95 (4-6cm) and 15.93 (0-2cm).

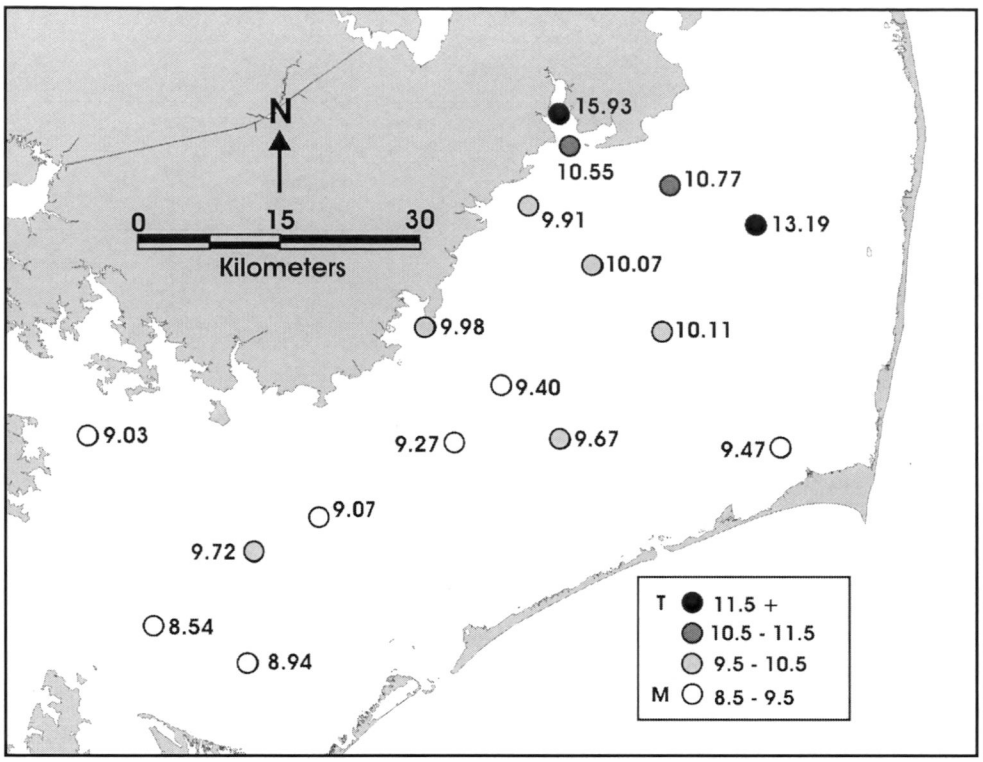

Figure 39: Surface (0-2cm) C:N ratios for Pamlico Sound.
T = terrestrial and M = marine.

Some localized variation in up-core trends is observed at S9, S10, S23, S30, and S59 (Figures 20, 21, 25, 28, and 34). Some rates of changes are greater than others, such as S30 (Figure 27). S30 displays the greatest amount of change in C:N values. The C:N value for the base (20-22cm) is 15.97 and the surface (0-2cm) is 9.98. At the base (34-36cm) of S9, the C:N ratio is 14.80, and at the surface (0-2cm) the ratio is 13.19. Mid-core, between the intervals representing 120 and 40 years BP, there is an abrupt shift towards increasing C:N values, peaking at 16.67 (16-18cm). The top 8cm of the core average out to a ratio of approximately 13.

S10 and S23 display a similar pattern mid-core as S30 (Figures 21 and 25). Within each core, there is a change up-core in the generally gentle and steady trend in decreasing ratio to a more abrupt and steeper gradient in decreasing ratios. For S10, at the base (28-30cm), the ratio is 14.71, which steadily decreases to 13.53 mid-core (12-14cm), then rapidly decreases to a ratio of 10.55 at the surface (0-2cm). The base of S23 (24-26cm) has a ratio of 13.38, which steadily decreases to 14.3 mid-core (10-12cm), then rapidly decreases to a ratio of 10.77 at the surface (0-2cm).

The pattern observed in the core at S59 is different from the general trends present in other cores (Figure 34). The C:N ratios increase from 9.92 at the base (30-33cm) to 11.04 mid-core (12-14cm), then the values begin to decrease for remaining intervals up-core to the surface (0-2cm) with a value of 9.72. S59 is located in the southern section of Pamlico Sound where the two rivers (Pamlico and Neuse) enter into the Sound. The observed shift from increasing C:N values to decreasing C:N values may be a result of the location for S59.

Percent Organic Carbon

The amount of organic carbon within Pamlico Sound is very low, averaging between less than one to approximately five percent. Greater percents of organic carbon (approximately 3% or greater) are found in areas containing fine sediment (silt and clay) and vary spatially throughout the study area (Figure 40).

Few sites display a slight increase in organic carbon up-core (S10, S11, S32, S60, and S61) (Figures 21, 22, 30, 35, and 36). These sites are either located next to a marsh

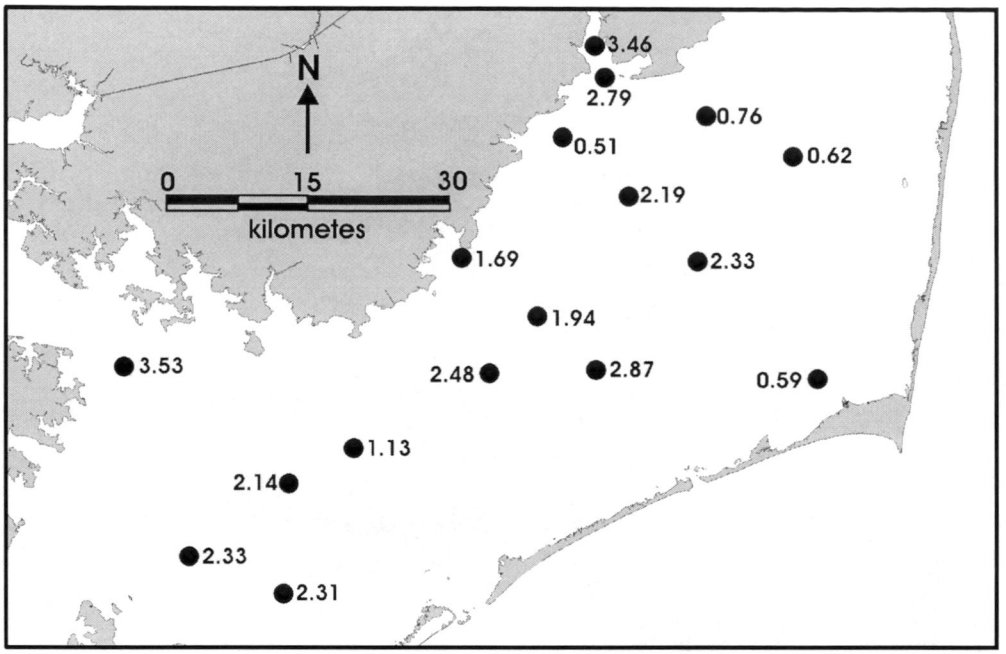

Figure 40: Surface (0-2cm) percent organic carbon values for Pamlico Sound.

(S10 and S11) or along the perimeter of the central basins which define the deepest sections of the Sound (S32, S60, and S61) (see Figure 2 for bathymetry).

The greatest change down-core in percent organic carbon is observed at S23 (Figure 25). Percent organic carbon fluctuates between 4.5 (near the base) and 0.53 (near the surface). An overall decrease in organic carbon is observed up-core. Sediment within the core is described as a sandy mud from the base (24-26cm) to mid-core (8-10cm), while the top 8cm is described as fine to coarse sands with shell fragments.

For the most part, the average percent of organic carbon present down-core in S30 is less than two percent (Figure 28). However, there is a spike of organic carbon (4.28%) at the 8-10cm interval. This interval is found just above the interval representing approximately 40yrs BP.

One-way Analysis of Variance (ANOVA) for Geochemical Results

A one-way ANOVA was used to test statistically the hypothesis that the geochemical results ($\delta^{13}C$, $\delta^{15}N$, and C:N ratios) at the three specified time slices (~120 yrs BP, ~40 yrs BP, and the modern) are significantly different. The analysis was run using SPSS. For each test, the null hypothesis was that there is no significant difference in values overtime (between ~120 yrs BP, ~40 yrs BP, and modern). The results are listed in Tables 9, 10, and 11. Any $p(F) < 0.05$ was considered significant (95% confidence). Therefore, the null hypothesis was accepted the ANOVA that compared $\delta^{13}C$ signatures; there is no significant change in $\delta^{13}C$ signatures over time. However with p(F) values equal to 0.000 and 0.030 for $\delta^{15}N$ and C:N ratios, respectively, the null hypothesis was rejected. There is a significant change in signatures and ratio values overtime. Figures 41, 42, and 43 display the mean proportions of the stable isotope signatures and C:N ratios for the three time slices.

Contrasts were set-up between the time slices to determine when the greatest change had occurred. The results are listed in Table 12. As determined before, there is no significant change in $\delta^{13}C$ signatures. However, $\delta^{15}N$ signatures are observed to have a statistically significant difference for each contrast except for the comparison of the ~40 yrs BP time slice with the modern and ~120 yrs BP time slices. This suggests that there is an increase (enrichment) of $\delta^{15}N$ signatures over time. Three contrasts show a significant change for C:N ratios, 1) between ~120 yrs BP and the modern time slices, 2) the modern time slice compared with both the ~120 and ~40 yrs BP time slices, and 3)

~120 yrs BP compared to both the modern and ~40 yrs BP time slices. This suggests that C:N ratios decrease down-core.

Table 9: ANOVA test results for $\delta^{13}C$ signatures. The value of the Sum of Squares between groups is the sum of the difference between averages (means) of the three time slices (120 yrs, 40 yrs, and modern). Since there are three groups, the degrees of freedom (df) is equal to 2 (3 groups–1=2). The Mean Square value is the Sum of Squares divided by the df. The F value is the ratio for the between group variance and the within group variance. The df for the Within Groups is found by number of samples/sites (49) minus the number of groups/time slices (3) which is equal to 46.

	Sum of Squares	df	Mean Square	F	Sig.
Between Groups	3.321	2	1.660	1.268	.291
Within Groups	60.208	46	1.309		
Total	63.529	48			

Table 10: ANOVA test results for $\delta^{15}N$ signatures. The value of the Sum of Squares between groups is the sum of the difference between averages (means) of the three time slices (120 yrs, 40 yrs, and modern). Since there are three groups, the degrees of freedom (df) is equal to 2 (3 groups–1=2). The Mean Square value is the Sum of Squares divided by the df. The F value is the ratio for the between group variance and the within group variance. The df for the Within Groups is found by number of samples/sites (49) minus the number of groups/time slices (3) which is equal to 46.

	Sum of Squares	df	Mean Square	F	Sig.
Between Groups	12.035	2	6.018	11.079	.000
Within Groups	24.985	46	.543		
Total	37.020	48			

Table 11: ANOVA test results for C:N ratios. The value of the Sum of Squares between groups is the sum of the difference between averages (means) of the three time slices (120 yrs, 40 yrs, and modern). Since there are three groups, the degrees of freedom (df) is equal to 2 (3 groups–1=2). The Mean Square value is the Sum of Squares divided by the df. The F value is the ratio for the between group variance and the within group variance. The df for the Within Groups is found by number of samples/sites (49) minus the number of groups/time slices (3) which is equal to 46.

	Sum of Squares	df	Mean Square	F	Sig.
Between Groups	25.686	2	12.843	3.770	.030
Within Groups	156.697	46	3.406		
Total	182.383	48			

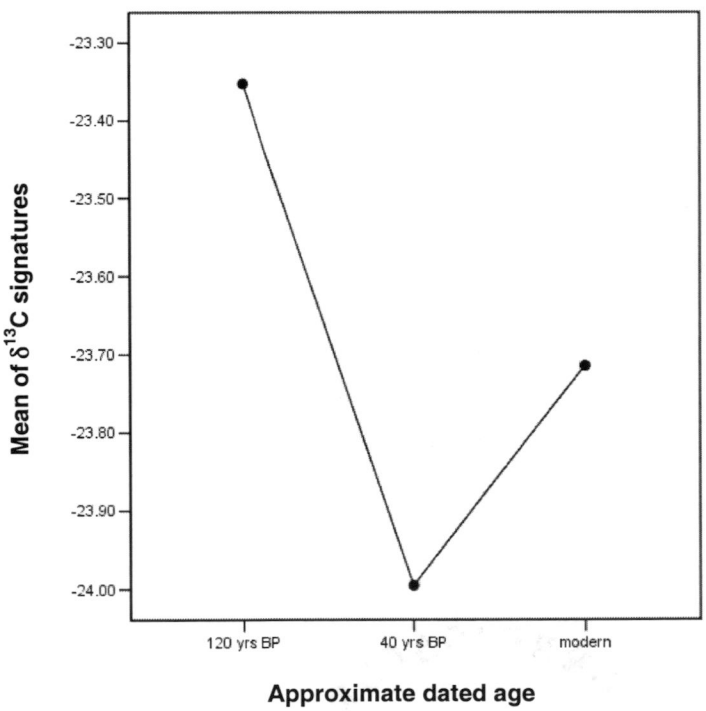

Figure 41: One-way ANOVA plot of means for time slices (as determined by radionuclides) vs $\delta^{13}C$ signatures.

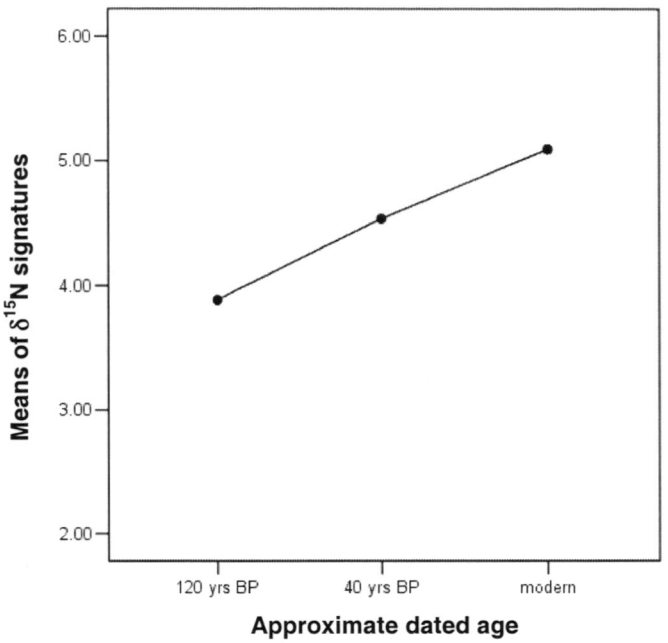

Figure 42: One-way ANOVA plot of means for time slices (as determined by radionuclides) vs $\delta^{15}N$ signatures.

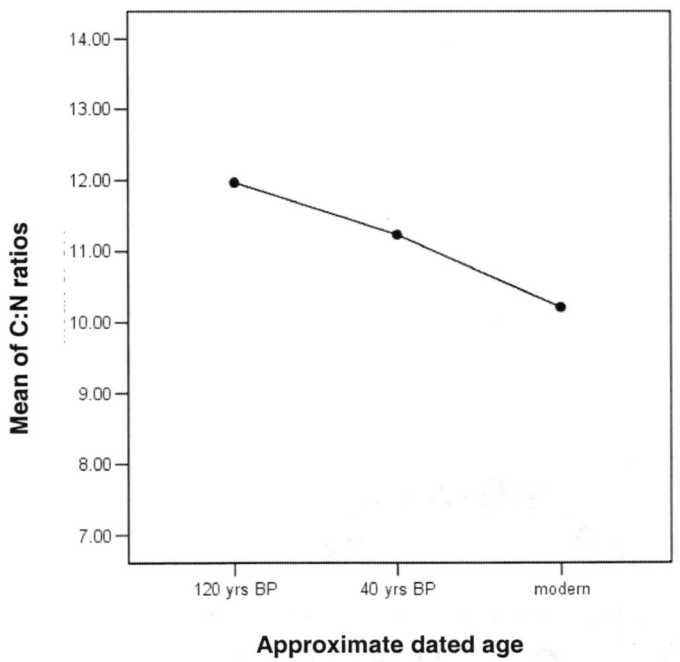

Figure 43: One-way ANOVA plot of means for time slices (as determined by radionuclides) vs C:N ratios.

Table 12: Contrasts for geochemistry compared to the three time slices, where p(F) < 0.05 is significant. 120 and 40 are in years BP.

Geochemical analysis	p(F) 120 vs 40	p(F) 120 vs modern	p(F) 40 vs modern	p(F) modern vs 120, 40	p(F) 40 vs modern, 120	p(F) 120 vs modern, 40
$\delta^{13}C$	0.119	0.369	0.484	0.907	0.192	0.157
$\delta^{15}N$	0.016	0.000	0.035	0.000	0.836	0.000
C:N	0.267	0.009	0.119	0.016	0.800	0.032

DISCUSSION

Combination of surficial foraminiferal and geochemical data gives an indication of environmental conditions that currently affect Pamlico Sound. Comparison between the modern surficial conditions with down-core data gives an indication of the paleoenvironmental conditions over the last approximately 120 years. To observe and compare the changing environments of Pamlico Sound, this discussion is divided into four parts; (1) description of the modern environment, (2) description of the paleoenvironment 120 years BP, (3) description of the paleoenvironment 40 years BP, and (4) explanations.

Description of the Modern Environment

Analysis of surficial foraminiferal data allowed the distinction of four biofacies; (1) Marine, (2) Estuarine Biofacies B, (3) Estuarine Biofacies A, and (4) Marsh Biofacies Biofacies. Canonical discriminant analysis (Figure 15) and species diversity (Table 8, Figure 19) were used to verify that these groups are different from one another. The distribution of the biofacies within Pamlico Sound appears to be related to the distribution of sediments, salinity, and to some extent, depth (Ellison and Nichols, 1970). Table 13 is a summary of the modern biofacies existing within Pamlico Sound.

The Marine Biofacies, located at Hatteras and Ocracoke inlets, (Figure 14) was completely dominated by calcareous foraminifera such as *Cibicides lobatulus, Elphidium galvestonense, Elphidium mexicanum, Elphidium subarcticum, Hanzawaia strattoni,* and

Table 13: Summary of modern biofacies described for Pamlico Sound, the key species, sites, and salinity readings. Salinity readings were recorded at time of collection. The salinity value for S4 is questionable due to faulty equipment.

Biofacies:	**Key Species:**	**Sites:**	**Salinity:**
Marsh Biofacies	*T. comprimata*	S1	24
	T. inflata	S2	24
	M. fusca	S5	22
	H. wilberti	S10	24
		S14	27
		S17A	26
		S38	21
		S45	33
		S46	33
Estuarine Biofacies A	*A. salsum*	S4	7.4 (?)
	A. crassus	S7	24
	E. excavatum	S9	25
		S11	22
		S12	22
		S15	29
		S22	25
		S23	25
		S26	27
		S27	27
		S35	25
		S39	21
		S40	21
		S44	27
		S50	7
		S63	20
Estuarine Biofacies B	*E. excavatum*	S24	25
	A. salsum	S25	25
		S30	27
		S31	26
		S32	30
		S41	22
		S42	24
		S59	15
		S60	14
		S61	15
Marine Biofacies	*E. excavatum*	S17	35
	H. strattoni	EB02S1	32
	C. lobatulus	EB02S2	34
	E. subarcticum	EB02S3	36
	Q. seminula		
	E. galvestonense		

Quinqueloculina seminula. Q. seminula species is typical of inlet environments (Grossman and Benson, 1967; Robinson and McBride, 2003). The salinity recorded at these sites was typically greater than 30 (Table 13). Sediment type recorded at the inlets is medium-grained sand (Figure 3), which is indicative of relatively high-energy environments.

The central and southern section of Pamlico Sound is the location of Estuarine Biofacies B (Figure 14), which also defines the deepest sections of the Sound (Figure 2). The average salinity for this biofacies is greater than 25, with the exception of the stations located to the south. Salinities in the southern section of the sound are influenced by freshwater discharge from the Neuse and Pamlico Rivers (Figure 5). Thus, overall salinity range is between 7 and 25. Calcareous foraminifera are found in great abundance within this biofacies as well as a significant amount of coarsely agglutinated foraminifera. Typical foraminifera present within this biofacies are *Elphidium excavatum, Ammonia parkinsoniana*, and *Ammotium salsum.* The surface sediment for the majority of these sites is silt (Figure 3). Environmental conditions described by this biofacies agree with the description of the Basin Biofacies located in the Rappahonnock Estuary (Ellison and Nichols, 1970).

Estuarine Biofacies A, generally located along the platforms of the basins (Figure 2), surrounds Estuarine Biofacies B (Figure 14). The average salinity for Estuarine Biofacies A is between 20 to 25 (Table 13) and the substrate is generally fine to very fine sand (Figure 3). Typical foraminifera belonging to this biofacies are coarsely agglutinated, such as *Ammotium salsum* and *Ammobaculies crassus*, as well as some

calcareous foraminifera, such as *Elphidium excavatum*. The environmental conditions for this biofacies are equivalent to the description of the Shoal Biofacies located in the Rappahonnock Estuary (Ellison and Nichols, 1970).

The Marsh Biofacies is located along the perimeter of the Sound (Figure 14) and is typically found at marsh locations. The Marsh Biofacies is comprised primarily of finely agglutinated foraminfera, such as *Trochammina inflata, Tiphotrocha comprimata, Miliammina fusca,* and *Haplophragmoides wilberti.* Average salinity recorded at time of collection for this biofacies was high, ranging between 21 to 33 (Table 13). Wide ranges in salinity are typical for salt marshes (Goldstein et al., 1995; Collins, 1996; Culver et al., 1996; Woo et al., 1997; Saffert and Thomas, 1998; Goldstein and Watkins, 1999; Scott et al., 2001). The faunal composition of the Pamlico Sound Marsh Biofacies is comparable to other marsh biofacies described along the east coast of the United States (Ellison and Nichols, 1970; Goldstein et al., 1995; Collins, 1996; Culver et al., 1996; Woo et al., 1997, Saffert and Thomas, 1998; Goldstein and Watkins, 1999; Robinson and McBride, 2003).

Surface $\delta^{13}C$ signatures are slightly less enriched with increasing distance from the inlets (Figure 37). This reflects a greater marine influence closer to the inlets. S27, located behind Cape Hatteras, has a signature of -19.10, which is very different from any other recorded value within the sound. The S27 value can most likely be attributed to a mixture between marine phytoplankton and C_4 plant organic matter (e.g. marsh) (Waller and Lewis, 1979; Letrick, 2003).

The most enriched surface $\delta^{15}N$ values are found at sites located in the center of Pamlico Sound (Figure 38). These sites are located in the deepest section of the Sound

(Figure 2) where the sediment is typically silt and clay (Figure 3). This suggests that greater activity (e.g., trawling) here (in comparison to the rest of the Sound) has caused an increase in biogeochemical processes to enrich the sediment.

The greatest reported C:N ratios are found in the northern section of Pamlico Sound (Figure 39). S11 has a C:N value of 15.93, the highest surface value recorded throughout the Sound (Figure 39). S11 is located next to a marsh. A comparison of the high ratio value, strongly depleted $\delta^{13}C$ signature (-24.09) (Figure 37), and locality, suggest that the erosion of a nearby marsh heavily influences this site.

Description of the Paleoenvironment 120 years Before Present

The foraminiferal assemblage representing approximately 120 years BP (as determined by radionuclide data) (Figure 18) is very different from the modern day surface assemblage (Figure 14). The high abundance of *Ammotium salsum* throughout the study area characterizes the majority of the sound as Estuarine Biofacies A. Estuarine Biofacies A is associated with more brackish conditions in comparison to the other three biofacies (Table 13). There are just two sites (S12 and S30) classified with Estuarine Biofacies B, and one site (S11) classified with the Marsh Biofacies (Figure 18).

$\delta^{13}C$ signatures ranged between –24.69 and –22.37 throughout Pamlico Sound approximately 120 years BP (Figure 44). The range signifies a predominantly terrestrial

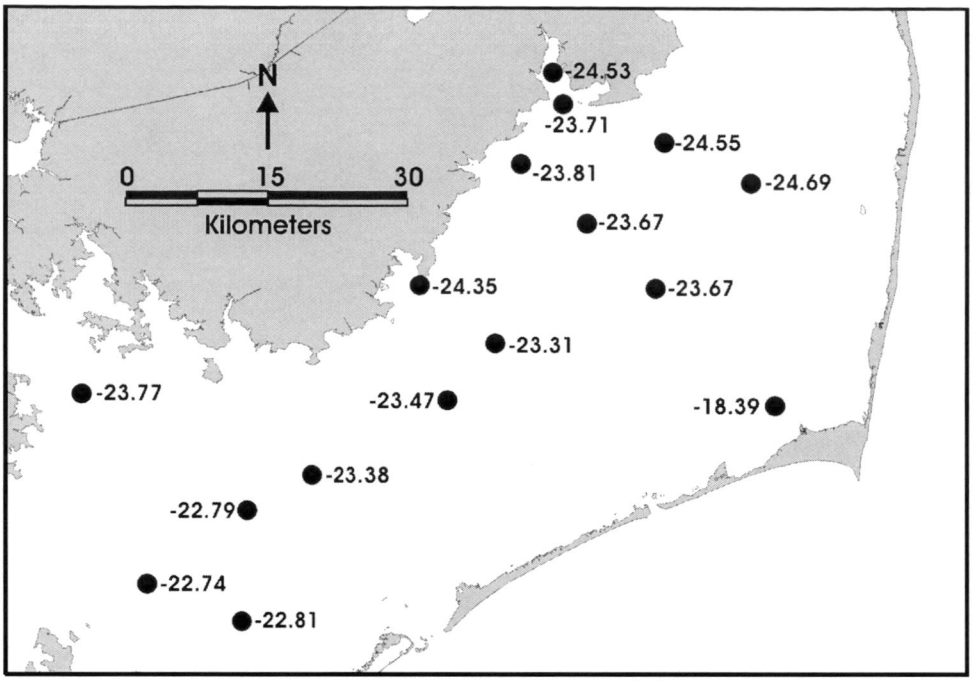

Figure 44: $\delta^{13}C$ signatures approximately 120 yrs BP (as determined by radionuclide data).

source (C_3 plants) for organic matter (Waller and Lewis, 1979). The distribution pattern (Figure 44) is comparable to the observed pattern at the surface (Figure 37) with typically more depleted values found in the northern section of the Sound. Similarities of the modern and 120 year old distribution patterns may be indicative of the same source area for organic matter and similar circulation/depositional patterns.

During this time interval, $\delta^{15}N$ values were scattered with no discernable pattern, ranging between 3.25 and 5.18 (Figure 45). However, the distribution pattern of C:N values at this time (approximately 120 years BP) (Figure 46) is comparable with the surface distribution (Figure 39). Ratios range between 10.22 and 15.67. Terrestrially influenced ratios (>12) are concentrated in the northern section of the Sound and gradually decrease to the south, indicative of terrestrially influenced organic matter

mixing with marine influenced organic matter. The similarity between distribution patterns (120 years BP compared to the surface/modern day) is indicative of a continued terrestrial influence in the northern section of Pamlico Sound.

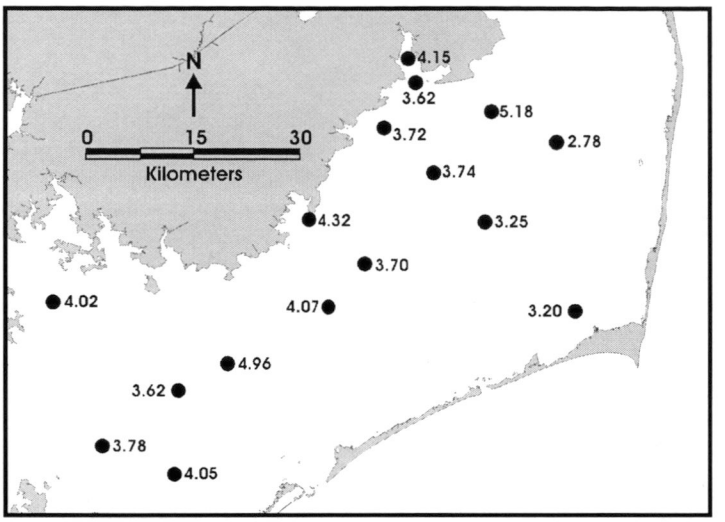

Figure 45: $\delta^{15}N$ signatures approximately 120 yrs BP (as determined by radionuclide data).

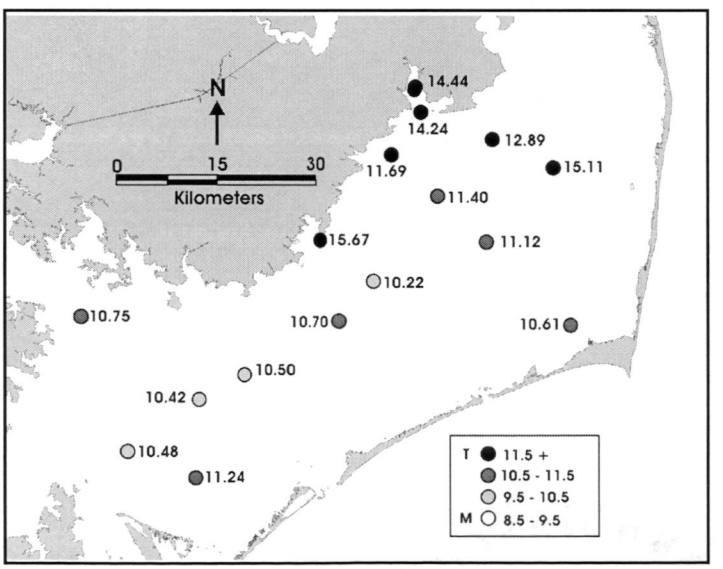

Figure 46: C:N ratios approximately 120 yrs BP (as determined by radionuclide data). T = terrestrial and M = marine.

Description of the Paleoenvironment 40 years Before Present to Present Day

Peak activity in ^{137}Cs data dates sediment to be approximately 40 years old (early 1960s). Many of the cores do not display a distinct peak in activity. These cores have several intervals that have similar elevated activities. It is possible that these intervals represent an extended period of time of intense mixing, resuspension, or maybe accumulation (Tully, 2004). Regardless, distinct changes (foraminiferal and geochemical) are recognized in all cores representing this time frame.

The foraminiferal assemblage represented at this time interval is comparable to the modern day surficial assemblage. The exceptions are two sites, S9 and S30; which are classified with the Marsh Biofacies (Figure 17). S9 and S30 are not located at a marsh. Therefore it is quite likely that marsh foraminifera present at these locations were washed into the Sound from another location. The smaller area classified as Estuarine Biofacies B (Figure 17) may suggest that the Sound was not as saline as it is today.

A significant change is not observed in the distribution pattern or range of $\delta^{13}C$ signatures between the 120 years BP time interval and the 40 years BP time interval (Figure 47). Some of the signatures recorded in the north are slightly more depleted than signatures deeper down-core. However, $\delta^{15}N$ signatures are enriched at nearly all of the sites (except two) and a slight distribution pattern has developed (Figure 48). Many of the cores display an increasing trend in $\delta^{15}N$ signatures mid-core either at or close to the interval representing the peak ^{137}Cs activity. The result of the ANOVA contrast demonstrated that there is a significant change in $\delta^{15}N$ signatures over time (Table 12). This suggests a change in biogeochemical processes to increase nitrification and

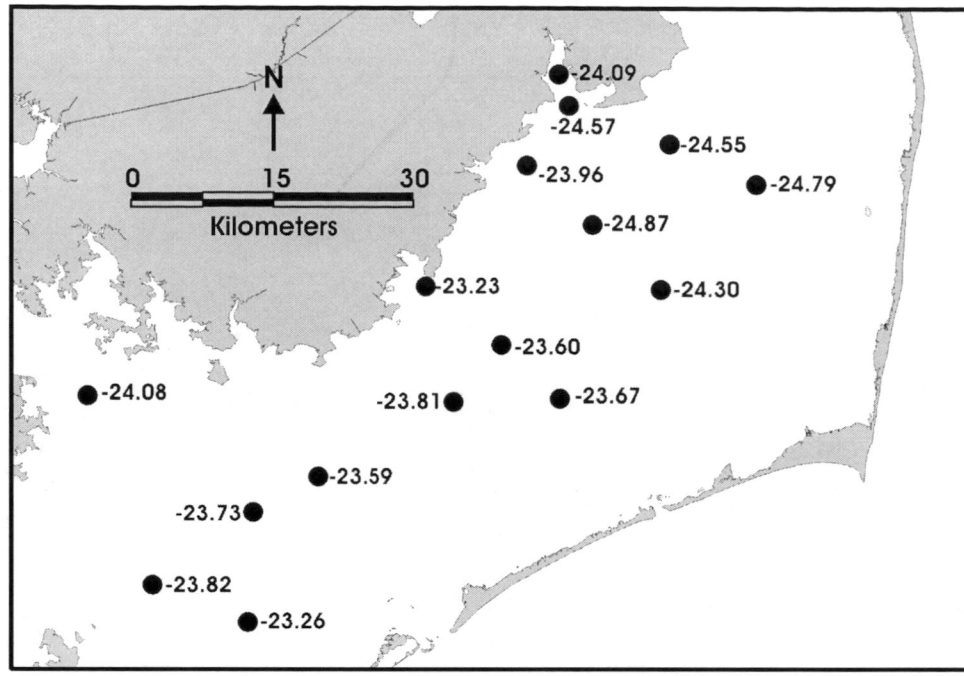

Figure 47: $\delta^{13}C$ signatures ratios approximately 40 yrs BP (as determined by radionuclide data).

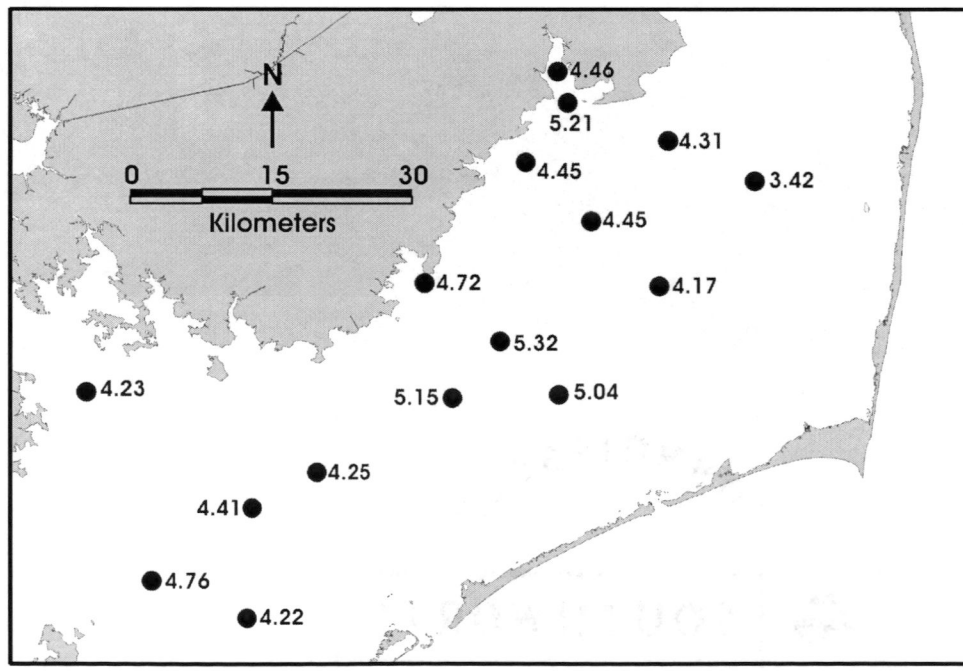

Figure 48: $\delta^{15}N$ signatures ratios approximately 40 yrs BP (as determined by radionuclide data).

denitrification and to deposit sediment enriched in ^{15}N. This trend of increasing enriched $\delta^{15}N$ values continues to the surface for many cores, which suggests denitrification has continually increased within Pamlico Sound over the last 40 years. This trend increases to the surface in many cores (S23, S24, S27, S30, and S41), which may indicate that these sections of the Sound are not stable and continue to be susceptible to changing environmental conditions.

The majority of the C:N values are lower at the interval representing 40 years BP (Figure 49) compared to values at the interval representing approximately 120 years BP (Figure 46). However, the distribution pattern is similar for both time intervals; greater ratio values are located in the northern section.

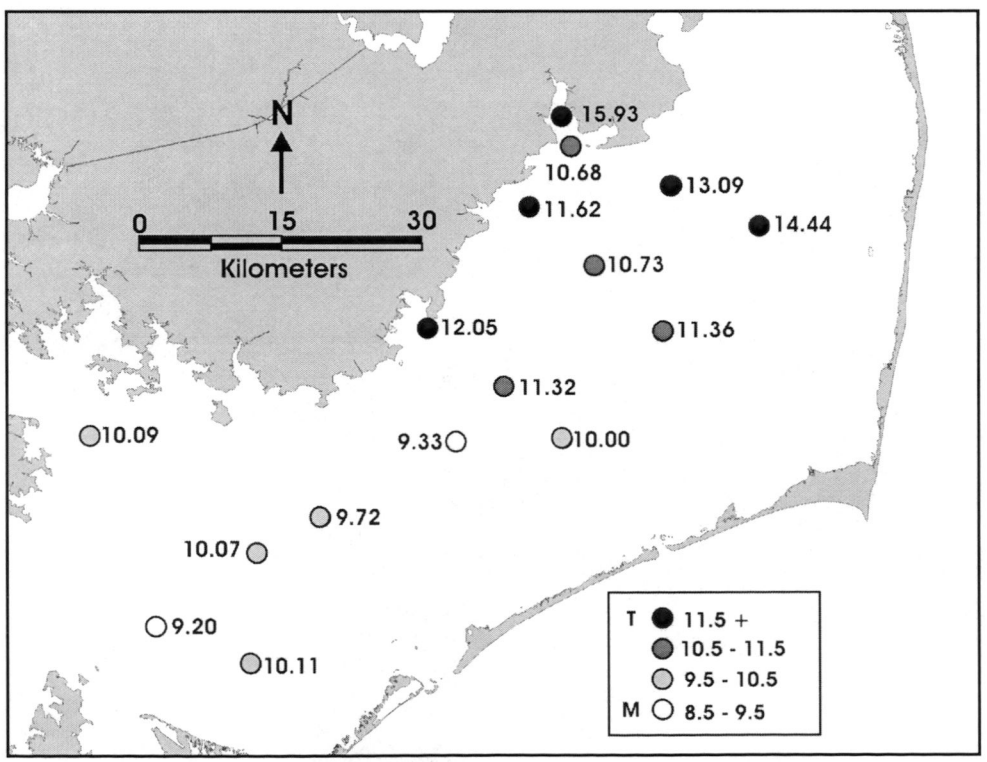

Figure 49: C:N ratios approximately 40 yrs BP (as determined by radionuclide data). T = terristrial and M = marine.

Explanations

Figure 50 presents a comparison of the three time slices (as determined by radionuclides) analyzed for surface and down-core foraminiferal assemblages. Based on salinity characteristics of Estuarine Biofacies A and B, there has been increase in salinity in Pamlico Sound over the last 120 years. Recorded storm events and C:N provide an explanation for this change.

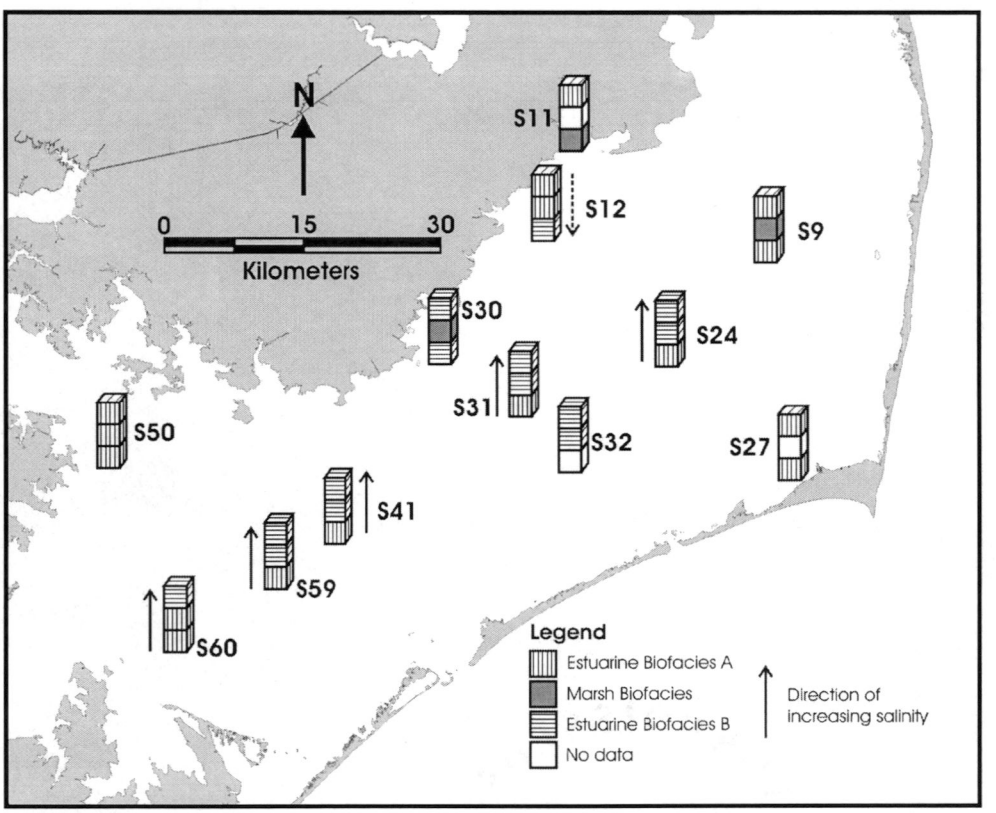

Figure 50: Comparison of foraminiferal assemblage changes over time. Bottom box represents approximately 120 years BP, the middle box represents approximately 40 years BP, and the top box represents present day. Arrows indicate direction of increasing salinity based on foraminifera present. Arrow is dashed at S12 because the discriminant analysis plots this sample very close to the territory boundary between Estuarine Biofacies A and B (see Figure 16 and Results section).

During the late 1870s to 1900, 12 hurricanes reached the shores of eastern North Carolina (Table 14). During some years there were more than one reported hurricane within a two-month interval. Increased amounts of freshwater have been reported to enter Pamlico Sound via the Pamlico and Neuse Rivers for an extended period of time after a wetter than average spring (Pietrafesa et al., 1986). Applying this concept to intense rainfall associated with hurricanes, it is possible that the brackish conditions indicated by the foraminiferal assemblage that accumulated approximately 120 years ago was caused by one or more of the several hurricanes.

Visual comparison of C:N ratios suggest a decrease in values up-core at all sites except one (S11). Results obtained from a one-way ANOVA test do suggest there are significant differences between C:N ratios over time (Tables 10 and 11). However, the general distribution pattern, with greater ratio values found in the northern section of the Sound, has not changed (Figure 39). The core intervals representing approximately 120 years BP display C:N ratios indicative of mixing between terrestrial and marine influenced organic matter (Figure 46). A comparison of the three time slices indicates that, a marine-influenced area (as determined by C:N ratios) has steadily increased in size and extended into the northern section of Pamlico Sound (Figure 51). Even though there has a been an increasing marine influence within the Sound over time, current ratios in the north are representative of mixed terrestrial and marine organic matter sources. Southerly currents from the Albemarle Sound flow through Roanoke and Croatan Sounds into Pamlico Sound (Singer and Knowles, 1975; Pietrafesa et al., 1986; Riggs et al., 2000). These currents flow across eroding peats rich in organic matter (Riggs et al.,

Table 14: Dates of hurricanes to reach coastal North Carolina between the years 1876 and 1899 (Barnes, 2001).

Year	Date(s) of Hurricane
1876	September 17
1879	September 18
1881	September 9
1882	September 11 September 22 October 22
1883	September 11
1885	August 25
1893	August 27-29 October 13
1899	August 16-18 October 30-31

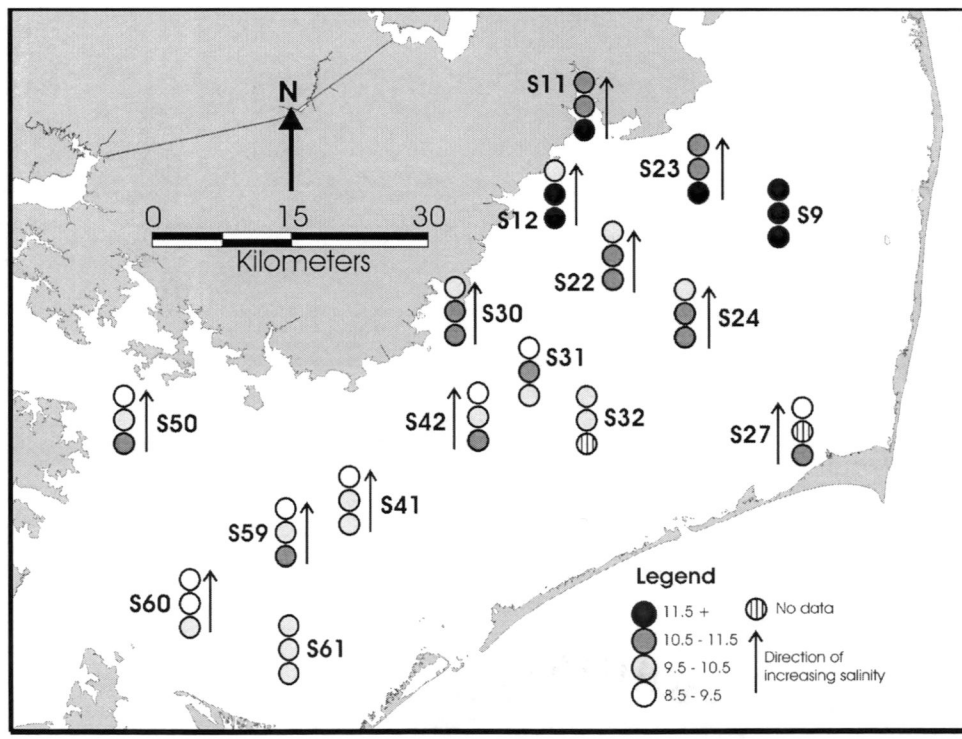

Figure 51: Comparison of C:N ratios changes over time. Bottom circle represents approximately 120 years BP, the middle circle represents approximately 40 years BP, and the top circle represents present day. Arrows indicate direction of increasing marine influence based on decreasing C:N ratios.

2000). Letrick (2003) reported high C:N values (range between 12.21 and 40), strongly depleted $\delta^{13}C$ signatures indicative of terrestrial input, and percent organic matter values ranging between 1.6 and 6.7 from Croatan Sound. It is possible to attribute the terrestrial signature recorded by the C:N ratios in the northern section of Pamlico Sound to these eroding peats and other terrestrial inputs from Croatan Sound.

Water draining through the Roanoke and Croatan Sounds into the northern section of Pamlico Sound is brackish. The foraminiferal assemblage in the northern section of Pamlico Sound (Estuarine Biofacies A) is indicative of brackish environments. This observation supports the interpretation of a terrestrial influence on the northern section of the Sound.

The amount of organic carbon present in cores has increased between the intervals representing 120 years BP and 40 years BP at some sites. The rate of increase has been steady for most sites (S31, S32, S41, S42, S50, S59, and S60), while other sites have had a dramatic increase (S10 and S11). These variations are indicative of changing depositional patterns and possible episodic erosion events. A number of variables are responsible for shoreline erosion, such as physical setting and boat traffic (Riggs and Ames, 2003). S10 and S11 are located near a marsh. The increased percentages of organic carbon found in the cores may be explained by erosion of the nearby marsh. S23 shows the greatest fluctuation in percent organic carbon between the intervals representing approximately 120 years and 40 years BP. There is also a change in lithology from sandy mud (silt and clay particles) to coarse sands with shell fragments. This evidence indicates that there has been a change in the distribution of sediments

within the Sound with coarse sediments indicative of higher energy environments. Increased percent organic carbon is observed in the top centimeters at S32, S60, and S61 as well. These sites are located along the platforms defining the central basins. The sediment found in the upper centimeters is fine, silty material with some shell fragments. The increased amount of organic carbon and fine sediment in the upper few centimeters and the location of these sites suggests that S32, S60, and S61 may act as regions of deposition for eroded material from the mainland.

Marsh foraminifera present at depth at sites S9 and S30 may be indicative of another storm event about 40 years ago. The Ash Wednesday Storm was a class 5 (as determined by the Dolan/Davis Northeaster Intensity scale, 1-5) nor'easter that impacted coastal North Carolina for two days in March 1962. Ranked as extreme, class 5 storms often cause up to 50m of beach erosion, extensive and widespread destruction of dunes, massive overwash, and inlet formation (Pilkey et al., 1998). The Ash Wednesday Storm is considered the most destructive nor'easter of the twentieth century. Strong winds and waves caused flooding and overwashing for large portions of the beach. Some areas flooded between 2 to 4 feet. Several breaches were cut into the barrier islands, including Buxton Inlet, exposing the once protected Pamlico Sound to the Atlantic Ocean (Pilkey et al., 1998).

Strong northeasterly winds push estuarine water to the southernmost section of Pamlico Sound. As a result, high standing water in the south flood the area while low standing water in the north erodes the shoreline (marsh shoreline) (Riggs and Ames, 2003). The affects of this storm could explain the presence of marsh foraminifera found

at depth at sites S9 and S30. These foraminifera may have been transported towards the center of the Sound following severe erosion of the marsh shoreline. Erosion supplies sand to the platforms and mud to the central basin of the Sound (Riggs, 1996). The Ash Wednesday Storm could also explain the strong peak (4.28%) in organic carbon seen at the 8-10cm interval at S30, which occurs just above the interval representing the peak activity in ^{137}Cs.

Figure 52 displays the relationship between $\delta^{13}C$ and $\delta^{15}N$ for the three time intervals determined by radionuclides. S27 is not included because the recorded $\delta^{13}C$ signatures down-core proved the site to be very different from the rest of the sites within Pamlico Sound.

There is an increasing direct relationship over time between $\delta^{13}C$ and $\delta^{15}N$ signatures in Pamlico Sound (Figure 52) but there is very little change in range for $\delta^{13}C$ signatures for the three time slices. Results from the one-way ANOVA test suggest that there is not significant change over time in $\delta^{13}C$ signatures (Tables 8 and 11). This indicates that the terrestrially influenced source of organic matter has not varied over the last century. However, the ANOVA results (Tables 9 and 11) indicate that there is an observed enrichment in $\delta^{15}N$ signatures over time. The greatest increase is observed between the 120 years BP and 40 years BP time slices. As mentioned before, a shift in $\delta^{15}N$ signatures is observed in the 40 years BP time slice in most cores. The change can be attributed to several processes. For example, an increase in NH_4^+ delivery into the water-column can result in the increase of nitrification-denitrification, and assimilation. All of these biogeochemical processes result in the enrichment of $\delta^{15}N$ signatures (see

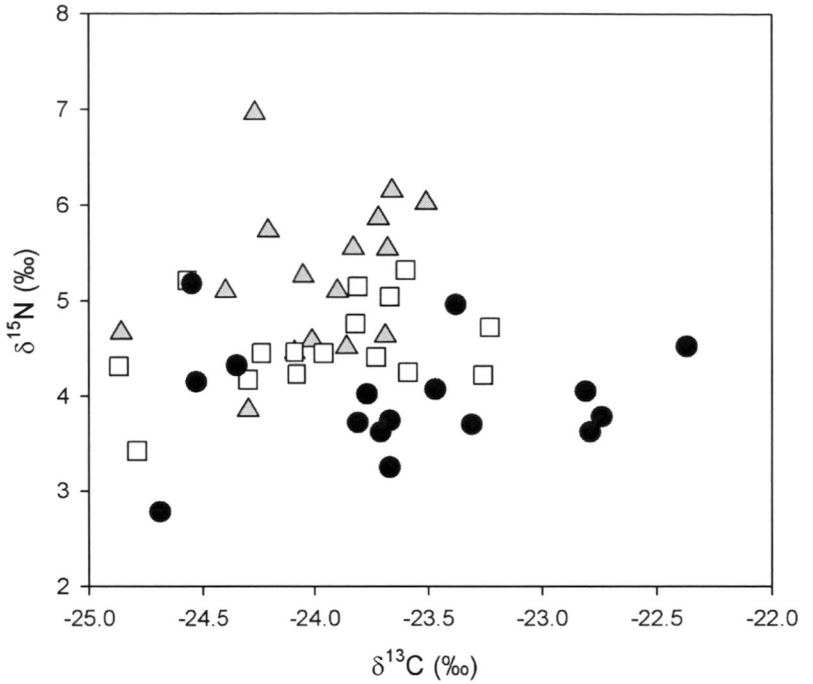

Figure 52: $\delta^{13}C$ signatures versus $\delta^{15}N$ signatures over the last approximate 120 years BP. Signatures are evaluated at three time slices, approximately 120 years BP (closed circles), approximately 40 years BP (open squares), and present day (shaded triangles).

Previous Works, significance of $\delta^{15}N$ signatures). A possible explanation for observed enrichment could be the amount of shrimp trawling within Pamlico Sound.

Shrimp trawling in Pamlico Sound began in 1912. The conditions found within Pamlico Sound make it an excellent environment for shrimp to proliferate. Shrimp breed all year long, making them a 'year long crop.' By the mid 1950s, trawlers were bringing in close to seven million pounds of shrimp a year. By the 1960s, it became apparent to shrimpers that the environmental conditions within the Sound would not allow shrimp to be overfished (NCFA, 2001). Trawling disturbs the seafloor by resuspending sediments. The large amount of trawling occurring in the Sound during the early 1960s may have continuously resuspended sediment. $\delta^{15}N$ signatures within sediment are a result of

nitrogen cycling within the water column and interactions with the surficial sediment (Bratton et al., 2003). The longer sediment is suspended in the water column, the longer the time frame for biogeochemical processes to enrich the sediment in ^{15}N.

CONCLUSIONS

Significant paleoenvironmental changes for Pamlico Sound, North Carolina, are observed in down-core sediments. Environmental conditions existing within the Sound over the last century were analyzed using foraminiferal data, stable isotope (C and N) data, C:N ratios, percent OC, and radionuclide data. For comparison, these changes were evaluated at three time slices (1) present day, or modern environment as determined by the surficial (0-2cm) sediments, (2) the intervals representing approximately 120 years BP, as determined by ^{210}Pb activity, and (3) the intervals representing approximately 40 years BP, as determined by ^{137}Cs activity.

There has been a steady increasing marine influence within Pamlico Sound over the last century based on foraminiferal assemblages and C:N ratios. Greater C:N ratios are observed at the depth representing approximately 120 years BP. C:N ratios steadily decrease up-core, which is indicative of a more marine influence of the Sound over time. The change in the foraminiferal assemblage patterns observed at the intervals representing approximately 120 years BP, 40 years BP, and the modern surficial (0-1cm) intervals confirm that salinity has increased over the last century within Pamlico Sound. Estuarine Biofacies A, which is indicative of a more brackish environment, was the dominant assemblage within Pamlico Sound approximately 120 years BP. The foraminiferal assemblage representing approximately 40 years BP is comparable to the modern day assemblage. However, Estuarine Biofacies B, which is characteristic of higher salinity, was not as widespread throughout the Sound as it is today. It is possible

to attribute these foraminiferal assemblage changes to major storm activity; hurricanes 120 years ago and the Ash Wednesday nor'easter 40 years ago.

An increasing trend is observed between $\delta^{13}C$ and $\delta^{15}N$ signatures over the last century. The average range for $\delta^{13}C$ signatures is typical of terrestrial sediment input and has changed little over time. This suggests that the source area for the sediments being deposited within Pamlico Sound has not changed.

The average range for $\delta^{15}N$ signatures has increased over time. Recorded signatures are more enriched in $\delta^{15}N$ at the surface than they were approximately 120 years BP. The greatest change is observed at intervals representing approximately the early 1960s as determined by radionuclide data. These changes can be explained by anthropogenic influences, in particular, shrimp trawling.

In the early 1960s, trawling for shrimp increased tremendously. Trawling resuspends sediment into the water column allowing more time for biogeochemical processes to occur before settling and re-depositing. For example, the longer sediment remains suspended, the more denitrification occurs thus enriching the $\delta^{15}N$ signature. The widespread continued increase (enrichment) in $\delta^{15}N$ signatures up-core indicates that these environmental processes are still occurring within Pamlico Sound.

REFERENCES

Anderson, H.V., 1952. Buccella, a new genus of the rotalid Foraminifera. Journal of the Washington Academy of Sciences 42, 143-151.

Anderson, WT., and Fourqurean, J.W., 2003. Intra- and interannual variability in seagrass carbon and nitrogen stable isotopes from south Florida, a preliminary study. Organic Geochemistry 34, 185-194.

Appleby, P.G., and Oldfield, F., 1992. Application of lead-210 to sedimentation studies, *in* Ivanovich, M., and Harmon, R.S., eds., Uranium-Series Disequilibrium: Applications to Earth, Marine, Environmental Problems: Oxford, UK, Clarendon Press, p. 731-778.

Bandy, O.L., 1954. Distribution of some shallow-water foraminifera in the Gulf of Mexico. Geological Survey Professional Paper 254-F, 125-139.

Barnes, J., 2001. North Carolina's hurricane history. The University of North Carolina Press, Chapel Hill, NC, 319p.

Benniger, L.K., and Wells, J.T., 1993. Sources of sediment to the Nuese River estuary, North Carolina. Marine Chemistry 43, 137-156.

Boltovskoy, E., and Wright, R., 1976. Recent Foraminifera. The Hague, 515p.

Bratton, J.F., Colman, S.M., and Seal, R.R. II, 2003. Eutrophication and carbon sources in Chesapeake Bay over the last 2700 yr: human impacts in context. Geochemica et Cosmochimica Acta 67, 3385-3402.

Buzas, M.A., 1965. The distribution and abundance of foraminifera in Long Island Sound. Smithsonian Miscellaneous Collections 149, 89p.

Buzas, M.A., 1979. Quantitative biofacies analysis, *in* Foraminiferal Ecology and Paleocology, SEPM Short Course No. 6, Houston, TX, p. 17-19.

Buzas, M.A., 1990. Another look at confidence limits for species proportions. Journal of Paleontology 64, 842-843.

Buzas, M.A., Culver, S.J., and Isham, L.B., 1985. A comparison of fourteen Elphidiid (Foraminiferida) taxa. Journal of Paleontology 59, 1075-1090.

Buzas, M.A., and Gibson, T.G., 1969. Species diversity: benthonic foraminifera of western North Atlantic. Science 163, 72-75.

Buzas-Stephens, P., Pessagon, E.A. Jr, and Bowen, C.J., 2003. Foraminiferal response to habitat desruption: Arroyo Colorado, Texas. Journal of Foraminiferal Research 33, 294-308.

Chmura, G.L., and Kosters, E.C., 1994. Storm deposition and Cs-137 Accumulation in fine-grained marsh sediments of the Mississippi delta plain. Estuarine, Coastal, and Shelf Science 39, 33-44.

Cifuentes, L.A., Sharp, J.H., Fogel, M.L., 1988. Stable carbon and nitrogen isotope biogeochemistry in the Delaware estuary. Limnology and Oceanography 33, 1102-1115.

Cifuentes, L.A., Coffin, R.B., Solorzano, L., Cardenas, W., Espinoza, J., and Twilley, R.R., 1996. Isotopic and elemental variations of carbon and nitrogen in a mangrove estuary. Estuarine, Coastal and Shelf Science 43, 781-800.

Collins, E.S., 1996. Marsh-estuarine benthic foraminiferal distributions and Holocene sea-level reconstructions along the South Carolina coastline. PhD Thesis, Dalhousie University, Halifax, Nova Scotia. 240p.

Corbett, D.R., Tully, L.S., Vance, D.J., Abbene, I.J., Smith, C.G., and Dail, M., 2004. Sediment dynamics in the Albemarle-Pamlico Estuarine System, North Carolina: A storm driven process?. GSA Abstracts with Programs 36, p.64.

Culver, S.J., and Buzas, M.A., 1980. Distribution of recent benthic foraminifera off the North American Atlantic coast. Smithsonian Contributions to the Marine Sciences, Smithsonian Institution Press, Washington, D.C., 512p.

Culver, S.J., and Buzas, M.A., 1981. Recent benthic foraminiferal provinces on the Atlantic continental margin of North America. Journal of Foraminiferal Research 11, 217-240.

Culver, S.J., Woo, H.J., Oertel, G.F., and Buzas, M.A., 1996. Foraminifera of coastal depositional environments, Virginia, U.S.A.: Distribuition and Taphonomy. Palaios 11, 459-486.

Cushman, J.A., 1947. New species and varieties of Foraminifera from off the southeastern coast of the United States. Contributions from the Cushman Laboratory for Foraminiferal Research 23 37-42.

Cushman, J.A., and Brönnimann, P., 1948a. Additional new species of arenaceous Foraminifera from the shallow waters of Trinidad. Contibutions from the Cushman Laboratory for Foraminifera Research 24, 37-42.

Cushman, J.A., and Brönnimann, P., 1948b. Some new genera and species of Foraminifera from brackish water of Trinidad. Contributions from the Cushman Laboratory for Foraminiferal Research 24, 15-21.

Davis, J.C., 1973. Statistics and Data Analysis in Geology. John Wiley and Sons, Inc., New York, NY, 550p.

Dellapenna, T.M., Kuehl, S.A., Schaffner, L.C., 1998. Sea-bed Mixing and Particle Residence Times in Biologically and Physically Dominated Estuarine Systems: a Comparison of Lower Chesapeake Bay and the York River Subestuary. Estuarine, Coastal and Shelf Science 46, 777 -795.

Donnelly, J.P., Roll, S., Wengren, M., Butler, J., Lederer, R., and Webb, III, T., 2001a. Sedimentary evidence of intense hurricane strikes from New Jersey Geology 29, 615-618.

Donnelly, J.P., Bryant, S.S., Butler, J., Dowling, J., Fan, L., Hausmann, N., Newby, P., Shuman, B., Stern, J., Westover, K., and Webb, III, T., 2001b. 700 yr sedimentary record of intense hurricane landfalls in southern New England. Geological Society of America Bulletin 113, 714-727.

Dortch, Q., Peterson, J. and Turner, R., 1998. Algal bloom resulting from the opening of the Bonnet Carre spillway in 1997. Fourth Bi-annual Basics of the Basin Symposium, 28-29.

Dyer, K.R., 1997. Estuaries, A Physical Introduction. John Wiley and Sons, Inc., New York, NY, 195p.

Ellison, R.L., and Nichols, M.M., 1970. Estuarine foraminifera from the Rappahannock River, Virginia. Contributions from the Cushman Foundation for Foraminiferal Research 21, 1-17.

Faure, G., 1998. Principles and applications of geochemistry, second edition. Prentice Hall, Upper Saddle River, NJ, 315-317.

Giese, G.l., Wilder, H.B., and Parker, Jr., G.G., 1985. Hydrology of major estuaries and sounds of North Carolina. USGS Water-Supply Paper 2221, 105p.

Graham, M.C., Eaves, M.A., Farmer, J.G., Dobson, J., Fallick, A.E., 2001. A study of carbon and nitrogen stable isotope and elemental ratios as potential indicators of source and fate of organic matter in sediments of the Forth Estuary, Scotland. Estuarine, Coastal and Shelf Science 52, 375-380.

Goldstein, S.T, and Wakins, G.T., 1999. Taphonomy of salt marsh foraminifera: an example from coastal Georgia. Palaeogeography, Palaeoclimatology, Palaeoecology 149, 103-114.

Goldstein, S.T., Watkins, G.T., and Kuhn, R.M., 1995. Microhabits of salt marsh foraminifera: St. Catherines Island, Georgia, USA. Marine Micropaleontolgy 26, 17-29.

Gordon, E.S., Goñi, M.A., Roberts, Q.N., Kineke, G.C., and Allison, M.A., 2001. Organic matter distribution and accumulation on the inner Louisiana shelf west of Atchafalaya River. Continental Shelf Research 21, 1691-1721.

Grossman, S., 1967. Part 1, Living and subfossil Rhisopod and Ostracode populations, In, Grossman, S., and Benson, R.H., Ecology of Rhizopodea and Ostracoda of southern Pamlico Sound region, North Carolina: Kansas University, Paleontology Contributions 44, 1-82.

Grossman, S., and Benson, R.H., 1967. Ecology of Rhizopodea and Ostracoda of southern Pamlico Sound region, North Carolina: Kansas University, Paleontology Contributions 44, 1-90.

Harris, D., Horwath, W.R., and Kessel, C.V., 2001. Acid fumigation of soils to remove carbonates prior to total organic carbon or carbon-13 isotope analysis. Soil Science Society of America Journal 65, 1853-1856.

Hayek, L.C., and Buzas, M.A., 1997. Surveying Natural Populations. Columbia University Press, New York, 563p.

Hazel, J.E., 1977. Use of certain multivariate and other techniques in assemblage zonal biostratigraphy: examples utilizing Cambrian, Cretaceous, Tertiary Benthic invertebrates, *in* Kauffman, E.G, and Hazel J.E., eds., Concepts and Methods of Biostratigraphy: Stroudsburg, PA, Dowden, Hutchinson and Ross, Inc., p. 210-211.

Jeter, H.W., 2000. Determining the ages of recent sediments using measurements of trace radioactivity. Terra et Aqua 78, 21-28.

Karlsen, A. A., Cronin, T.M, Ishman, S.E., Wilard, D.A., Holmes, C.W., and Kerhin, R., 2000. Historical trends in Chesapeake Bay dissolved oxygen based on benthic foraminifera from sediment cores. Estuaries 23, 488-508.

Kemp, W.M., Sampou, P., Caffrey, J., and Mayer, M., 1990. Ammonium recycling versus denitrification in Chesapeake Bay sediments. Limnology and Oceanography 35, 1545-1563.

Koch, C.F., 1987. Prediction of sample size effects on the measured temporal and geographic distribution of species. Paleobiology 13, 100-107.

Kornfield, M.M., 1931. Recent littoral Foraminifera from Texas and Louisiana. Contributions from the Department of Geology of Stanford University, 1, 77-101.

Lehmann, M.F., Bernasconi, B.M., Barbieri, A., McKenzie, J.A., 2002. Preservation of organic matter and alteration of its carbon and nitrogen isotope composition during simulated and in situ early sedimentary diagenesis. Geochimica et Cosmoschimica Acta 66, 3573-3584.

LeFurgey, A., 1976. Recent benthic foraminifera from Roanoke, Croatan, and northern Pamlico Sounds, North Carolina. PhD Dissertation, University of North Carolina Chapel Hill, Chapel Hill, NC. 382p.

Letrick, E., 2003. Sedimentology and geochemistry of estuarine sediments from the Albemarle Sound and adjacent tributaries in Eastern North Carolina. MS Thesis, East Carolina University, Greenville, NC.143p.

Lewis, R.C., Coale, K.H., Edwards, B.d., Marot, M., Douglas, J.N., Burton, E.J., 2002. Accumulation rate and mixing of shelf sediments in the Monterey Bay National Marine Sanctuary. Marine Geology 181, 157-169.

Loeblick, A.R., Jr., and Tappan, H., 1994. Foraminifera of the Sahul Shelf and Timor Sea. Cushman Foundation for Foraminiferal Research, Special Publication No. 31, 661p.

Maksymowska, D., Richard, P., Piekarek-Jankowska, H., Riera, P., 2000. Chemical and isotopic composition of the organic matter sources in the Gulf of Gdansk (Southern Baltic Sea). Estuarine, Coastal and Shelf Science 51, 585-598.

Marshall, N., 1951. Hydrography of North Carolina marine waters. Harden A. Taylor and Associates, Survey of Marine Fisheries of North Carolina. University of North Carolina Press, Chapel Hill, 1-76.

Matson, E.A., and Brinson, M.M., 1990. Stable carbon isotopes and the C:N ratio in the estuaries of the Pamlico and Neuse Rivers, North Carolina. Limnology and Oceanography 35, 1290-1300.

Mello, J.F., and Buzas, M.A., 1968. An application of cluster analysis as a method of determining biofacies. Journal of Paleontology 42, 747-758.

Middleburg, J.J., and Nieuwenhuize, J., 1998. Carbon and nitrogen stable isotopes in suspended matter and sediments from the Schelde Estuary. Marine Chemistry 60, 217-225.

MODMON, 2001. Modeling and Monitoring of the Neuse River Estuary. www.marine.unc.edu/neuse/modmon/publications/publications.html

Montoya, J.P., Korrigan, S.G., and McCarthy, J.J., 1991. Rapid, storm-induced changes in the natural abundance of 15N in a planktonic ecosystem, Chesapeake Bay, USA. Geochimica et Cosmochimica Acta 55, 3627-3638.

Munsterman, D., and Kerstholt, S., 1996. Sodium polytungstate, a new non-toxic alternative to bromoform in heavy liquid separation. Review of Palaeobotany and Palynology 91, 417-422.

Müller, A., and Voss, M., 1999. The palaeoenvironments of coastal lagoons in the southern Baltic Sea, II. $\delta^{13}C$ and d15N ratios of organic matter-sources and sediments. Palaeography, Palaeoclimatology, Palaeoecology 145, 17-32.

Murray, J.W., 1973. Distribution and Ecology of Living Benthic Foraminiferids. Heinemann Educational Books Limited, London, England, 274p.

Neubauer, S.C., Anderson, I.C., Constantine, J.A., and Kuehl, S.A., 2002. Sediment Deposition and Accretion in a Mid-Atlantic (U.S.A.) Tidal Freshwater Marsh. Estuarine, Coastal, and Shelf Science 54, 713-727.

NCFA, 2001. North Carolina Fisheries Association, Shrimp Trawling. www.ncfish.org/2001/july/archives.htm

Nichols, M., and Norton, W., 1969. Foraminiferal populations in a coastal plain estuary. Palaeogeography, Palaeoclimatology, Palaeoecology 6, 197-213.

Paerl, H.W., Bales, J.D., Ausley, L.W., Buzzelli, C.P., Crowder, L.B., Eby, L.A., Fear, J. M., Go, M., Peierls, B.L., Richardson, T.L., and Ramus, J.S., 2001. Ecosystem impacts of three sequential hurricanes (Dennis, Floyd, and Irene) on the United States' largest lagoonal estuary, Pamlico Sound, NC. Proceedings of the National Academy of Sciences 98, 5655-5660.

Parker, F.L., 1952a. Foraminiferal distribution in the Long Island Sound – Buzzards Bay area. Bulletin of the Museum of Comaparative Zoology 111, 451-588.

Parker, F.L., 1952b. Foraminiferal species off Portsmouth, New Hampshire. Bulletin of the Museum of Comparative Zoology 106, 391-423.

Parker, R.L., and Athearn, W.D., 1959. Ecology of marsh foraminifera in Poponesset Bay, Massachusetts. Journal of Paleontology 33, 333-343.

Peters, K.E., Sweeney, R.E., and Kaplan, 1978. Correlation of carbon and nitrogen stable isotope ratios in sedimentary organic matter. Limnology and Oceanography 23, 598-604.

Peterson, B.J., Howarth, R.W., and Garritt, R.H., 1985. Multiple stable isotopes used to trace the flow of organic matter in estuarine food webs. Science 227, 1361-1363.

Pietrafesa, L.J., Janowitz, G.S., Chao, T.Y., Weisberg, R.H., Askari, F., and Noble, E., 1986. The physical oceanography of Pamlico Sound. UNC Sea Grant Publication UNC-WP-86-5.

Pilkey, O.H., neal, W.J., Riggs, S.R., Webb, C.A., Bush, D.M., Pilkey, D.F., Bullock, J., and Cowan, B.A., 1998. The North Carolina shore and its barrier islands, restless ribbons of sand. Duke University Press, Durham, NC, 318p.

Ravichandran, M., Baskaran, M., Santschi, P.H., Bianchi, T.S., 1995. Geochronology of sediments in the Sabine-Neches estuary, Texas, U.S.A. Chemical Geology (Isotopic Geosciences Section) 125, 291-306.

Riggs, S.R., York, L.L., Wehmiller, J.F., and Snyder, S.W., 1992. Depositional patterns resulting from high-frequency Quaternary sea-level fluctuations in northeastern North Carolina. Quaternary Coasts of the United States: Marine and Lacustrine Systems, SEPM Special Publication No. 48, p.141-153.

Riggs, S.R., Cleary, W.J., Synder, S.W., 1995. Influence of inherited geologic framework on barrier shoreface morphology and dynamics. Marine Geology 126, 213-234.

Riggs, S.R., Rudolph, G.L., and Ames, D.V., 2000. Erosional scour and geologic evolution of Croatan Sound, Northeastern North Carolina. CTE/NCDOT Joint Environmental Research Program, report number: FHWA/NC/2000-002.

Riggs, S.R., and Ames, D.V., 2003. Drowning the North Carolina coast: sea-level rise and estuarine dynamics. North Carolina Sea Grant, North Carolina University, Raleigh, NC, 152p.

Robinson, M.M., and McBride, R.A., 2003. Old Currituck Inlet, VA/NC: Inlet history documented by foraminiferal evidence (Part II). Proceedings Coastal Sediments '03, ASCE Press, 14pp.

Roelofs, E.W., and Bumpus, D.F., 1953. The hydrography of Pamlico Sound: Bulletin Marine Science, Gulf and Caribbean 3, 181-205.

Saffert, H., and Thomas, E., 1998. Living foraminifera and total populations in salt marsh peat cores: Kelsey Marsh (Clinton, CT) and the Great Marshes (Barnstable, MA). Marine Micropaleontolgy 33, 175-202.

Saunders, J.B., 1957. Trochamminidae and certain Lituolidae (Foraminifera) from the Recent brackish-water sediments of Trinidad, Bristh West Indies. Smithsonian Miscellaneous Collections 134, 16pp.

Schafer, C.T., and Cole, F.E., 1978. Distribution of Foraminifera in Chaleur Bay, Gulf of St. Lawrence. Geological Survey of Canada 77-30, 1-55.

Schlesinger, W.H., 1997. Biogeochemistry, an analysis of global change, second edition. Academic Press, San Diego, CA, 588p.

Schnitker, D., 1971. Distribution of foraminifera on the North Carolina continental shelf. Tulane Studies in Geology and Paleontology 8 169-215.

Scott, D.B. and Medioli, F.S., 1980. Living vs. total foraminiferal populations: their usefulness in paleoecology. Journal of Paleontology 54, 814-831.

Scott, D.B., Medioli, F.S., and Schafer, C.T., 1977. Temporal changes in foraminiferal distributions in Miramichi River estuary, New Brunswick. Canadian Journal of Earth Sciences 14, 1566-1587.

Scott, D.B., Medioli, F.S., and Schafer, C.T., 2001. Monitoring in coastal environments using foraminifiera and thecamoebian indicators. Cambridge University Press, NY, 167p.

Sen Gupta, B.K., 1971. the benthonic foraminifera of the tail of the Grand Banks. Micropaleontology 17, 69-98.

Singer, J.J., and Knowles, C.E., 1975. Hydrology and circulation patterns in the vicinity of Oregon Inlet and Roanoke Island, North Carolina. University of North Carolina Sea Grant Program Publication, UNC-SG-75-15, 171p.

Struck, U., Emeis, K.C., Voss, M., Christiansen, C., and Kunzendorf, H., 2000. Records of southern and central Baltic Sea eutrophication in $\delta^{13}C$ and $\delta^{15}N$ of sedimentary organic matter. Marine Geology 164, 157-171.

Smith, R.L., and Smith, T.M., 1998 Elements of Ecology, forth edition. Benjamin/Cummings Science Publishing, San Francisco, CA. 99: 21-25.

Thomas, E., Gapotchenko, T., Varekamp, J.C., Mecray, E.L., Buchholtz ten Brink, M.R., 2000. Benthic Foraminifera and Environmental Changes in Long Island Sound. Journal of Coastal Research 16, 641-655.

Thornton, S.F., and McManus, J., 1994. Application of Organic Carbon and Nitrogen Stable Isotope and C/N Ratios as Source Indicators of Organic Matter Provenance in Estuarine Systems: Evidence from the Tay Estuary, Scotland. Estuarine, Coastal, and Shelf Science 38, 219-233.

Todd, R., and Brönnimann, P., 1957. Recent Foraminifera and Thecamoebina from the Eastern Gulf of Paria. Contributions from the Cushman Foundation for Foraminiferal Research 12, 5-21.

Tully, L.S., 2004. Evaluation of sediment dynamics using geochemical tracers in the Pamlico Sound estuarine system, North Carolina. MS Thesis, East Carolina University, Greenville, NC, 168p.

Usui, T., Koike, I., and Ogura, N., 2001. N_2O production, nitrification and denitrification in an estuarine sediment. Estuarine, Coastal and Shelf Science 52, 769-781.

Vance, D.J., 2004. Modern and historic trends in foraminiferal distributions and sediment dynamics in the Albemarle estuarine system, North Carolina. MS Thesis, East Carolina University, Greenville, NC, 249p.

Voss, M., Larsen, B., Leivuori, M., and Vallius, H., 2000. Stable isotope signals of eutrophication in Baltic Sea sediments. Journal of Marine Systems 25, 287-298.

Waller, S.S., and Lewis, J.K., 1979. Occurrence of C_3 and C_4 photosynthetic pathways in North American grasses. Journal of Range Management 32, 12-28.

Walton, W.R., 1952. Techniques for recognition of living foraminifera. Contributions from the Cushman Foundation for Foraminiferal Research 3, 56-60.

Warren, A.D., 1957. Foraminifera of the Buras-Scofield Bayou-region, southeast Louisisana. Contributions from the Cushman foundation for Foraminiferal Research 8, 29-40.

Wells, J.T., and Kim, S., 1989. Sedimentation in the Albemarle-Pamlico lagoonal system: synthesis and hypotheses. Marine Geology 88, 263-284.

Williams, A.B., Posner, G.S., Woods, W.J., and Deubler, Jr., E.E., 1973. A hydrographic atlas of larger North Carolina sounds. Sea Grant Publication No UNC-SG-73-02, University of North Carolina, Chapel Hill, NC.

Woo, H.J., Culver, S.J., and Oertel, G.F., 1997. Benthic foraminiferal communities of a barrier-lagoon system, Virginia, U.S.A. Journal of Coastal Research 13, 1192-1200.

Woo, H.J., 1992. Distribution of foraminifera and pollen in coastal depositional environments of the Southern Delmarva Peninsula, Virginia, U.S.A. PhD. Dissertation, Old Dominion University, Norfolk, VA, 298p.

Workman, Jr., R.R., 1981. Foraminiferal assemblages of the nearshore inner continental shelf, Nags Head, and Wilmington areas, North Carolina. M.S. Thesis, East Carolina University, Greenville, NC, 162p.

Zimmerman, A.R., and Canuel, E.A., 2000. A geochemical record of eutrophication and anoxia in Chesapeake Bay sediments: anthropogenic influence on organic matter composition. Marine Chemistry 69, 117-137.

PLATE 1

(bar = 50 μm)

Figures

1	*Ammoastuta inepta* Cushman and McCulloch; lateral view
2	*Ammobaculites crassus* Warren: lateral view
3	*Ammobaculites dilatatus* Cushman and Brönnimann; lateral view
4	*Ammobaculites exiguus* Cushman and Brönnimann; lateral view
5, 6	*Ammonia parkinsoniana* (d'Orbigny); dorsal and ventral view
7, 11	*Ammonia tepida* (Cushman); dorsal and ventral view
8	*Ammotium salsum* (Cushman and Brönnimann); lateral view
9, 10	*Arenoparrella mexicana* (Kornfield); dorsal and ventral view
12, 13	*Asterigerinata carinata* d'Orbigny; dorsal and ventral view
14, 15	*Buccella frigida* (Cushman); dorsal and ventral view
16, 17	*Buccella inusitata* Andersen; dorsal and ventral view
18, 19	*Cibicides lobatulus* (Walker and Jacob); dorsal and ventral view

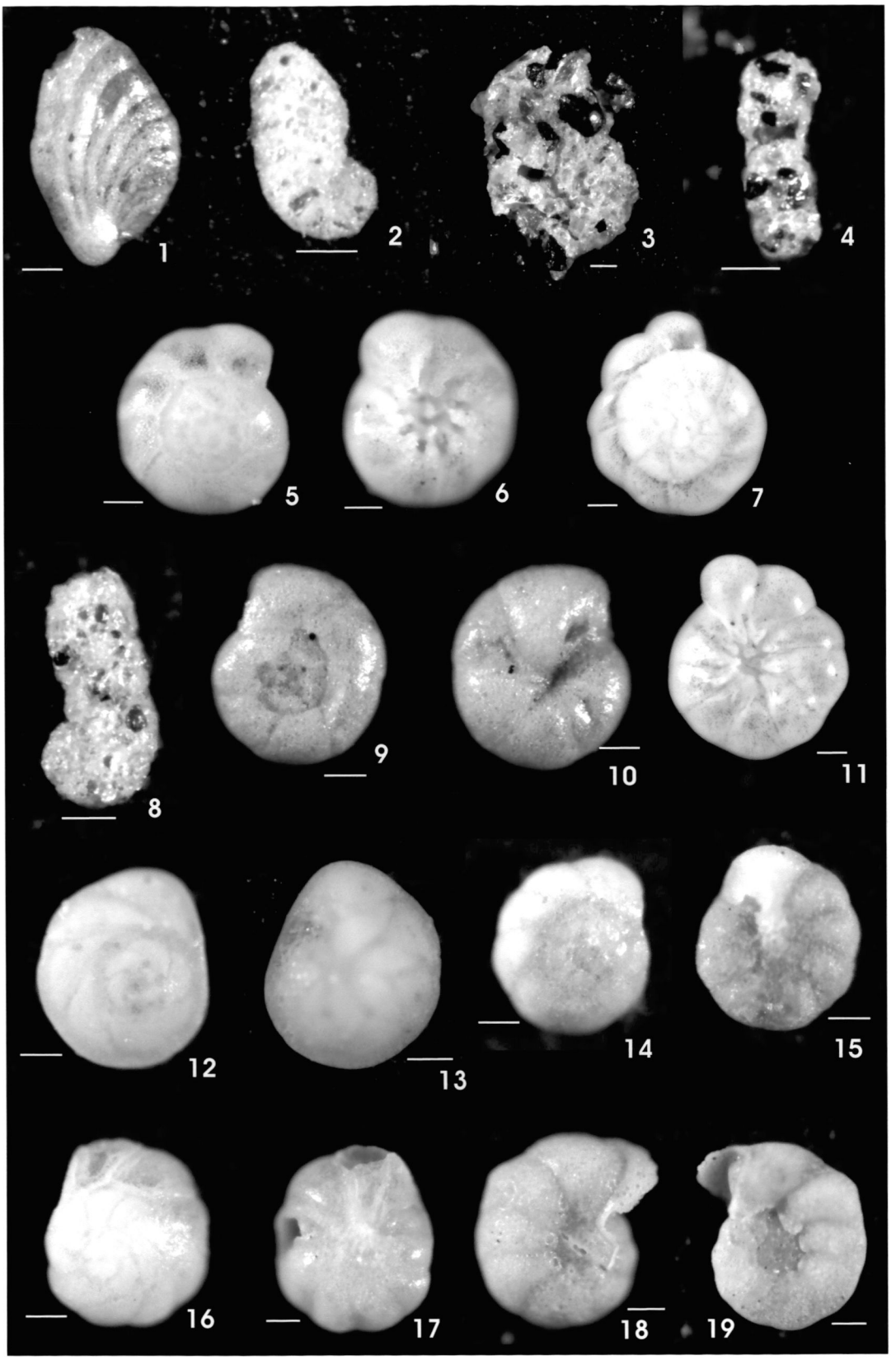
1
2
3
4
5
6
7
8
9
10
11
12
13
14
15
16
17
18
19

PLATE 2

(bar = 50 μm)

Figures

1, 2 *Cibicides refulgens* Montfort; dorsal and ventral view

3 *Elphidium excavatum* (Terquem); lateral view

4 *Elphidium galvestonense* Kornfield; lateral view

5 *Elphidium gunteri* Cole; lateral view

6 *Elphidium mexicanum* (Kornfield); lateral view

7 *Elphidium* cf. *E. mexicanum*; lateral view

8 *Elphidium subarcticum* Cushman; lateral view

9, 10 *Hanzawaia strattoni* (Applin); dorsal and ventral view

11 *Haplophragmoides bonplandi* Todd and Brönnimann; lateral view

12 *Haplophragmoides wilberti* Andersen; lateral view

13 *Haynesina germanica* (Ehrenberg); lateral view

14, 15 *Jadammina macrescens* (Brady); dorsal and ventral view

16 *Miliammina fusca* (Brady); lateral view

17 *Miliammina petila* Saunders; lateral view

18 *Pseudoclavulina gracilis* Cushman and Brönnimann; lateral view

19 *Nonionella atlantica* Cushman; lateral view

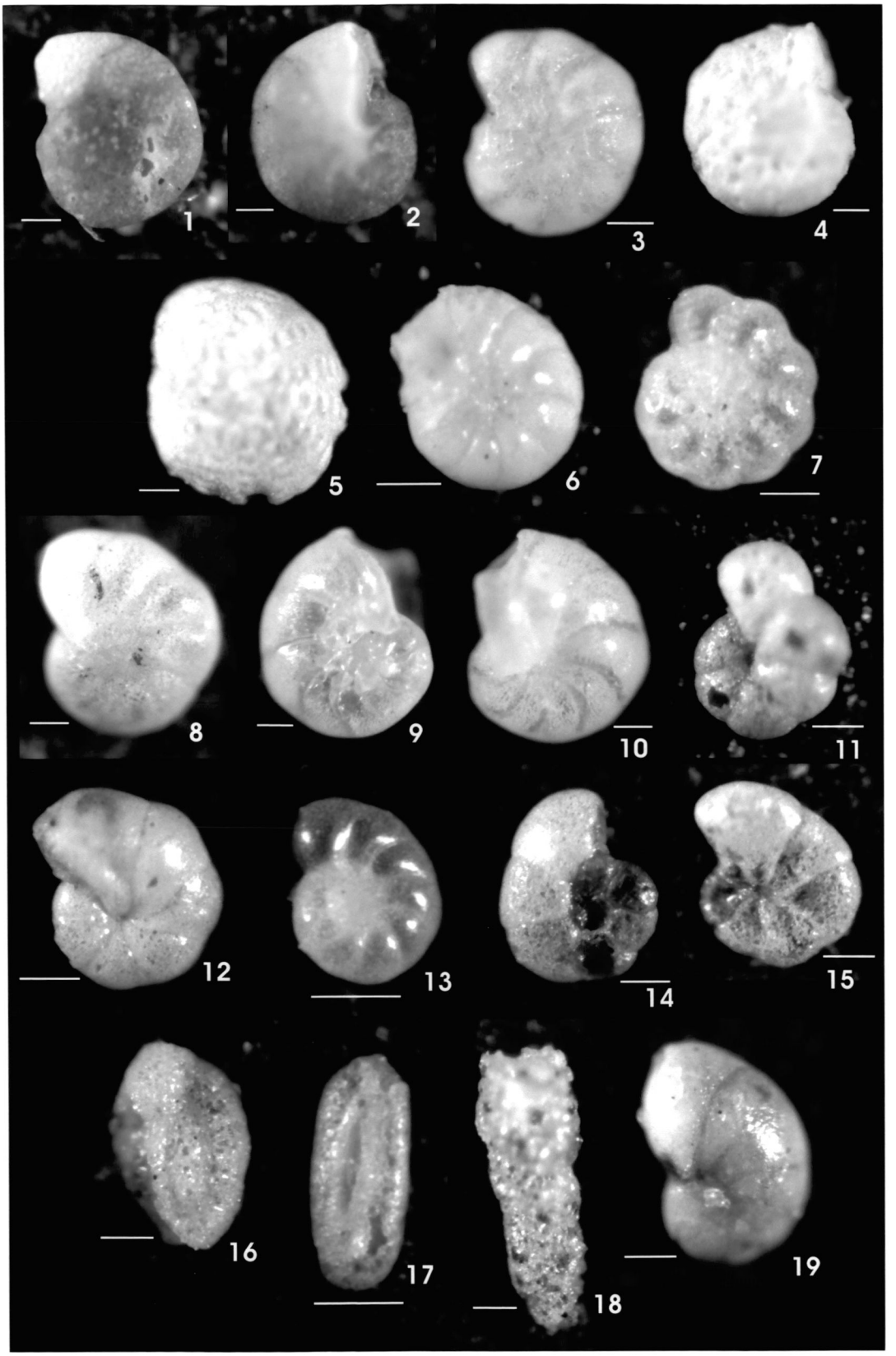
1
2
3
4
5
6
7
8
9
10
11
12
13
14
15
16
17
18
19

PLATE 3

(bar = 50 μm)

Figures

1, 2 *Poroeponides lateralis* (Terquem); dorsal and ventral view

3 *Quinqueloculina lamarckiana* d'Orbigny; lateral view

4 *Quinqueloculina jugosa* (Cushman); lateral view

5 *Quinqueloculina seminula* (Linné); lateral view

6 *Quinqueloculina* sp. C; lateral view

7 *Reophax* sp.; lateral view

8, 9 *Siphotrochammina lobata* Saunders; dorsal and ventral view

10 *Textularia earlandi* Phleger; lateral view

11 *Textularia* cf. *T. gramen* (Todd and Brönnimann); lateral view

12 *Textularia* sp.; lateral view

13, 17 *Tiphotrocha comprimata* (Cushman and Brönnimann); dorsal and ventral view

14, 15 *Trochammina inflata* (Montagu); dorsal and ventral view

16 *Trochamminita irregularis* Cushman and Brönnimann; lateral view

18 *Trochammina* sp.; lateral view

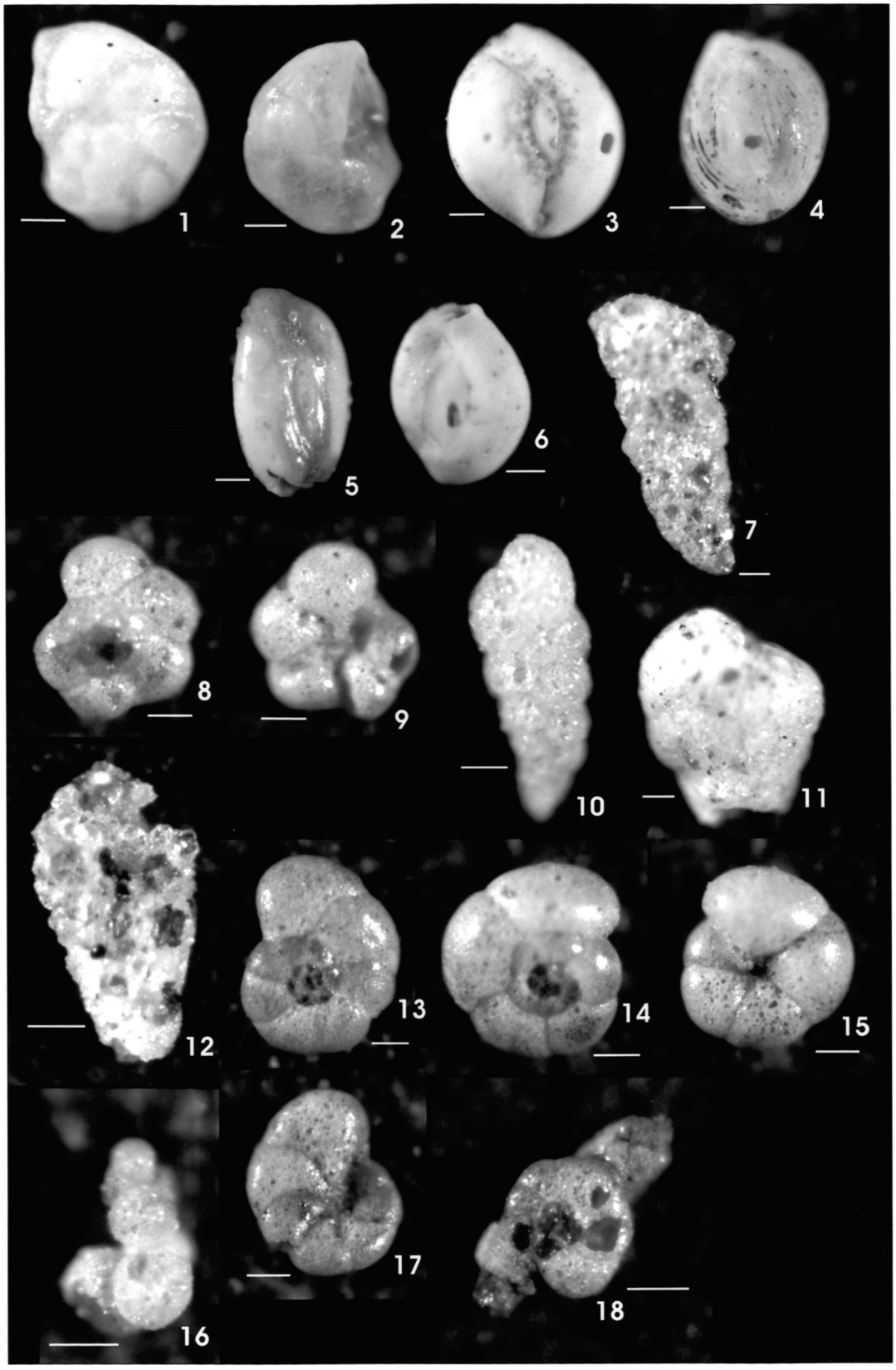
1
2
3
4
5
6
7
8
9
10
11
12
13
14
15
16
17
18

Appendix A: References useful in identifying taxa to the species level

Ammoastuta inepta (Cushman and McCulloch); Grossman, 1967:47, pl. 2:fig. 9. Parker, 1952a, pl. 2:figs. 1,2. [as *A. salsa*]

Ammobaculites crassus Warren: Warren, 1957:35, pl. 3:figs. 5-7. Grossman, 1967:48, pl. 1: figs. 4,5,10.

Ammobaculites dilatatus Cushman and Brönnimann: Cushman and Brönnimann, 1948b:39, pl. 7:figs. 10,11. Parker and Athearn, 1959:340, pl. 50:figs. 4,5.

Ammobaculites exiguus Cushman and Brönnimann: Ellison and Nichols, 1970:15, pl. 2:fig. 6 [as *Ammobaculites* cf. *A. exiguus*].

Ammonia parkinsoniana (d'Orbigny): Grossman, 1967:56, pl.10:figs. 1,2 [as *A. limbatobeccarii*].

Ammonia tepida (Cushman): Grossman, 1967:56, pl. 9: figs. 5,9. Loeblich and Tappan, 1994:166, pl. 371:figs. 5-10.

Ammotium salsum (Cushman and Brönnimann): Grossman, 1967:49, pl. 2:figs. 1,2,8. Scott, et al., 1977:1578, pl. 2:figs. 4,5.

Arenoparrella mexicana (Kornfield): Kornfield, 1931:86, pl. 13:figs. 5a-c [as *Trochammina inflata* var. *mexicana*]. Saunders, 1957:13, pl. 4:fig. 5. Grossman 1967:55, pl.6:figs.2-4.

Asterogeroma carinata d'Orbigny: Parker, 1954:532, pl. 10:figs. 16, 17. Schnitker, 1971:204, pl. 6:figs. 9a-c.

Buccella frigida (Cushman): Anderson, 1952:147, figs. 4-6.

Buccella inusitata Anderson: Anderson, 1952:147, fig 10, 11.

Cibicides lobatulus (Walker and Jacob): Todd and Brönnimann, 1957:41, pl. 12:figs. 11a-c. Sen Gupta, 1971:89, pl. 2:figs. 34-36.

Cibicides refulgens Montfort: Todd and Brönnimann, 1957:41, pl. 12:figs. 12a-c.

Elphidium advenum Cushman: Parker, 1954:508, pl. 6:fig. 14. Buzas et al., 1985:1081, figs. 6.1, 6.2.

Elphidium excavatum (Terquem): Buzas et al., 1985:1083, figs. 6.7-6.10, 7.1, 7.2.

Elphidium galvestonense Kornfield: Grossman, 1967:60, pl. 7:figs. 1,2.

Elphidium gunteri Cole: Grossman, 1967:59, pl. 8:figs 1-4. Buzas et al., 1985:1084, figs. 7.4, 7.5.

Elphidium mexicanum (Kornfield): Buzas et al., 1985:1086, figs. 7-9, 10.

Elphidium cf. *E. mexicanum*

Elphidium subarcticum Cushman: Buzas et al., 1985:1087, figs. 8.1, 8.2.

Hanzawaia strattoni (Applin): Bandy, 1954:136, pl. 31:fig. 4. Grossman, 1967:62, pl. 10:figs. 3-5 [as *H.* sp. cf. *H. strattoni*].

Haplophragmoides bonplandi Todd and Brönnimann: Todd and Brönnimann, 1957:23, pl. 2: fig. 2. Scott and Medioli 1980:40, pl. 2:figs. 4, 5.

Haplophragmoides wilberti Andersen. Grossman, 1967:47, pl. 2:figs. 12-14.

Haynesina germanica (Ehrenberg): Buzas et al., 1985:1088, figs 8.4, 8.5.

Jadammina macrescens (Brady): Parker, 1952a:408, pl. 4:figs. 8 a, b. Parker, 1952b:460, pl. 3:figs 3 a, b.

Miliammina fusca (Brady): Parker, 1952b:452, pl. 2:figs. 6 a, b. Parker and Athearn 1959:340, pl. 50:figs. 11, 12. Grossman, 1967:46, pl. 2:figs. 3-5.

Miliammina petila Saunders: Saunders, 1958:88, pl. 1:10, 11.

Nonionella atlantica Cushman: Cushman, 1947:90, pl. 30:figs, 4,5. Parker, 1954:507, pl. 6:figs. 6,7.

Poroeponides lateralis (Terquem): Bandy, 1954:137, pl. 30:fig. 1. Grossman, 1967:56, pl. 10:figs. 6-8.

Pseudoclavulina gracilis Cushman and Brönnimann: Cushman and Brönnimann, 1948b:40, pl. 7:fig. 18.

Quinqueloculina lamarckiana d'Orbigny: Grossman, 1967:52, pl. 3:figs. 1-3. Schnitker, 1971:208, pl. 2:figs. 16a-c.

Quinqueloculina jugosa (Cushman): Grossman, 1967:51, pl. 4:figs. 7,11,12. Schnitker, 1971:208, pl. 2:fig. 15a-c.

Quinqueloculina seminula (Linné): Kornfield, 1931:83-84, pl. 14: figs. 4a-c [as *Q. seminulum*]. Grossman, 1967:53, pl. 4:figs. 13,14,18. Schnitker, 1971:208, pl. 3:figs. 1a-c.

Quinqueloculina sp. C

Reophax sp.

Siphotrochammina lobata Saunders. Saunders, 1957:9 pl. 3:figs. 1,2.

Textularia earlandi Phleger: Schafer and Cole, 1978:29, pl. 3:fig. 4.

Textularia c.f. *T. gramen* (Todd and Brönnimann): Todd and Brönnimann, 1957:11, pl. 2:fig. 18.

Textularia sp.

Tiphotrocha comprimata (Cushman and Brönnimann): Saunders, 1957:11, pl. 4:figs. 1 4. Grossman, 1967:50, pl. 6:figs. 1,5.

Trochammina inflata (Montagu): Buzas, 1964:57, pl. 1:figs. 9a, 9b.

Trochammina sp.

Trochamminita irregularis Cushman and Brönnimann: Cushman and Brönnimann, 1948a:17, pl. 4:figs. 1-3. Saunders, 1957:4, pl. 2:figs. 2-8.

Appendix B: Raw Census Data (surface)

Raw census data (numbers of live and dead specimens) for surface samples in Pamlico Sound. S37 is not listed because it was barren of foraminifera.

Raw Data (Live & Dead)

Station ID		S1	S2	S4	S5	S7	S9	S10	S11	S12	S14	S15	S17	S17A	S22	S23	S24	S25	S26	S27	S30	S31	S32
Number of live specimens		113	0	30	1	1	0	3	3	0	2	3	70	16	8	0	5	1	5	5	14	9	48
Number of dead specimens		174	268	277	348	2	249	30	283	251	35	28	202	283	289	183	258	18	30	227	130	273	259
Total number of specimens		287	268	307	349	3	249	33	286	251	37	31	272	299	297	183	263	19	35	232	144	282	307
Ammoastuta inepta	L																						
	D	1	37																				
Ammobaculites crassus	L																						
	D	2		7	1			1	6							5				1	8		
Ammobaculites dilatatus	L																						
	D											1											
Ammobaculites exiguus	L											1								1			
	D											2								15			
Ammonia parkinsoniana	L	20		26	1	1		1	1		2		1	3			5				1		2
	D	100		57	282		1	3	35		19		8	4	14		18				6	33	37
Ammonia tepida	L																						1
	D							7	6				2										24
Ammotium salsum	L	15		4								1		3	5					2	3	1	
	D	18	75	188	56	2	234		220	216	12	18		4	218	148	19	11	24	203	33	4	9
Arenoparrella mexicana	L																						
	D						1	1	1					28							6		
Asterigerina carinata	L																						
	D												1										1
Buccella frigida	L																						
	D																						
Buccella inusitata	L																						
	D												2										
Cibicides lobatulus	L																						
	D												5										
Cibicides refulgens	L																						
	D												4										
Elphidium advenum	L																						
	D																						
Elphidium excavatum	L	3							1					6	3			1	5		10	8	38
	D	6			7		13	1	10	35	1		146		55	27	220	5	3	2	59	236	84
Elphidium galvestonense	L													1									
	D												2										

Raw Data (Live & Dead)

Station ID		S1	S2	S4	S5	S7	S9	S10	S11	S12	S14	S15	S17	S17A	S22	S23	S24	S25	S26	S27	S30	S31	S32
Elphidium gunteri	L	3							1														
	D								1				1										1
Elphidium mexicanum	L											1	69	1									
	D												6										
Elphidium cf. *E. mexicanum*	L																						7
	D																						100
Elphidium subarcticum	L	3																					
	D												9										
Hanzawaia strattoni	L																						
	D												9								2		
Haplophragmoides bonplandi	L																						
	D		6											2									
Haplophragmoides wilberti	L	1																					
	D	3	5	1				9	1			2		114						2	4		
Haynesina germanica	L																						
	D																						3
Jadammina macrescens	L																						
	D		39					2	1					10							2		
Miliammina fusca	L	68						1															
	D	42	53	24	1			1	1							1					3		
Miliammina petila	L																						
	D		4											3									
Nonionella atlantica	L																						
	D												3										
Poroeponides lateralis	L																						
	D																						
Pseudoclavulina gracilis	L																						
	D														1								
Quinqueloculina lamarckiana	L																						
	D																						

Station ID		S1	S2	S4	S5	S7	S9	S10	S11	S12	S14	S15	S17	S17A	S22	S23	S24	S25	S26	S27	S30	S31	S32
Quinqueloculina jugosa	L																						
	D																						
Quinqueloculina seminula	L																						
	D												2										
Quinqueloculina sp. C	L																						
	D																						
Reophax sp.	L							1															
	D																						
Siphotrochammina lobata	L													1									
	D													3		1							
Textularia earlandi	L																			2			
	D																		1				
Texularia cf. *T. gramen*	L																						
	D												2										
Textularia sp.	L																						
	D														1								
Tiphotrocha comprimata	L													1									
	D		41					1						14		1					4		
Trochammina inflata	L																						
	D	2						4	1			2		87				1	2		3		
Trochamminita irregularis	L																						
	D													6									
Trochammina sp.	L																						
	D		1											3									
Indeterminate agglutinated	L																						
	D		7																				
Indeterminate calcareous	L																						
	D																1						
Organic lining	L																						
	D				1						3	3		5				1		4			

Raw Data (Live & Dead)

Station ID		S35	S38	S39	S40	S41	S42	S44	S45	S46	S50	S59	S60	S61	S63	EB02 S1	EB02 S2	EB02 S3
Number of live specimens		0	15	5	11	22	4	27	55	23	119	2	61	21	37	0	1	4
Number of dead specimens		1	179	211	318	316	302	75	165	36	198	330	242	229	234	111	11	143
Total number of specimens		1	194	216	329	338	306	102	220	59	317	332	303	250	271	111	12	147
Ammoastuta inepta	L																	
	D																	
Ammobaculites crassus	L														1			
	D			3														
Ammobaculites dilatatus	L																	
	D																	
Ammobaculites exiguus	L							2										
	D							4										
Ammonia parkinsoniana	L					6		5		9			3	5	18			
	D					5	49	4		2	6	18	58	69		12	1	5
Ammonia tepida	L																	
	D																	
Ammotium salsum	L			3			4	6			85		4	8	14			
	D	1	5	200	225	129	93	56	8		144	6	42	16	232			
Arenoparrella mexicana	L								1									
	D		21	1						4								
Asterigerina carinata	L																	
	D																	3
Buccella frigida	L																	
	D																	1
Buccella inusitata	L																	
	D																	
Cibicides lobatulus	L																	
	D															2		6
Cibicides refulgens	L																	
	D																	
Elphidium advenum	L																	
	D																	1
Elphidium excavatum	L			2	11	16					34	2	54	8				
	D			4	89	181	153	3	1		48	306	131	143		69	6	97
Elphidium galvestonense	L							1		10					4			
	D							1		1						1		3

Raw Data (Live & Dead)

Station ID		S35	S38	S39	S40	S41	S42	S44	S45	S46	S50	S59	S60	S61	S63	EB02 S1	EB02 S2	EB02 S3
Elphidium gunteri	L																	
	D							1										
Elphidium mexicanum	L		2					11										
	D															1	3	2
Elphidium cf. *E. mexicanum*	L																	
	D																	
Elphidium subarcticum	L																	
	D															3		1
Hanzawaia strattoni	L																	
	D															4	1	11
Haplophragmoides bonplandi	L																	
	D																	
Haplophragmoides wilberti	L		1															
	D		20	1														
Haynesina germanica	L																	
	D																	
Jadammina macrescens	L																	
	D		17															
Miliammina fusca	L																	
	D		7						2					1				
Miliammina petila	L																	
	D																	
Nonionella atlantica	L																	
	D																	1
Poroeponides lateralis	L																	
	D																	1
Pseudoclavulina gracilis	L																	
	D																	
Quinqueloculina lamarckiana	L																	
	D															3		2

Raw Data (Live & Dead)

Station ID		S35	S38	S39	S40	S41	S42	S44	S45	S46	S50	S59	S60	S61	S63	EB02 S1	EB02 S2	EB02 S3
Quinqueloculina jugosa	L																1	1
	D																	1
Quinqueloculina seminula	L																	3
	D															12		8
Quinqueloculina sp. C	L																	
	D															3		
Reophax sp.	L																	
	D				3		1											
Siphotrochammina lobata	L									2								
	D		4						22	8								
Textularia earlandi	L							2										
	D				1			2							1			
Texularia cf. *T. gramen*	L																	
	D																	
Textularia sp.	L																	
	D					1												
Tiphotrocha comprimata	L		2															
	D		23	2					8	1								
Trochammina inflata	L		10						53	1								
	D		82						122	18					1			
Trochamminita irregularis	L																	
	D																	
Trochammina sp.	L								1									
	D								2									
Indeterminate agglutinated	L																	
	D																	
Indeterminate calcareous	L																	
	D						6						11			1		
Organic lining	L									1								
	D							4		2								

Appendix C: Relative Abundance Data (surface)

Relative abundance data (expressed as percents) of the 31 species comprising two percent or more of the assemblage in any one sample.

Relative Abundance:

Station ID	S1	S2	S4	S5	S7	S9	S10	S11	S12	S14	S15	S17	S17A	S22	S23	S24	S25	S26
Number of specimens	174	268	277	348	2	249	30	283	251	35	28	202	283	289	183	258	18	30
Ammoastuta inepta	0.6	13.8	0	0	0	0	0	0	0	0	0	0	0	0	0	0	0	0
Ammonia parkinsoniana	57.5	0	20.6	81.0	0	0.4	10.0	12.4	0	54.3	0	4.0	1.4	4.8	0	7.0	0	0
Ammonia tepida	0	0	0	0	0	0	23.3	2.1	0	0	0	1.0	0	0	0	0	0	0
Ammotium salsum	10.3	28.0	67.9	16.1	100.0	94.0	0	77.7	86.1	34.3	64.3	0	1.4	75.4	80.9	7.4	61.1	80.0
Arenoparrella mexicana	0	0	0	0	0	0.4	3.3	0.4	0	0	0	0	9.9	0.0	0	0	0	0
Asterigerina carinata	0	0	0	0	0	0	0	0	0	0	0	0.5	0	0	0	0	0	0
Ammobaculites crassus	1.1	0	2.5	0.3	0	0	3.3	2.1	0	0	0	0	0	0	2.7	0	0	0
Ammobaculites dilatatus	0	0	0	0	0	0	0	0	0	0	3.6	0	0	0	0	0	0	0
Ammobaculites exiguus	0	0	0	0	0	0	0	0	0	0	7.1	0	0	0	0	0	0	0
Cibicides lobatulus	0	0	0	0	0	0	0	0	0	0	0	2.5	0	0	0	0	0	0
Cibicides refulgens	0	0	0	0	0	0	0	0	0	0	0	2.0	0	0	0	0	0	0
Elphidium excavatum	3.4	0	0	2.0	0.0	5.2	3.3	3.5	13.9	2.9	0	72.3	0	19.0	14.8	85.3	27.8	10.0
Elphidium galvestonense	0	0	0	0	0	0	0	0	0	0	0	1.0	0	0	0	0	0	0
Elphidium mexicanum	0	0	0	0	0	0	0	0	0	0	0	3.0	0	0	0	0	0	0
Elphidium cf. *E. mexicanum*	0	0	0	0	0	0	0	0	0	0	0	0.0	0	0	0	0	0	0
Elphidium subarcticum	0	0	0	0	0	0	0	0	0	0	0	4.5	0	0	0	0	0	0
Hanzawaia strattoni	0	0	0	0	0	0	0	0	0	0	0	4.5	0	0	0	0	0	0
Haplophragmoides bonplandi	0	2.2	0	0	0	0	0	0	0	0	0	0	0.7	0	0	0	0	0
Haplophragmoides wilberti	1.7	1.9	0.4	0	0	0	30.0	0.4	0	0	7.1	0	40.3	0	0	0	0	0
Jadammina macrescens	0	14.6	0	0	0	0	6.7	0.4	0	0	0	0	3.5	0	0	0	0	0
Miliammina fusca	24.1	19.8	8.7	0.3	0	0	3.3	0.4	0	0	0	0	0	0	0.5	0	0	0
Quinqueloculina lamarckiana	0	0	0	0	0	0	0	0	0	0	0	0	0	0	0	0	0	0
Quinqueloculina seminula	0	0	0	0	0	0	0	0	0	0	0	1	0	0	0	0	0	0
Quinqueloculina sp. C	0	0	0	0	0	0	0	0	0	0	0	0	0	0	0	0	0	0
Siphotrochammina lobata	0	0	0	0	0	0	0	0	0	0	0	0	1.1	0	0.5	0	0	0
Textularia earlandi	0	0	0	0	0	0	0	0	0	0	0	0	0	0	0	0	0	3.3
Tiphotrocha comprimata	0	15.3	0	0	0	0	3.3	0	0	0	0	0	4.9	0	0.5	0	0	0.0
Trochammina inflata	1.1	0	0	0	0	0	13.3	0.4	0	0	7.1	0	30.7	0	0	0	5.6	6.7
Indeterminate agglutinated	0	2.6	0	0	0	0	0	0	0	0	0	0	0	0	0	0	0	0
Indeterminate calcareous	0	0	0	0	0	0	0	0	0	0	0	0	0	0	0	0.4	0	0
Organic lining	0	0	0	0.3	0	0	0	0	0	8.6	10.7	0	1.8	0	0	0	5.6	0

Relative Abundance:

Station ID	S27	S30	S31	S32	S35	S38	S39	S40	S41	S42	S44	S45	S46	S50	S59	S60	S61	S63
Number of specimens	227	130	273	259	1	179	211	318	316	302	75	165	36	198	330	242	229	234
Ammoastuta inepta	0	0	0	0	0	0	0	0	0	0	0	0	0	0	0	0	0	0
Ammonia parkinsoniana	0	4.6	12.1	14.3	0	0	0	0	1.6	16.2	5.3	0	5.6	3.0	5.5	24.0	30.1	0
Ammonia tepida	0	0	0	9.3	0	0	0	0	0	0	0	0	0	0	0	0	0	0
Ammotium salsum	89.4	25.4	1.5	3.5	100.0	2.8	94.8	70.8	40.8	30.8	74.7	4.8	0	72.7	1.8	17.4	7.0	99.1
Arenoparrella mexicana	0	4.6	0	0	0	11.7	0.5	0	0	0	0	0	11.1	0	0	0	0	0
Asterigerina carinata	0	0	0	0.4	0	0	0	0	0	0	0	0	0	0	0	0	0	0
Ammobaculites crassus	0.4	6.2	0	0	0	0	1.4	0	0	0	0	0	0	0	0	0	0	0
Ammobaculites dilatatus	0	0	0	0	0	0	0	0	0	0	0	0	0	0	0	0	0	0
Ammobaculites exiguus	6.6	0	0	0	0	0	0	0	0	0	5.3	0	0	0	0	0	0	0
Cibicides lobatulus	0	0	0	0	0	0	0	0	0	0	0	0	0	0	0	0	0	0
Cibicides refulgens	0	0	0	0	0	0	0	0	0	0	0	0	0	0	0	0	0	0
Elphidium excavatum	0.9	45.4	86.4	32.4	0	0	1.9	28.0	57.3	50.7	4.0	0.6	0	24.2	92.7	54.1	62.4	0
Elphidium galvestonense	0	0	0	0	0	0	0	0	0	0	1.3	0.0	2.8	0	0	0	0	0
Elphidium mexicanum	0	0	0	0	0	0	0	0	0	0	0	0	0	0	0	0	0	0
Elphidium cf. *E. mexicanum*	0	0	0	38.6	0	0	0	0	0	0	0	0	0	0	0	0	0	0
Elphidium subarcticum	0	0	0	0	0	0	0	0	0	0	0	0	0	0	0	0	0	0
Hanzawaia strattoni	0	2	0	0	0	0	0	0	0	0	0	0	0	0	0	0	0	0
Haplophragmoides bonplandi	0	0	0	0	0	0	0	0	0	0	0	0	0	0	0	0	0	0
Haplophragmoides wilberti	0.9	3.1	0.0	0	0	11	0	0	0	0	0	0	0	0	0	0	0	0
Jadammina macrescens	0	1.5	0	0	0	9.5	0	0	0	0	0	0	0	0	0	0	0	0
Miliammina fusca	0	2.3	0	0	0	3.9	0	0	0	0	0	1.2	0	0	0	0	0.4	0
Quinqueloculina lamarckiana	0	0	0	0	0	0	0	0	0	0	0	0	0	0	0	0	0	0
Quinqueloculina seminula	0	0	0	0	0	0	0	0	0	0	0	0	0	0	0	0	0	0
Quinqueloculina sp. C	0	0	0	0	0	0	0	0	0	0	0	0	0	0	0	0	0	0
Siphotrochammina lobata	0	0	0	0	0	2.2	0	0	0	0	0	13.3	22.2	0	0	0	0	0
Textularia earlandi	0	0	0	0	0	0	0	0.3	0	0	2.7	0	0	0	0	0	0	0.4
Tiphotrocha comprimata	0	3.1	0	0	0	12.8	0.9	0	0	0	0	4.8	2.8	0	0	0	0	0
Trochammina inflata	0	2.3	0	0	0	45.8	0	0	0	0	0	73.9	50.0	0	0	0	0	0.4
Indeterminate agglutinated	0	0	0	0	0	0	0	0	0	0	0	0	0	0	0	0	0	0
Indeterminate calcareous	0	0	0	0	0	0	0	0	0	2.0	0	0	0	0	0	4.5	0	0
Organic lining	1.8	0	0	0	0	0	0	0	0	0	5.3	0	5.6	0	0	0	0	0

Relative Abundance:

Station ID	EB02 S1	EB02 S2	EB02 S3
Number of specimens	111	11	143
Ammoastuta inepta	0	0	0
Ammonia parkinsoniana	10.8	9.1	3.5
Ammonia tepida	0	0	0
Ammotium salsum	0	0	0
Arenoparrella mexicana	0	0	0
Asterigerina carinata	0	0	2.1
Ammobaculites crassus	0	0	0
Ammobaculites dilatatus	0	0	0
Ammobaculites exiguus	0	0	0
Cibicides lobatulus	1.8	0	4.2
Cibicides refulgens	0	0	0
Elphidium excavatum	62.2	54.5	67.8
Elphidium galvestonense	0.9	0	2.1
Elphidium mexicanum	0.9	27.3	1.4
Elphidium cf. *E. mexicanum*	0	0	0
Elphidium subarcticum	2.7	0	0.7
Hanzawaia strattoni	3.6	9.1	7.7
Haplophragmoides bonplandi	0	0	0
Haplophragmoides wilberti	0	0	0
Jadammina macrescens	0	0	0
Miliammina fusca	0	0	0
Quinqueloculina lamarckiana	2.7	0	1.4
Quinqueloculina seminula	10.8	0	5.6
Quinqueloculina sp. C	2.7	0	0
Siphotrochammina lobata	0	0	0
Textularia earlandi	0	0	0
Tiphotrocha comprimata	0	0	0
Trochammina inflata	0	0	0
Indeterminate agglutinated	0	0	0
Indeterminate calcareous	0.9	0	0
Organic lining	0	0	0

Appendix D: Transformed Abundance Data (surface)

Transformed abundance data of the 31 species comprising two percent or more of the assemblage in any one sample.

Transformed Abundance:

Station ID	S1	S2	S4	S5	S7	S9	S10	S11	S12	S14	S15	S17
Ammoastuta inepta	0.1518	0.7614	0.0000	0.0000	0.0000	0.0000	0.0000	0.0000	0.0000	0.0000	0.0000	0.0000
Ammobaculites crassus	0.2148	0.0000	0.3193	0.1073	0.0000	0.0000	0.3672	0.2923	0.0000	0.0000	0.0000	0.0000
Ammobaculites dilatatus	0.0000	0.0000	0.0000	0.0000	0.0000	0.0000	0.0000	0.0000	0.0000	0.0000	0.3803	0.0000
Ammobaculites exiguus	0.0000	0.0000	0.0000	0.0000	0.0000	0.0000	0.0000	0.0000	0.0000	0.0000	0.5411	0.0000
Ammonia parkinsoniana	1.7208	0.0000	0.9417	2.2404	0.0000	0.1268	0.6435	0.7187	0.0000	1.6566	0.0000	0.4007
Ammonia tepida	0.0000	0.0000	0.0000	0.0000	0.0000	0.0000	1.0083	0.2923	0.0000	0.0000	0.0000	0.1993
Ammotium salsum	0.6549	1.1149	1.9363	0.8255	3.1416	2.6456	0.0000	2.1589	2.3762	1.2511	1.8605	0.0000
Arenoparrella mexicana	0.0000	0.0000	0.0000	0.0000	0.0000	0.1268	0.3672	0.1190	0.0000	0.0000	0.0000	0.0000
Asterigerina carinata	0.0000	0.0000	0.0000	0.0000	0.0000	0.0000	0.0000	0.0000	0.0000	0.0000	0.0000	0.1408
Cibicides lobatulus	0.0000	0.0000	0.0000	0.0000	0.0000	0.0000	0.0000	0.0000	0.0000	0.0000	0.0000	0.3160
Cibicides refulgens	0.0000	0.0000	0.0000	0.0000	0.0000	0.0000	0.0000	0.0000	0.0000	0.0000	0.0000	0.2824
Elphidium excavatum	0.3736	0.0000	0.0000	0.2846	0.0000	0.4611	0.3672	0.3782	0.7654	0.3397	0.0000	2.0326
Elphidium galvestonense	0.0000	0.0000	0.0000	0.0000	0.0000	0.0000	0.0000	0.0000	0.0000	0.0000	0.0000	0.1993
Elphidium mexicanum	0.0000	0.0000	0.0000	0.0000	0.0000	0.0000	0.0000	0.0000	0.0000	0.0000	0.0000	0.3464
Elphidium cf. *E. mexicanum*	0.0000	0.0000	0.0000	0.0000	0.0000	0.0000	0.0000	0.0000	0.0000	0.0000	0.0000	0.0000
Elphidium subarcticum	0.0000	0.0000	0.0000	0.0000	0.0000	0.0000	0.0000	0.0000	0.0000	0.0000	0.0000	0.4254
Hanzawaia strattoni	0.0000	0.0000	0.0000	0.0000	0.0000	0.0000	0.0000	0.0000	0.0000	0.0000	0.0000	0.4254
Haplophragmoides bonplandi	0.0000	0.3004	0.0000	0.0000	0.0000	0.0000	0.0000	0.0000	0.0000	0.0000	0.0000	0.0000
Haplophragmoides wilberti	0.2634	0.2740	0.1202	0.0000	0.0000	0.0000	1.1593	0.1190	0.0000	0.0000	0.5411	0.0000
Jadammina macrescens	0.0000	0.7828	0.0000	0.0000	0.0000	0.0000	0.5223	0.1190	0.0000	0.0000	0.0000	0.0000
Miliammina fusca	1.0272	0.9217	0.5976	0.1073	0.0000	0.0000	0.3672	0.1190	0.0000	0.0000	0.0000	0.0000
Quinqueloculina lamarckiana	0.0000	0.0000	0.0000	0.0000	0.0000	0.0000	0.0000	0.0000	0.0000	0.0000	0.0000	0.0000
Quinqueloculina seminula	0.0000	0.0000	0.0000	0.0000	0.0000	0.0000	0.0000	0.0000	0.0000	0.0000	0.0000	0.1993
Quinqueloculina sp. C	0.0000	0.0000	0.0000	0.0000	0.0000	0.0000	0.0000	0.0000	0.0000	0.0000	0.0000	0.0000
Siphotrochammina lobata	0.0000	0.0000	0.0000	0.0000	0.0000	0.0000	0.0000	0.0000	0.0000	0.0000	0.0000	0.0000
Textularia earlandi	0.0000	0.0000	0.0000	0.0000	0.0000	0.0000	0.0000	0.0000	0.0000	0.0000	0.0000	0.0000
Tiphotrocha comprimata	0.0000	0.8037	0.0000	0.0000	0.0000	0.0000	0.3672	0.0000	0.0000	0.0000	0.0000	0.0000
Trochammina inflata	0.2148	0.0000	0.0000	0.0000	0.0000	0.0000	0.7476	0.1190	0.0000	0.0000	0.5411	0.0000
Indeterminate agglutinated	0.0000	0.3247	0.0000	0.0000	0.0000	0.0000	0.0000	0.0000	0.0000	0.0000	0.0000	0.0000
Indeterminate calcareous	0.0000	0.0000	0.0000	0.0000	0.0000	0.0000	0.0000	0.0000	0.0000	0.0000	0.0000	0.0000
Organic lining	0.0000	0.0000	0.0000	0.1073	0.0000	0.0000	0.0000	0.0000	0.0000	0.5942	0.6669	0.0000

Transformed Abundance:

Station ID	S17A	S22	S23	S24	S25	S26	S27	S30	S31	S32	S35	S38
Ammoastuta inepta	0.0000	0.0000	0.0000	0.0000	0.0000	0.0000	0.0000	0.0000	0.0000	0.0000	0.0000	0.0000
Ammobaculites crassus	0.0000	0.0000	0.3321	0.0000	0.0000	0.0000	0.1328	0.5014	0.0000	0.0000	0.0000	0.0000
Ammobaculites dilatatus	0.0000	0.0000	0.0000	0.0000	0.0000	0.0000	0.0000	0.0000	0.0000	0.0000	0.0000	0.0000
Ammobaculites exiguus	0.0000	0.0000	0.0000	0.0000	0.0000	0.0000	0.5200	0.0000	0.0000	0.0000	0.0000	0.0000
Ammonia parkinsoniana	0.2383	0.4438	0.0000	0.5346	0.0000	0.0000	0.0000	0.4330	0.7102	0.7752	0.0000	0.0000
Ammonia tepida	0.0000	0.0000	0.0000	0.0000	0.0000	0.0000	0.0000	0.0000	0.0000	0.6186	0.0000	0.0000
Ammotium salsum	0.2383	2.1044	2.2363	0.5496	1.7949	2.2143	2.4792	1.0561	0.2427	0.3750	3.1416	0.3358
Arenoparrella mexicana	0.6400	0.0000	0.0000	0.0000	0.0000	0.0000	0.0000	0.4330	0.0000	0.0000	0.0000	0.6992
Asterigerina carinata	0.0000	0.0000	0.0000	0.0000	0.0000	0.0000	0.0000	0.0000	0.0000	0.1244	0.0000	0.0000
Cibicides lobatulus	0.0000	0.0000	0.0000	0.0000	0.0000	0.0000	0.0000	0.0000	0.0000	0.0000	0.0000	0.0000
Cibicides refulgens	0.0000	0.0000	0.0000	0.0000	0.0000	0.0000	0.0000	0.0000	0.0000	0.0000	0.0000	0.0000
Elphidium excavatum	0.0000	0.9028	0.7885	2.3538	1.1102	0.6435	0.1880	1.4784	2.3876	1.2118	0.0000	0.0000
Elphidium galvestonense	0.0000	0.0000	0.0000	0.0000	0.0000	0.0000	0.0000	0.0000	0.0000	0.0000	0.0000	0.0000
Elphidium mexicanum	0.0000	0.0000	0.0000	0.0000	0.0000	0.0000	0.0000	0.0000	0.0000	0.0000	0.0000	0.0000
Elphidium cf. *E. mexicanum*	0.0000	0.0000	0.0000	0.0000	0.0000	0.0000	0.0000	0.0000	0.0000	1.3410	0.0000	0.0000
Elphidium subarcticum	0.0000	0.0000	0.0000	0.0000	0.0000	0.0000	0.0000	0.0000	0.0000	0.0000	0.0000	0.0000
Hanzawaia strattoni	0.0000	0.0000	0.0000	0.0000	0.0000	0.0000	0.0000	0.2487	0.0000	0.0000	0.0000	0.0000
Haplophragmoides bonplandi	0.1683	0.0000	0.0000	0.0000	0.0000	0.0000	0.0000	0.0000	0.0000	0.0000	0.0000	0.0000
Haplophragmoides wilberti	1.3752	0.0000	0.0000	0.0000	0.0000	0.0000	0.1880	0.3526	0.0000	0.0000	0.0000	0.6816
Jadammina macrescens	0.3782	0.0000	0.0000	0.0000	0.0000	0.0000	0.0000	0.2487	0.0000	0.0000	0.0000	0.6265
Miliammina fusca	0.0000	0.0000	0.1480	0.0000	0.0000	0.0000	0.0000	0.3050	0.0000	0.0000	0.0000	0.3981
Quinqueloculina lamarckiana	0.0000	0.0000	0.0000	0.0000	0.0000	0.0000	0.0000	0.0000	0.0000	0.0000	0.0000	0.0000
Quinqueloculina seminula	0.0000	0.0000	0.0000	0.0000	0.0000	0.0000	0.0000	0.0000	0.0000	0.0000	0.0000	0.0000
Quinqueloculina sp. C	0.0000	0.0000	0.0000	0.0000	0.0000	0.0000	0.0000	0.0000	0.0000	0.0000	0.0000	0.0000
Siphotrochammina lobata	0.2063	0.0000	0.1480	0.0000	0.0000	0.0000	0.0000	0.0000	0.0000	0.0000	0.0000	0.3001
Textularia earlandi	0.0000	0.0000	0.0000	0.0000	0.0000	0.3672	0.0000	0.0000	0.0000	0.0000	0.0000	0.0000
Tiphotrocha comprimata	0.4486	0.0000	0.1480	0.0000	0.0000	0.0000	0.0000	0.3526	0.0000	0.0000	0.0000	0.7332
Trochammina inflata	1.1754	0.0000	0.0000	0.0000	0.4759	0.5223	0.0000	0.3050	0.0000	0.0000	0.0000	1.4869
Indeterminate agglutinated	0.0000	0.0000	0.0000	0.0000	0.0000	0.0000	0.0000	0.0000	0.0000	0.0000	0.0000	0.0000
Indeterminate calcareous	0.0000	0.0000	0.0000	0.1246	0.0000	0.0000	0.0000	0.0000	0.0000	0.0000	0.0000	0.0000
Organic lining	0.2666	0.0000	0.0000	0.0000	0.4759	0.0000	0.2663	0.0000	0.0000	0.0000	0.0000	0.0000

Transformed Abundance:

Station ID	S39	S40	S41	S42	S44	S45	S46	S50	S59	S60	S61	S63
Ammoastuta inepta	0.0000	0.0000	0.0000	0.0000	0.0000	0.0000	0.0000	0.0000	0.0000	0.0000	0.0000	0.0000
Ammobaculites crassus	0.2390	0.0000	0.0000	0.0000	0.0000	0.0000	0.0000	0.0000	0.0000	0.0000	0.0000	0.0000
Ammobaculites dilatatus	0.0000	0.0000	0.0000	0.0000	0.0000	0.0000	0.0000	0.0000	0.0000	0.0000	0.0000	0.0000
Ammobaculites exiguus	0.0000	0.0000	0.0000	0.0000	0.4661	0.0000	0.0000	0.0000	0.0000	0.0000	0.0000	0.0000
Ammonia parkinsoniana	0.0000	0.0000	0.2522	0.8292	0.4661	0.0000	0.4759	0.3499	0.4715	1.0232	1.1621	0.0000
Ammonia tepida	0.0000	0.0000	0.0000	0.0000	0.0000	0.0000	0.0000	0.0000	0.0000	0.0000	0.0000	0.0000
Ammotium salsum	2.6809	1.9988	1.3862	1.1766	2.0867	0.4440	0.0000	2.0427	0.2705	0.8594	0.5350	2.9564
Arenoparrella mexicana	0.1378	0.0000	0.0000	0.0000	0.0000	0.0000	0.6797	0.0000	0.0000	0.0000	0.0000	0.0000
Asterigerina carinata	0.0000	0.0000	0.0000	0.0000	0.0000	0.0000	0.0000	0.0000	0.0000	0.0000	0.0000	0.0000
Cibicides lobatulus	0.0000	0.0000	0.0000	0.0000	0.0000	0.0000	0.0000	0.0000	0.0000	0.0000	0.0000	0.0000
Cibicides refulgens	0.0000	0.0000	0.0000	0.0000	0.0000	0.0000	0.0000	0.0000	0.0000	0.0000	0.0000	0.0000
Elphidium excavatum	0.2762	1.1149	1.7169	1.5840	0.4027	0.1559	0.0000	1.0296	2.5955	1.6535	1.8223	0.0000
Elphidium galvestonense	0.0000	0.0000	0.0000	0.0000	0.2315	0.0000	0.3349	0.0000	0.0000	0.0000	0.0000	0.0000
Elphidium mexicanum	0.0000	0.0000	0.0000	0.0000	0.0000	0.0000	0.0000	0.0000	0.0000	0.0000	0.0000	0.0000
Elphidium cf. *E. mexicanum*	0.0000	0.0000	0.0000	0.0000	0.0000	0.0000	0.0000	0.0000	0.0000	0.0000	0.0000	0.0000
Elphidium subarcticum	0.0000	0.0000	0.0000	0.0000	0.0000	0.0000	0.0000	0.0000	0.0000	0.0000	0.0000	0.0000
Hanzawaia strattoni	0.0000	0.0000	0.0000	0.0000	0.0000	0.0000	0.0000	0.0000	0.0000	0.0000	0.0000	0.0000
Haplophragmoides bonplandi	0.0000	0.0000	0.0000	0.0000	0.0000	0.0000	0.0000	0.0000	0.0000	0.0000	0.0000	0.0000
Haplophragmoides wilberti	0.1378	0.0000	0.0000	0.0000	0.0000	0.0000	0.0000	0.0000	0.0000	0.0000	0.0000	0.0000
Jadammina macrescens	0.0000	0.0000	0.0000	0.0000	0.0000	0.0000	0.0000	0.0000	0.0000	0.0000	0.0000	0.0000
Miliammina fusca	0.0000	0.0000	0.0000	0.0000	0.0000	0.2206	0.0000	0.0000	0.0000	0.0000	0.1323	0.0000
Quinqueloculina lamarckiana	0.0000	0.0000	0.0000	0.0000	0.0000	0.0000	0.0000	0.0000	0.0000	0.0000	0.0000	0.0000
Quinqueloculina seminula	0.0000	0.0000	0.0000	0.0000	0.0000	0.0000	0.0000	0.0000	0.0000	0.0000	0.0000	0.0000
Quinqueloculina sp. C	0.0000	0.0000	0.0000	0.0000	0.0000	0.0000	0.0000	0.0000	0.0000	0.0000	0.0000	0.0000
Siphotrochammina lobata	0.0000	0.0000	0.0000	0.0000	0.0000	0.7476	0.9818	0.0000	0.0000	0.0000	0.0000	0.0000
Textularia earlandi	0.0000	0.1122	0.0000	0.0000	0.3281	0.0000	0.0000	0.0000	0.0000	0.0000	0.0000	0.1308
Tiphotrocha comprimata	0.1950	0.0000	0.0000	0.0000	0.0000	0.4440	0.3349	0.0000	0.0000	0.0000	0.0000	0.0000
Trochammina inflata	0.0000	0.0000	0.0000	0.0000	0.0000	2.0701	1.5708	0.0000	0.0000	0.0000	0.0000	0.1308
Indeterminate agglutinated	0.0000	0.0000	0.0000	0.0000	0.0000	0.0000	0.0000	0.0000	0.0000	0.0000	0.0000	0.0000
Indeterminate calcareous	0.0000	0.0000	0.0000	0.2828	0.0000	0.0000	0.0000	0.0000	0.0000	0.4297	0.0000	0.0000
Organic lining	0.0000	0.0000	0.0000	0.0000	0.4661	0.0000	0.4759	0.0000	0.0000	0.0000	0.0000	0.0000

Transformed Abundance:

Station ID	EB02 S1	EB02 S2	EB02 S3
Ammoastuta inepta	0.0000	0.0000	0.0000
Ammobaculites crassus	0.0000	0.0000	0.0000
Ammobaculites dilatatus	0.0000	0.0000	0.0000
Ammobaculites exiguus	0.0000	0.0000	0.0000
Ammonia parkinsoniana	0.6701	0.6126	0.3762
Ammonia tepida	0.0000	0.0000	0.0000
Ammotium salsum	0.0000	0.0000	0.0000
Arenoparrella mexicana	0.0000	0.0000	0.0000
Asterigerina carinata	0.0000	0.0000	0.2907
Cibicides lobatulus	0.2693	0.0000	0.4126
Cibicides refulgens	0.0000	0.0000	0.0000
Elphidium excavatum	1.8165	1.6618	1.9355
Elphidium galvestonense	0.1901	0.0000	0.2907
Elphidium mexicanum	0.1901	1.0989	0.2371
Elphidium cf. *E. mexicanum*	0.0000	0.0000	0.0000
Elphidium subarcticum	0.3303	0.0000	0.1674
Hanzawaia strattoni	0.3820	0.6126	0.5621
Haplophragmoides bonplandi	0.0000	0.0000	0.0000
Haplophragmoides wilberti	0.0000	0.0000	0.0000
Jadammina macrescens	0.0000	0.0000	0.0000
Miliammina fusca	0.0000	0.0000	0.0000
Quinqueloculina lamarckiana	0.3303	0.0000	0.2371
Quinqueloculina seminula	0.6701	0.0000	0.4776
Quinqueloculina sp. C	0.3303	0.0000	0.0000
Siphotrochammina lobata	0.0000	0.0000	0.0000
Textularia earlandi	0.0000	0.0000	0.0000
Tiphotrocha comprimata	0.0000	0.0000	0.0000
Trochammina inflata	0.0000	0.0000	0.0000
Indeterminate agglutinated	0.0000	0.0000	0.0000
Indeterminate calcareous	0.1901	0.0000	0.0000
Organic lining	0.0000	0.0000	0.0000

Appendix E: Raw Census Data (down-core)

Raw census data (number of dead specimens) for 21 species recorded in down-core samples. 'a' indicates those intervals corresponding with the ^{137}Cs peak (1963-1964). 'b' indicates those intervals dated by ^{210}Pb to be approximately 120 years old.

Down-core Raw data

Station ID:	S9a	S9b	S11b	S12a	S12b	S24a	S24b	S27b	S30a	S30b	S31a	S31b	S32a	S41a	S41b	S50a	S50b	S59a	S59b	S60a	S60b
interval (cm):	8-10	18-20	14-16	16-18	20-22	12-14	28-30	12-14	10-12	16-18	16-18	51-54	10-12	12-14	24-26	16-18	36-39	4-6	20-22	12-14	28-30
Number of Specimens:	294	288	293	323	271	328	328	122	294	356	278	310	395	285	283	268	278	408	107	280	281
Ammoastuta inepta			1																		
Ammonia parkinsoniana						20	7	1	7	37	13	29	118	1		21		17	3	25	2
Ammonia tepida							2			3		2									
Ammotium salsum	281	276	281	313	256	33	288	112	253	126	88	180	3	151	249	240	277	133	66	249	272
Arenoparrella mexicana		1																			
Ammobaculites crassus	2	5	11	10	13		6	2	9	2	1	3		1							
Ammobaculites dilatatus																					
Ammobaculites exiguus																					1
Elphidium excavatum		4			2	274	24	7	14	187	176	96	271	132	34	7		255	37	6	6
Elphidium galvestonense										1											
Elphidium gunteri													1					1			
Elphidium mexicanum							1														
Elphidium cf. *E. mexicanum*													2								
Haplophragmoides wilberti	4								3												
Jadammina macrescens	1	1																			
Reophax sp.	2								1												
Textularia sp.																		1			
Tiphotrocha comprimata																		1			
Trochammina inflata	2					1			7												
Trochammina sp.		1																	1		
Organic lining	2																1				

Appendix F: Relative Abundance Data (down-core)

Relative abundance data of down-core samples expressed as percents. 'a' indicates those intervals corresponding with the ^{137}Cs peak (1963-1964). 'b' indicates those intervals dated by ^{210}Pb to be approximately 120 years old.

Relative Abundance:

Station ID:	S9a	S9b	S11b	S12a	S12b	S24a	S24b	S27b	S30a	S30b	S31a	S31b	S32a	S41a	S41b	S50a	S50b	S59a	S59b	S60a	S60b
interval (cm):	8-10	18-20	14-16	16-18	20-22	12-14	28-30	12-14	10-12	16-18	16-18	51-54	10-12	12-14	24-26	16-18	36-39	4-6	20-22	12-14	28-30
Ammoastuta inepta	0	0	0.3	0	0	0	0	0	0	0	0	0	0	0	0	0	0	0	0	0	0
Ammonia parkinsoniana	0	0	0	0	0	6.1	2.1	0.8	2.4	10.4	4.7	9.4	29.9	0.4	0	7.8	0	4.2	2.8	8.9	0.7
Ammonia tepida	0	0	0	0	0	0	0.6	0	0	0.8	0	0.6	0	0	0	0	0	0	0	0	0
Ammotium salsum	95.6	95.8	95.9	96.9	94.5	10.1	87.8	91.8	86.1	35.4	31.7	58.1	0.8	53.0	88.0	89.6	99.6	32.6	61.7	88.9	96.8
Arenoparrella mexicana	0	0.3	0	0	0	0	0	0	0	0	0	0	0	0	0	0	0	0	0	0	0
Ammobaculites crassus	0.7	1.7	3.8	3.1	4.8	0	1.8	1.6	3.1	0.6	0.4	1.0	0	0.4	0	0	0	0	0	0	0
Ammobaculites dilatatus	0	0	0	0	0	0	0	0	0	0	0	0	0	0	0	0	0	0	0	0	0
Ammobaculites exiguus	0	0	0	0	0	0	0	0	0	0	0	0	0	0	0	0	0	0	0	0	0.4
Elphidium excavatum	0	1.4	0	0	0.7	83.5	7.3	5.7	4.8	52.5	63.3	31.0	68.6	46.3	12.0	2.6	0	62.5	34.6	2.1	2.1
Elphidium galvestonense	0	0	0	0	0	0	0	0	0	0.3	0	0	0	0	0	0	0	0	0	0	0
Elphidium gunteri	0	0	0	0	0	0	0	0	0	0	0	0	0.3	0	0	0	0	0.2	0	0	0
Elphidium mexicanum	0	0	0	0	0	0	0.3	0	0	0	0	0	0	0	0	0	0	0	0	0	0
Elphidium cf. *E. mexicanum*	0	0	0	0	0	0	0	0	0	0	0	0	0.5	0	0	0	0	0	0	0	0
Haplophragmoides wilberti	1.4	0	0	0	0	0	0	0	1.0	0	0	0	0	0	0	0	0	0	0	0	0
Jadammina macrescens	0.3	0.3	0	0	0	0	0	0	0	0	0	0	0	0	0	0	0	0	0	0	0
Reophax sp.	0.7	0	0	0	0	0	0	0	0.3	0	0	0	0	0	0	0	0	0	0	0	0
Textularia sp.	0	0	0	0	0	0	0	0	0	0	0	0	0	0	0	0	0	0.2	0	0	0
Tiphotrocha comprimata	0	0	0	0	0	0	0	0	0	0	0	0	0	0	0	0	0	0.2	0	0	0
Trochammina inflata	0.7	0	0	0	0	0.3	0	0	2.4	0	0	0	0	0	0	0	0	0	0	0	0
Trochammina sp.	0	0.3	0	0	0	0	0	0	0	0	0	0	0	0	0	0	0	0	0.9	0	0
Organic lining	0.7	0	0	0	0	0	0	0	0	0	0	0	0	0	0	0	0.4	0	0	0	0

Appendix G: Transformed Abundance Data (down-core)

Transformed abundance data of down-core samples. 'a' indicates those intervals corresponding with the ^{137}Cs peak (1963-1964). 'b' indicates those intervals dated by ^{210}Pb to be approximately 120 years old.

Transformed Abundance:

Station ID:	S9a	S9b	S11b	S12a	S12b	S24a	S24b	S27b	S30a	S30b	S31a	S31b	S32a	S41a	S41b	S50a	S50b	S59a	S59b	S60a	S60b
interval (cm):	8-10	18-20	14-16	16-18	20-22	12-14	28-30	12-14	10-12	16-18	16-18	51-54	10-12	12-14	24-26	16-18	36-39	4-6	20-22	12-14	28-30
Ammoastuta inepta	0	0	0.12	0	0	0	0	0	0	0	0	0	0	0	0	0	0	0	0	0	0
Ammonia parkinsoniana	0.17	0.26	0.39	0.35	0.44	0	0.27	0.26	0.35	0.15	0.12	0.20	0	0.12	0	0	0	0	0	0	0
Ammonia tepida	0	0	0	0	0	0	0	0	0	0	0	0	0	0	0	0	0	0	0	0	0
Ammotium salsum	0	0	0	0	0	0	0	0	0	0	0	0	0	0	0	0	0	0	0	0	0.12
Arenoparrella mexicana	0	0	0	0	0	0.50	0.29	0.18	0.31	0.66	0.44	0.62	1.16	0.12	0	0.57	0	0.41	0.34	0.61	0.17
Ammobaculites crassus	0	0	0	0	0	0	0.16	0	0	0.18	0	0.16	0	0	0	0	0	0	0	0	0
Ammobaculites dilatatus	2.72	2.73	2.73	2.79	2.67	0.65	2.43	2.56	2.38	1.27	1.20	1.73	0.17	1.63	2.43	2.48	3.02	1.22	1.81	2.46	2.78
Ammobaculites exiguus	0	0.12	0	0	0	0	0	0	0	0	0	0	0	0	0	0	0	0	0	0	0
Elphidium excavatum	0	0.24	0	0	0.17	2.31	0.55	0.48	0.44	1.62	1.84	1.18	1.95	1.50	0.71	0.32	0	1.82	1.26	0.29	0.29
Elphidium galvestonense	0	0	0	0	0	0	0	0	0	0.11	0	0	0	0	0	0	0	0	0	0	0
Elphidium gunteri	0	0	0	0	0	0	0	0	0	0	0	0	0.10	0	0	0	0	0.10	0	0	0
Elphidium mexicanum	0	0	0	0	0	0	0.11	0	0	0	0	0	0	0	0	0	0	0	0	0	0
Elphidium cf. *E. mexicanum*	0	0	0	0	0	0	0	0	0	0	0	0	0.14	0	0	0	0	0	0	0	0
Haplophragmoides wilberti	0.23	0	0	0	0	0	0	0	0.20	0	0	0	0	0	0	0	0	0	0	0	0
Jadammina macrescens	0.12	0.12	0	0	0	0	0	0	0	0	0	0	0	0	0	0	0	0	0	0	0
Reophax sp.	0.17	0	0	0	0	0	0	0	0.12	0	0	0	0	0	0	0	0	0	0	0	0
Textularia sp.	0	0	0	0	0	0	0	0	0	0	0	0	0	0	0	0	0	0.10	0	0	0
Tiphotrocha comprimata	0	0	0	0	0	0	0	0	0	0	0	0	0	0	0	0	0	0.10	0	0	0
Trochammina inflata	0.17	0	0	0	0	0.11	0	0	0.31	0	0	0	0	0	0	0	0	0	0	0	0
Trochammina sp.	0	0.12	0	0	0	0	0	0	0	0	0	0	0	0	0	0	0	0	0.19	0	0
Organic lining	0.17	0	0	0	0	0	0	0	0	0	0	0	0	0	0	0	0.12	0	0	0	0

Appendix H: Geochemical Data

Geochemical data for cores collected in Pamlico Sound. Data are listed by site number and interval. $\delta^{15}N$ signatures are given in respect to the $\delta^{15}N$ signature of air. $\delta^{13}C$ signatures are given in respect to the $\delta^{13}C$ signature of the Pee Dee Belemnite. The last column (F/NF) represents those samples that were re-sent for either a second or third time to the stable isotope lab. 'F' represents a sample that was fumigated with acid while 'NF' represents a sample that was not fumigated with acid before being re-sent. Samples noted with 'F & NF' represent an averaged signature between fumigated and non-fumigated samples. A '*' indicates samples that were not used in the analysis because the values are still questionable and were not re-sent to the lab to be double-checked.

Site	Interval	Micro g N	Delta Air	Micro g C	Delta PDB	C/N	%OC	F/NF
S9	(0-2)	24.1	3.85	317.9	-24.30	13.19	0.62	
	(2-4)	22.3	3.66	287.6	-24.95	12.89	0.57	
	(4-6)	11.3	3.25	147.0	-24.59	12.95	0.29	
	(6-8)	15.2	3.43	197.5	-24.78	12.99	0.39	
	(8-10)	21.3	3.42	307.3	-24.79	14.44	0.61	
	(10-12)	20.6	3.04	323.7	-24.80	15.70	0.63	
	(12-14)	20.5	3.40	290.3	-24.61	14.13	0.57	
	(14-16)	22.4	2.84	372.9	-24.90	16.65	0.73	
	(16-18)	23.6	2.52	393.2	-24.68	16.67	0.78	
	(18-20)	22.8	2.78	345.0	-24.69	15.11	0.68	
	(20-22)	22.4	3.30	307.7	-24.22	13.74	0.60	
	(22-24)	24.2	2.98	333.5	-23.95	13.75	0.66	
	(24-26)	26.8	3.05	367.3	-24.13	13.72	0.72	
	(26-28)	27.2	2.96	397.0	-24.07	14.59	0.79	
	(28-30)	22.1	2.68	326.1	-24.10	14.76	0.65	
	(30-32)	25.9	3.05	392.5	-24.28	15.16	0.77	
	(32-34	17.6	2.81	256.8	-24.03	14.61	0.51	
	(34-36)	16.6	2.78	245.9	-24.03	14.80	0.48	
S10	(0-2)	64.1	5.10	676.5	-24.40	10.55	2.79	
	(2-4)	52.2	5.21	557.3	-24.57	10.68	2.70	
	(4-6)	44.4	4.95	489.0	-24.73	11.01	2.38	
	(6-8)	66.8	4.60	826.9	-24.79	12.35	1.90	F
	(8-10)	36.38	3.81	514.18	-26.64	14.13	1.64	NF
	(10-12)	31.48	3.17	461.28	-24.57	14.65	1.31	NF
	(12-14)	48.6	3.93	657.5	-24.30	13.53	0.73	NF
	(14-16)	33.95	3.62	483.52	-23.71	14.24	0.51	NF
	(16-18)	33.80	3.66	478.09	-23.38	14.14	0.60	NF
	(18-20)	41.0	6.14	601.5	-22.88	14.66	0.59	*
	(20-22)	31.90	3.74	431.30	-22.76	13.52	0.40	NF
	(22-24)	47.3	7.57	696.3	-22.12	14.73	0.71	*
	(24-26)	29.12	3.02	402.52	-22.20	14.13	0.70	F & NF
	(26-28)	36.82	2.72	519.12	-21.88	14.10	0.37	NF
	(28-30)	50.82	2.58	738.92	-20.01	14.71	1.02	F
S11	(0-2)	84.3	4.46	1342.5	-24.09	15.93	3.46	
	(2-4)	58.1	4.52	851.5	-24.85	14.66	1.05	
	(4-6)	54.21	5.02	502.16	-24.65	12.08	0.54	F & NF
	(6-8)	51.26	4.44	718.78	-25.18	14.02	0.55	NF
	(8-10)	35.5	2.96	556.9	-24.97	15.67	0.68	F
	(10-12)	63.4	3.78	936.2	-24.73	14.77	1.22	F
	(12-14)	71.6	4.11	1024.5	-24.79	14.30	1.11	F
	(14-16)	52.8	4.15	762.8	-24.53	14.44	1.15	F
	(16-18)	39.3	3.93	581.2	-24.66	14.79	0.86	F
	(18-20)	55.7	3.21	750.0	-24.29	13.46	1.01	
	(20-22)	61.5	3.22	882.3	-24.32	14.34	1.18	
	(22-24)	60.0	3.23	852.9	-23.93	14.22	0.97	
	(24-26)	62.9	3.24	772.0	-23.35	12.27	1.15	
S12	(0-2)	42.2	5.26	417.8	-24.05	9.91	0.51	F
	(2-4)	40.50	5.36	399.97	-23.91	9.88	0.29	NF
	(4-6)	17.78	5.41	161.62	-23.58	9.08	0.16	F & NF
	(6-8)	47.31	5.29	479.57	-24.21	10.14	0.35	NF
	(8-10)	54.51	5.50	578.45	-24.18	10.61	0.38	NF
	(10-12)	41.2	4.77	434.1	-24.09	10.70	0.35	F
	(12-14)	49.7	4.23	566.9	-23.87	11.40	0.55	
	(14-16)	32.7	4.99	368.8	-24.12	11.23	0.49	F

Site	Interval	Micro g N	Delta Air	Micro g C	Delta PDB	C/N	%OC	F/NF
S12	(16-18)	36.1	4.45	419.8	-23.96	11.62	0.48	
	(18-20)	19.1	4.27	221.0	-23.93	11.59	0.20	
	(20-22)	36.4	3.72	425.6	-23.81	11.69	0.99	
	(22-24)	42.2	4.00	459.5	-23.61	10.90	0.36	F
	(24-26)	47.7	4.38	534.6	-23.89	11.21	0.41	F
	(26-28)	56.88	4.76	667.44	-23.86	11.73	0.34	NF
	(28-30)	29.29	3.79	333.72	-22.84	11.39	0.33	NF
	(30-32)	52.73	4.28	614.98	-23.39	11.35	0.62	F
S22	(0-2)	73.9	5.73	744.8	-24.21	10.07	2.19	F
	(2-4)	77.2	5.67	808.4	-24.47	10.47	2.62	F
	(4-6)	66.2	4.72	684.5	-24.24	10.34	2.30	
	(6-8)	76.8	4.45	823.5	-24.24	10.73	2.35	
	(8-10)	59.2	4.22	639.7	-24.24	10.81	2.36	
	(10-12)	59.7	4.51	630.1	-24.10	10.55	2.30	
	(12-14)	40.4	4.12	441.2	-23.86	10.92	2.03	
	(14-16)	46.1	4.18	519.8	-23.93	11.29	1.98	
	(16-18)	59.3	4.02	689.0	-23.98	11.62	2.12	
	(18-20)	50.6	3.50	568.4	-23.71	11.23	2.24	
	(20-22)	48.1	3.47	540.4	-23.66	11.24	2.25	
	(22-24)	59.4	3.56	691.2	-23.73	11.63	2.19	
	(24-26)	57.8	3.74	658.7	-23.67	11.40	2.23	
	(26-28)	49.7	3.86	563.2	-23.64	11.33	2.37	
	(28-30)	47.6	3.76	596.3	-23.50	12.52	2.30	
	(30-32)	49.4	3.63	532.3	-23.37	10.78	1.85	
	(32-34)	41.9	3.79	443.4	-22.83	10.58	1.59	
S23	(0-2)	62.0	5.55	667.6	-23.83	10.77	0.76	
	(2-4)	50.7	4.80	579.8	-24.63	11.44	0.53	
	(4-6)	60.9	4.31	797.1	-24.87	13.09	1.00	
	(6-8)	42.2	3.73	650.0	-24.51	15.41	1.51	
	(8-10)	60.1	3.78	757.3	-23.94	12.60	2.47	
	(10-12)	21.8	3.22	311.8	-24.66	14.30	0.81	
	(12-14)	27.4	3.93	384.6	-24.51	14.01	1.65	
	(14-16)	29.5	3.81	395.4	-24.66	13.40	1.87	
	(16-18)	29.1	3.54	391.9	-24.68	13.48	1.02	
	(18-20)	45.0	4.54	603.7	-24.58	13.40	2.90	
	(20-22)	34.5	5.18	444.8	-24.55	12.89	1.91	
	(22-24)	47.8	3.40	586.8	-23.95	12.27	4.51	
	(24-26)	46.3	3.64	619.8	-24.48	13.38	4.37	
S24	(0-2)	105.4	6.96	1066.1	-24.27	10.11	2.33	
	(2-4)	72.1	4.52	706.5	-24.22	9.80	2.27	
	(4-6)	80.9	4.29	786.7	-24.19	9.72	2.02	
	(6-8)	72.1	6.38	779.3	-24.27	10.81	2.13	
	(8-10)	74.8	4.20	808.7	-24.26	10.81	2.11	
	(10-12)	76.2	5.13	816.1	-24.16	10.71	2.07	
	(12-14)	67.3	4.17	764.6	-24.30	11.36	2.19	
	(14-16)	72.8	4.18	830.8	-24.33	11.42	2.01	
	(16-18)	71.4	4.32	838.1	-24.11	11.74	1.83	
	(18-20)	62.8	4.13	703.6	-24.10	11.20	1.84	
	(20-22)	67.9	4.09	772.0	-24.11	11.36	1.82	
	(22-24)	65.1	4.12	735.2	-24.10	11.29	1.87	
	(24-26)	74.1	4.02	860.2	-23.98	11.60	1.96	
	(26-28)	81.6	3.58	941.1	-23.77	11.53	2.05	
	(28-30)	71.4	3.25	794.0	-23.67	11.12	1.95	

Site	Interval	Micro g N	Delta Air	Micro g C	Delta PDB	C/N	%OC	F/NF
S27	(0-2)	65.3	2.62	618.3	-19.10	9.47	0.59	
	(2-4)	74.8	3.11	697.0	-19.25	9.32	0.52	
	(4-6)	56.6	2.93	605.0	-19.49	10.69	0.60	
	(6-8)	67.8	2.04	735.2	-19.02	10.84	0.71	
	(8-10)	69.4	1.86	727.1	-18.76	10.48	0.72	
	(10-12)	70.1	2.58	742.6	-18.53	10.60	0.83	
	(12-14)	62.3	3.20	661.0	-18.39	10.61	0.78	
	(14-16)	61.5	2.94	708.7	-18.47	11.53	0.66	
	(16-18)	64.4	4.42	728.6	-18.68	11.31	0.60	
	(18-20)	71.1	1.98	819.6	-19.04	11.53	0.73	
S30	(0-2)	70.6	6.15	703.9	-23.66	9.98	1.69	F
	(2-4)	61.65	5.27	573.50	-23.99	9.30	0.72	NF
	(4-6)	55.76	5.07	563.62	-24.14	10.11	0.76	NF
	(6-8)	60.6	4.12	705.9	-23.41	11.65	1.47	
	(8-10)	53.02	3.92	728.82	-24.00	13.75	4.28	F &NF
	(10-12)	61.55	4.72	741.60	-23.23	12.05	0.44	NF
	(12-14)	48.24	4.35	643.04	-22.33	13.33	0.61	NF
	(14-16)	47.7	4.49	687.7	-24.63	14.41	0.99	NF
	(16-18)	50.7	4.32	794.1	-24.35	15.67	1.69	
	(18-20)	42.5	3.58	672.8	-24.25	15.85	1.88	
	(20-22)	73.98	4.42	1181.62	-21.25	15.97	1.83	NF
S31	(0-2)	60.46	6.02	568.48	-23.51	9.40	1.94	NF
	(2-4)	70.89	6.04	657.55	-23.91	9.28	2.10	NF
	(4-6)	52.9	6.05	494.0	-23.96	9.33	2.06	F
	(6-8)	42.8	5.58	400.7	-23.92	9.36	1.57	F
	(8-10)	57.2	5.42	554.8	-24.01	9.70	1.47	F
	(10-12)	54.1	5.14	547.7	-23.96	10.12	1.60	F
	(12-14)	55.5	5.13	588.3	-24.00	10.60	1.71	F
	(14-16)	34.8	5.54	393.4	-23.35	11.29	1.79	
	(16-18)	35.8	5.32	405.1	-23.60	11.32	1.96	
	(18-20)	33.4	6.05	381.6	-23.41	11.44	1.87	
	(20-22)	38.0	5.60	419.8	-23.44	11.06	1.67	
	(22-24)	58.2	4.32	591.1	-23.68	10.15	1.98	
	(24-26)	45.6	3.79	469.8	-23.61	10.31	2.19	
	(26-28)	60.0	4.10	598.5	-23.60	9.98	2.39	
	(28-30)	57.1	4.00	618.3	-23.41	10.82	2.37	
	(30-33)	40.5	3.71	428.6	-23.62	10.57	2.14	
	(33-36)	47.8	3.68	504.4	-23.51	10.55	2.25	
	(36-39)	49.5	3.72	527.1	-23.61	10.65	2.22	
	(39-42)	51.2	3.73	537.4	-23.41	10.49	1.85	
	(42-45)	57.8	3.46	611.7	-23.25	10.58	2.31	
	(45-48)	52.0	3.66	540.4	-23.25	10.39	2.36	
	(48-51)	55.0	3.95	572.7	-23.27	10.41	1.89	
	(51-54)	41.2	3.70	420.5	-23.31	10.22	1.68	
S32	(0-2)	46.1	5.10	445.2	-23.90	9.67	2.87	
	(2-4)	43.2	5.64	438.2	-24.03	10.14	2.85	
	(4-6)	39.6	5.17	404.8	-23.95	10.22	2.63	
	(6-8)	39.8	5.19	411.9	-23.89	10.34	2.65	
	(8-10)	38.2	5.24	382.3	-23.74	10.01	2.49	
	(10-12)	38.6	5.04	385.7	-23.67	10.00	2.50	
	(12-14)	34.0	4.88	361.5	-23.29	10.62	2.39	
	(14-16)	30.7	4.76	353.8	-23.01	11.52	2.34	
	(16-18)	29.6	4.80	338.2	-23.12	11.43	2.18	
	(18-20)	26.5	4.57	308.5	-22.67	11.62	2.01	

Site	Interval	Micro g N	Delta Air	Micro g C	Delta PDB	C/N	%OC	F/NF
S32	(20-22)	27.0	4.61	303.9	-22.95	11.26	2.01	
	(22-24)	27.0	4.50	306.3	-23.23	11.35	2.00	
	(24-26)	28.8	4.39	333.8	-22.71	11.57	2.15	
	(26-28)	28.0	4.52	329.2	-22.37	11.74	2.14	
S41	(0-2)	93.2	5.86	845.5	-23.72	9.07	1.13	
	(2-4)	93.2	5.58	830.8	-23.73	8.92	0.96	
	(4-6)	93.9	5.65	867.6	-23.68	9.24	1.44	
	(6-8)	91.1	4.92	860.2	-23.67	9.44	1.44	
	(8-10)	66.2	4.48	630.8	-23.60	9.52	1.24	
	(10-12)	70.1	4.78	672.0	-23.63	9.59	1.21	
	(12-14)	67.9	4.25	660.2	-23.59	9.72	1.54	
	(14-16)	68.7	4.33	698.5	-23.48	10.17	1.44	
	(16-18)	56.6	4.05	588.2	-23.40	10.39	1.33	
	(18-20)	65.8	3.97	699.2	-23.47	10.63	1.25	
	(20-22)	85.0	4.08	926.4	-23.32	10.90	1.49	
	(22-24)	65.4	4.11	680.1	-23.40	10.40	1.43	
	(24-26)	65.2	4.96	684.5	-23.38	10.50	1.34	
	(26-28)	50.0	3.91	523.5	-23.25	10.47	1.32	
S42	(0-2)	80.9	5.54	749.9	-23.68	9.26	2.48	
	(2-4)	109.5	5.50	1021.9	-23.76	9.33	2.46	
	(4-6)	78.9	5.19	719.8	-23.77	9.12	2.13	
	(6-8)	84.3	5.15	786.7	-23.81	9.33	2.43	
	(8-10)	82.3	5.21	757.3	-23.80	9.20	2.00	
	(10-12)	79.6	4.62	772.0	-23.78	9.70	1.95	
	(12-14)	72.1	4.70	713.2	-23.74	9.89	1.99	
	(14-16)	58.8	4.46	588.2	-23.70	10.00	1.95	
	(16-18)	82.98	4.64	845.50	-23.64	10.19	1.62	
	(18-20)	60.1	4.21	611.0	-23.62	10.17	1.75	
	(20-22)	54.3	5.09	540.4	-23.50	9.94	1.98	
	(22-24)	70.7	4.04	749.9	-23.50	10.60	1.95	
	(24-26)	78.2	4.08	867.6	-23.45	11.09	1.90	
	(26-28)	70.1	4.07	749.9	-23.47	10.70	1.99	
	(28-30)	75.5	6.35	808.7	-23.26	10.71	1.85	
	(30-32)	56.8	3.43	621.3	-23.47	10.94	2.02	
S50	(0-2)	64.9	4.66	585.3	-24.86	9.03	3.53	
	(2-4)	81.0	4.70	700.2	-24.26	8.65	3.55	
	(4-6)	68.4	4.35	640.1	-24.29	9.36	3.44	
	(6-8)	85.6	4.53	776.8	-24.09	9.07	3.11	
	(8-10)	75.7	4.53	689.3	-24.07	9.11	3.22	
	(10-12)	75.7	4.18	749.5	-23.97	9.90	3.10	
	(12-14)	89.6	4.50	820.6	-24.03	9.16	3.14	
	(14-16)	64.3	4.36	601.8	-23.81	9.36	3.10	
	(16-18)	77.0	4.23	776.8	-24.08	10.09	3.04	
	(18-20)	83.6	4.60	804.2	-24.41	9.61	3.12	
	(20-22)	59.8	4.36	618.2	-24.19	10.34	3.15	
	(22-24)	66.2	4.62	634.6	-23.85	9.59	2.64	
	(24-26)	60.6	4.73	585.3	-23.72	9.66	2.65	
	(26-28)	69.0	4.60	716.6	-23.79	10.38	2.70	
	(28-30)	75.7	4.73	744.0	-23.79	9.83	2.81	
	(30-33)	59.5	4.40	629.1	-23.74	10.57	2.68	
	(33-36)	63.3	4.28	623.6	-23.81	9.86	3.02	
	(36-39)	63.1	4.02	678.3	-23.77	10.75	3.07	
	(39-42)	80.3	3.90	798.7	-23.73	9.94	2.96	
	(42-45)	80.3	3.82	853.4	-23.55	10.63	3.16	

Site	Interval	Micro g N	Delta Air	Micro g C	Delta PDB	C/N	%OC	F/NF
S50	(45-48)	89.6	4.04	864.3	-23.42	9.65	2.60	
	(48-50)	79.7	3.94	847.9	-23.50	10.65	2.62	
S59	(0-2)	77.7	4.51	754.9	-23.86	9.72	2.14	
	(2-4)	88.3	4.57	891.7	-23.92	10.10	2.14	
	(4-6)	77.7	4.41	782.3	-23.73	10.07	2.31	
	(6-8)	85.6	4.44	891.7	-23.71	10.41	2.11	
	(8-10)	73.0	4.19	771.3	-23.77	10.56	2.15	
	(10-12)	69.03	4.00	754.93	-23.65	10.94	2.09	
	(12-14)	68.4	4.09	754.9	-23.51	11.04	1.98	
	(14-16)	67.7	3.92	744.0	-23.52	10.99	2.22	
	(16-18)	69.0	3.98	749.5	-23.46	10.86	1.94	
	(18-20)	60.9	3.87	645.5	-23.32	10.60	2.00	
	(20-22)	67.7	3.62	705.7	-22.79	10.42	1.21	
	(22-24)	66.4	3.70	678.3	-22.80	10.22	1.00	
	(24-26)	63.3	3.88	634.6	-22.82	10.03	1.24	
	(26-28)	69.7	3.84	694.8	-22.73	9.97	1.52	
	(28-30)	63.7	3.78	640.1	-22.66	10.04	1.80	
	(30-33)	71.7	4.09	711.2	-22.68	9.92	1.66	
S60	(0-2)	73.7	4.58	629.1	-24.01	8.54	2.33	
	(2-4)	92.3	4.50	809.6	-24.23	8.77	2.46	
	(4-6)	98.9	4.72	864.3	-24.33	8.74	2.67	
	(6-8)	79.0	4.74	733.1	-24.44	9.28	2.68	
	(8-10)	93.6	4.82	826.1	-24.35	8.83	2.35	
	(10-12)	88.3	4.94	787.8	-24.10	8.92	2.22	
	(12-14)	85.63	4.76	787.76	-23.82	9.20	2.08	
	(14-16)	90.9	4.54	902.6	-23.86	9.93	1.98	
	(16-18)	81.6	4.58	820.6	-23.65	10.05	1.84	
	(18-20)	62.2	4.36	656.5	-23.33	10.55	1.82	
	(20-22)	67.7	4.39	700.2	-23.25	10.34	1.68	
	(22-24)	62.4	4.04	640.1	-23.27	10.26	1.64	
	(24-26)	61.8	4.13	645.5	-23.30	10.45	1.63	
	(26-28)	76.3	3.80	809.6	-23.28	10.61	1.67	
	(28-30)	68.4	3.78	716.6	-22.74	10.48	1.72	
	(30-33)	60.7	3.72	640.1	-22.45	10.54	1.81	
S61	(0-2)	78.3	4.63	700.2	-23.69	8.94	2.31	
	(2-4)	85.0	4.68	776.8	-23.62	9.14	2.09	
	(4-6)	68.4	4.63	651.0	-23.51	9.52	2.11	
	(6-8)	73.7	4.52	727.6	-23.56	9.87	2.07	
	(8-10)	75.0	4.58	754.9	-23.43	10.06	1.94	
	(10-12)	73.7	4.52	760.4	-23.42	10.32	2.03	
	(12-14)	49.2	4.22	497.3	-23.26	10.11	2.12	
	(14-16)	70.4	4.30	733.1	-23.42	10.42	1.98	
	(16-18)	65.8	4.37	689.3	-23.31	10.47	1.92	
	(18-20)	56.6	4.14	596.3	-23.10	10.54	1.59	
	(20-22)	58.1	4.11	618.2	-23.01	10.64	1.37	
	(22-24)	54.5	4.05	612.7	-22.81	11.24	0.87	
	(24-26)	50.4	4.06	563.5	-22.64	11.17	1.04	
	(26-28)	44.3	3.99	495.1	-22.50	11.17	1.15	
	(28-30)	54.6	4.13	612.7	-22.57	11.22	1.20	
	(30-33)	53.2	4.12	596.3	-22.56	11.20	0.68	